ISSN 8755-6839

SCIENCE OF **TSUNAMI HAZARDS**

Journal of Tsunami Society International

Volume 42 Number 3 2023

TSUNAMI SOCIETY INTERNATIONAL
1325 South 33rd Avenue, Hollywood, Florida 33021, USA.

SCIENCE OF TSUNAMI HAZARDS is a CERTIFIED OPEN ACCESS Journal included in the prestigious international academic journal database DOAJ.
SCIENCE OF TSUNAMI HAZARDS is also preserved, archived and disseminated by the National Library, The Hague, NETHERLANDS, the Library of Congress, Washington D.C., USA, the Electronic Library of Los Alamos, National Laboratory, New Mexico, USA, the EBSCO Publishing databases and ELSEVIER Publishing in Amsterdam. The vast dissemination gives the journal additional global exposure and readership in 90% of the academic institutions worldwide, including nation-wide access to databases in more than –as of now – 80 countries.

OBJECTIVE: Tsunami Society International publishes this interdisciplinary journal to increase and disseminate knowledge about tsunamis and their hazards.

DISCLAIMER: Although the articles in SCIENCE OF TSUNAMI HAZARDS have been technically reviewed by peers, Tsunami Society International is not responsible for the veracity of any statement, opinion or consequences.

Submit manuscripts of research papers, notes or letters to the Editor. If a research paper is accepted for publication, the author(s) must submit a scan-ready manuscript, in Microsoft Doc, TeX or an PDF file in the established journal format.

Issues of the journal are published electronically in PDF format. There is a minimal publication fee for authors to cover costs of production, of worldwide mailing and

distribution of the journal to libraries and to recipients in more than 80 countries.

CD-ROMs of pastvolumes may be purchased by contacting:
Tsunami Society International at postmaster@tsunamisociety.org Issues of the journal from 1982 through 2005 are also available in PDF format at the U.S. Los Alamos National Laboratory Library http://epubs.lanl.gov/tsunami/

ISSN 8755-6839

SCIENCE OF TSUNAMI HAZARDS

Journal of Tsunami Society International

Volume 42 Number 3 2023

GLOBAL OVERVIEW ON THE RECENT STUDIES OF GEOHAZARDS: A DYNAMIC POPULATION APPROACH

Nadi Suprapto[1,*], Akhmad Zamroni[2,5], Decibel V. Faustino-Eslava[2], Eduardo C. Calzeta[2], Cristino L. Tiburan Jr.[3], Yeni Rachmawati[4], and Ronnel C. Nolos[2]

[1]*Physics Education Program, Universitas Negeri Surabaya,* ***Indonesia***
[2]*School of Environmental Science and Management, University of the Philippines, Los Baños, Laguna 4031,* ***Philippines***
[3]*Environmental Remote Sensing and Geo-Information Laboratory, Institute of Renewable Natural Resources, College of Forestry and Natural Resources, University of the Philippines, Los Baños, Laguna 4031,* ***Philippines***
[4]*Early Childhood Education Department, Universitas Pendidikan Indonesia,* ***Indonesia***
[5]*Department of Geological Engineering, Institut Teknologi Nasional Yogyakarta,* ***Indonesia***
[*]Email: nadisuprapto@unesa.ac.id

ABSTRACT - Geohazards are often present in highly populated areas. Dynamic changes in population exposure to geohazards have resulted from shifting population numbers, spatial dispersion, and mobility. In addition, the changing vulnerability distribution of the population is a crucial consideration when establishing an effective evacuation strategy. Therefore, exploring the link between geohazards and population exposure is vital to avert disasters. This paper reviewed geohazards around the world based on a dynamic population approach. It identifies and synthesizes evidence of links between certain parts of the dynamic population and geohazard risk management. The major search engine in this investigation was Google Scholar. "Geohazards", "dynamic population", and keywords related to geohazards like landslides, floods, drought, earthquake, and tsunami were used, followed by terms related to dynamic population. The review shows that geohazards based on a dynamic population approach include socioeconomic status; gender and gender relations; migration, residency, and mobility; education and knowledge; and religions and beliefs. Understanding those elements is essential to managing geohazard risks because it can assist the government in its financial commitment and allocation in the event of a disaster, constructing effective policies and adaptation plans, and including communities in managing geohazard risks.

Keywords: *Geohazards, Dynamic population, Vulnerability, Adaptation, Risk management*

Vol. 42 No 3, page 159 (2023)

1. INTRODUCTION

Geohazards are geological, environmental, geomorphological, and anthropogenic characteristics or actions that may endanger human life, property, or the environment (Dikshit et al., 2021; Hidaayatullaah & Suprapto, 2022). Two main types of geohazards are natural hazards (earthquakes, volcanic eruptions, floods, landslides, and tsunamis) and human-induced hazards (land subsidence consequent to groundwater extraction, water contamination, and atmospheric pollution) (Tomás & Li, 2017). Although geohazards as a topic are extensive due to the numerous potential generators, earthquakes, landslides, floods, droughts, debris flows, and glacial lake eruptions are the six most devastating geohazards (Dikshit et al., 2021). In many cases, geohazards can be triggered and result in disasters with little to no warnings, emphasizing the significance of researching and monitoring the endangered areas for risk management objectives (Pappalardo et al., 2021). Furthermore, some geohazards have high-frequency rates or return periods, particularly large-scale geohazards that also have the potential to impact broader spatial extents. Such geohazards pose higher risks that are difficult to manage are widely spread and pose a higher risk; as a result, the risk is difficult to manage. It is critical and vital to examine geohazard conditions, including their relationship to spatial patterns (the distribution of settlement and socio-economic level) and human activities (Zhang et al., 2012).

Geohazards are often present in highly populated areas. The capacity to monitor geohazards from many locations could be an essential tool for determining the degree of hazard and, as a result, for predicting and preventing accidents and deaths (Prasetya et al., 2021). The world's population has exploded in the last two centuries, reaching over 7 billion people in 2011. The increased population has resulted in rapid urbanization and increased land occupation, as well as increased demand for primary resources (water, food, electricity, building materials, etc.), as well as increased anthropogenic impact on the environment (industries, traffic, wastes, pollution) (Gutiérrez et al., 2014). Furthermore, due to the tremendous increase in air pollution emissions caused by industrial and economic growth over the previous century, air quality has become a global environmental issue. A growing amount of evidence implies that massive changes occur in our environment, including changes in the atmosphere and temperature. These changes impact the biosphere, human environment, and biodiversity, particularly global warming caused by human activities. Mitigating and reversing the effects of these alterations are significant problems (D'Amato et al., 2015; Suprapto et al., 2022). Human activities supporting industrial and economic growth can also cause waste in the aquatic environment, such as heavy metal pollution (Agarin et al., 2021; Asih et al., 2022; Nolos et al., 2022), increase in turbidity and pH of water that is not suitable for daily needs (Zamroni et al., 2022). In addition, the development of coastal cities will also cause a groundwater deficit and trigger seawater intrusion (Zamroni et al., 2021). For instance, Deschênes and Greenstone (2011) found a statistically significant link between mortality and daily temperatures, with frigid and hot days being linked to higher mortality rates. Only a few studies document regional scale-to-global-scale effects, varying by climate zone, temperature measures, and geographical area. River and coastal floods have also been thoroughly examined in the future. However, these methodologies frequently overlook human vulnerability, reporting the population potentially affected (e.g., individuals living in flooded areas) without stating the fraction of people who could die. The lack of robust vulnerability models based on observation-driven statistics makes estimating human consequences difficult (Forzieri et al., 2017).

Risk reduction and natural hazards research explains the relationship between demographics and natural hazard risk management. Most articles, however, have emphasized cities in recent years, focusing on links between rising settlements and hazard exposure following the global urbanization trend. Despite the evident reality that urban and rural areas are vulnerable in different ways, areas experiencing population decrease and shrinking are frequently overlooked (Clar, 2019). The changing vulnerability distribution of the population is a crucial consideration when establishing an effective evacuation strategy. Many factors can influence population susceptibility, including population density, age, race, health, and other related aspects. Population density significantly impacts area vulnerability of all these factors, as more powerful concentrations of people mean more difficult evacuation. An evacuation plan's dynamic population density distribution should be given greater attention because it incorporates specific population characteristics such as the elderly, children, and the unemployed (Zhang et al., 2013). For evaluating and mapping communities' risk to geohazards, the calculation of social vulnerability is essential, with population exposure being one of the most critical factors and pre-assessment requisites. Although a quantitative assessment of geohazard risk is required to enable spatial planning and local governments to provide population protection, more work has gone into understanding geohazards than calculating possible impacts on people and infrastructure. As a result, the first stage in geohazard preparedness is identifying and mapping population concentrations (Freire et al., 2013). Dynamic changes in population exposure to geohazards resulted from shifting population numbers, spatial dispersion, and mobility. Therefore, exploring the link between geohazards and population exposure is crucial (Zhang et al., 2018). This paper reviewed geohazards around the world based on a dynamic population approach. It identifies and synthesizes evidence of links between certain parts of the dynamic population and geohazard risk management. Specifically, this review paper aims to answer the following questions:

1. What elements of the dynamic population are linked to managing geohazard risks?
2. How are the links between certain parts of the dynamic population and geohazard risk management?

2. RESEARCH METHOD

The major search engine in this investigation was Google Scholar (GS), which can provide access to a recognizable corpus of academic literature and so is a better tool for the objectives of this study than Scopus or Web of Science (WoS) (Nguyen et al., 2019). GS covers most subjects, and the findings from Scopus and WoS are relatively similar (Harzing et al., 2016). The library sector has done most of the research on GS as an educational information search tool. The search engine was excellent for an institution, person, journal, or other scholarly communication channels to access 100% of the online knowledge (Martín-Martín et al., 2017). GS indexes individual academic articles from journals and conferences, academic publications, theses and dissertations, abstracts, preprints, technical reports, and other scholarly material from various fields. This search engine is also accessible through a university library, allowing scholars to link to papers in GS using library resources. GS can link other articles that mention a specific theme, connect readers to comparable publications, set up notifications to track publications for research areas and preserve a personalized library of papers (Zientek et al., 2018). It is also a free service for retrieving scholarly journals (Halevi et al., 2017). In addition, a thorough grasp of this case study requires reviewing some initial research (Zamroni et al., 2020).

This investigation also used the keywords technique. It is user-friendly and straightforward, with reasonable retrieval precision, while semantically rich ontology solves the need for complete text retrieval descriptions and improves retrieval precision. Text retrieval, web page retrieval, summarization, text clustering, text mining, and other applications benefit from keyword extraction. Choosing which document to read is simple to learn the relationship between texts by extracting necessary keywords (Poulimenou et al., 2014). The main keywords represent an article's title and indicate that piece's content. It can make finding related publications easier for others, including scholars (Mohaghegh et al., 2018). "Geohazards," "dynamic population," and keywords related to geohazards like landslides, floods, drought, earthquake, and tsunami were used, followed by words related to dynamic population like demographic, socioeconomic, residency, migration, mobility, gender, gender relations, knowledge, education, religion, and beliefs. The kinds of literature used are only currently available (2011 to 2022). The authors sought a thorough search of data using these keywords, considering all study aspects. To exclude unnecessary records, publication titles, and abstracts were checked. Reading abstracts to comprehend the main idea of the previous study has been conducted to select references. It is essential to read the complete text to add more understanding (Suprapto et al., 2017).

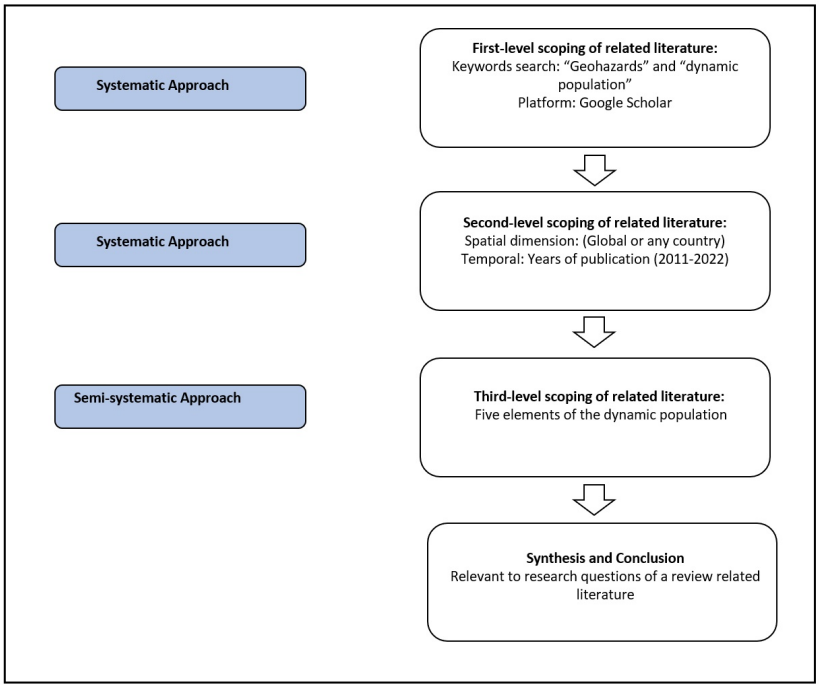

Figure 1. The methodological framework of the study

Figure 1 shows the methodological framework for this literature review, adopted from Snyder (2019). A systematic review approach aims to synthesize and compare literature

evidence. This step is focused on the keywords search "geohazards" and "dynamic population" in the first-level scoping and the Spatio-temporal dimension in the second level.

Meanwhile, a semi-systematic review approach aims to overview the research area and track development over time. In this step, the authors focus on five elements of the dynamic population. The last stage is to conclude that it is relevant to research questions of review-related literature.

3. FINDINGS

3.1 Geohazards based on a dynamic population approach

According to Clar (2019), the dynamic population discussion includes “socioeconomic status; gender and gender relations; migration, residency, and mobility; education and knowledge; and religions and beliefs”. These elements will be linked to the management of geohazard risks.

1. Socioeconomic status

Only two of the factors of vulnerability are society and the economy. Social vulnerability is a complicated and dynamic concept that changes through time and geography, making it difficult to represent with a single variable. It depicts the multidimensionality of catastrophes by emphasizing the entirety of interactions in each social scenario, which, when combined with environmental forces like geohazards, result in a disaster. The economic dimension of vulnerability is the propensity for financial loss due to physical asset destruction and business interruption (services, activities, or delivery of products). Another crucial factor to consider is the relationship between economic and social components (Contreras et al., 2020). Socioeconomic factors such as population characteristics, industrial structure, and spatial dispersion influenced geohazards (Ding et al., 2020). There is no indication of a link between disaster effects, such as the number of fatalities or the impacted population, and Gross Domestic Product (GDP) growth. Nonetheless, it suggests that the extent of damage caused by a disaster will harm GDP growth. As a result, it is critical to combine the number of injuries and fatalities with the financial loss caused by a disaster (Contreras et al., 2020). Within the exposure index, land use and regional development inequalities are compatible with the spatial characteristics of population density in the presence of socioeconomic change. From the municipal and commercial building standpoint, a high population density signifies a dynamic economy and accelerated urban growth, leading to centralized disaster threats. As a result, regional vulnerability may increase. Hazards are not just a natural process; they also impact the distribution of economic resources. Government support becomes the principal source of resilience when a community's ability to cope with geohazards is insufficient. In such cases, the government's financial investment and allocation will directly impact the tenacity of personnel and assets regarding relief assistance, which might improve authorities' emergency response capacity regarding public health care and expertise. As a result, to meet a significant need for help, the amount of government funding available has become extremely important (Gao et al., 2021). Geohazards frequently result in fatalities and significant economic losses. Disaster risk reduction and societal resilience, and emergency response capability are concerns that must be addressed. The rapid expansion of society has accelerated environmental changes, which has increased the potential for natural disaster harm. As a result,

academics are increasingly paying attention to social vulnerability (Miao & Ding, 2015). Communities' socioeconomic situation should be one factor examined while evaluating disaster management plans. Floods, for example, are inextricably tied to socioeconomic vulnerability. Flood damage to structures is more common among high-income people than low-income people. Lower-income people, on the other hand, have disproportionately higher death rates. Multiple vulnerability studies show that marginalized people cannot protect themselves from floods, return home or work after a flood, and access social safety nets before and after a disaster. Obtaining flood insurance modulates adaptive capacity and sensitivity, while mandated flood insurance is directly linked to exposure. Policy reforms to the national flood insurance program disproportionately affect low-income and minority groups (i.e., vulnerable populations) and have the potential to exacerbate pre-existing vulnerabilities (Frazier et al., 2020). In Bangladesh, middle-income families were more likely to migrate due to their awareness of disaster hazards. Although poorer village members migrate for income rather than safety, some from the unskilled and the better educated seek opportunities abroad, such as in India (Penning-Rowsell et al., 2013). However, several governments have given this subject significant thought. For example, Iran's disaster management system has seen significant advancements recently. Several laws and regulations have been passed at various levels, some of which are related to the socioeconomic aspects of disaster risk reduction. For instance, "the national Constitution was approved in 1979 and revised ten years later (Government of Iran, 1979, 1989). Articles 29 and 31 refer to the right to welfare and decent housing, respectively. These provisions refer implicitly to the government's responsibility to assist the population when disasters damage housing and render people destitute. Despite their importance to national life, the Constitution does not refer directly to disasters" (Amini Hosseini et al., 2013).

As a result, the influence of human activities on regional geohazards must not be overlooked. To continue rapid socioeconomic development in the future, it must adhere to a development strategy that places equal emphasis on development and preservation. As feasible, land development and use should avoid locations with a high risk of geohazards. Prohibited development zones should be developed in areas that meet various combination characteristics to safeguard the ecological environment, avoid increasing regional environmental deterioration, and induce geological risks. Ecological restorations are also necessary for locations with a significant danger of geological disasters to repair and rebuild regional ecosystem stability (Lin et al., 2021). Furthermore, comprehensive stabilization is not possible. In that case, installing monitoring and early warning systems in hazard zones, particularly for locations vulnerable to large-scale instabilities or inhabited regions, could be a solution. It is critical to have a broad understanding of the physical and socioeconomic circumstances of the target area while designing such systems. The relevant laws, rules, and organizational arrangements for decreasing geohazard consequences must also be addressed based on local socioeconomic situations, and appropriate risk reduction strategies should be offered accordingly. The results of these efforts can be reflected in master, comprehensive, and implementation plans that regional planners can employ in land-use planning (Amini Hossein & Ghayamghamian, 2012). The management of geohazards requires socioeconomic views. From a socioeconomic standpoint, the following factors can be considered throughout the post-earthquake recovery and reconstruction process: (1) the earthquake-stricken area's industrial and employment structures' compatibility and adaptation, and (2) the rate of economic development in the earthquake-stricken area. The employment structure represents the allocation and usage of regional labor resources, a significant determinant of macroeconomic

development and growth (Liu et al., 2020).

2. Gender and gender relations

In the context of geohazards, gender, and vulnerability are crucial considerations. Natural catastrophes affect men and women differently around the world. Men's and women's adaptable capacity is governed by their access to capital assets and livelihood activities, and gender influences disaster adaptation. Examples are physical disparities, gendered societal roles and relationships, the domestic environment, and employment (Naz & Saqib, 2021). In this scenario, gender may play a function similar to that played while dealing with hazards. Women appeared more confident in recognizing the geohazards' local impact, like the broader tendency to be more concerned about risk's negative implications (Gioia et al., 2021). However, there is a significant gender disparity in fatality rates in catastrophe situations, with women at higher risk than men. Physical injuries, hunger, infectious diseases, reproductive tract infections, miscarriage, extended psychological stress, chronic weariness, and gender-based violence against women are all factors that contribute to high rates of death and morbidity among women (Fatouros & Capetola, 2021).

On the one hand, several quantitative and qualitative research in risk perception revealed that gender disparities in risk perception might differ among various risks. Males, for example, maybe more concerned about health and safety hazards, physical aggression, and industrial accidents. In contrast, females may be more concerned about environmental hazards, sexual assault, overexertion injuries, and infectious infections. On the other hand, several studies have consistently shown that females have higher risk perceptions than males in various environmental and occupational risks (Kung & Chen, 2012).

Gender-based inequalities in time usage (concerning housework, employment, and care activities), varied access to assets and credit, and limited access to policymaking venues can all affect vulnerability to natural disasters (Strambo et al., 2021). According to previous studies, women are far more vulnerable to disasters than men, and women are always regarded as the worst victims, making them the most vulnerable group in society (Paul & Routray, 2011). The gender and age of the household head are particularly linked to non-land loss during natural disasters. Given that only 2% of household heads are female, the link between gender and environmental risks may not be substantial. According to the findings, female-headed households and homes with older heads have a more significant risk of experiencing loss than male-headed households and households with younger leaders. This finding is consistent with prior research showing that women in the Indian Sundarban are more exposed to the adverse effects of natural disasters because they have fewer options for livelihood, earn lower earnings, and have less control over their income and assets (Hajra et al., 2017). Women are disproportionately affected by natural catastrophes in communities where "women and girls have less access to and control over resources".

On the other hand, men are less likely to evacuate because they believe they can effectively guard their homes, putting them at risk. This may also be true for women responsible for the household and children, particularly in developing nations. In addition, there is a strong link between the female gender and fragility, owing to the more significant percentage of females living to be old. Females also have a more robust risk perception and readiness to act than males (Werg et al., 2013). Female survivors also reported more anxieties and threats to their lives and more financial loss than male survivors.

According to the risk-as-feelings theory, the results could indicate the effect of the "early-warning/experiential" system, which translated unclear and frightening components of the environment into affective reactions. Survivors affected by earthquakes were more sensitive to the risk of earthquakes and hence expressed increased sensitivity to earthquakes and their harmful effects (Hidaayatullaah & Suprapto, 2022; Kung & Chen, 2012).

Women in developing nations like Bangladesh are frequently involved in occupations that rely on natural resources. These jobs do not generate consistent and steady income. Inequitable rights to and access to land, resources, and capital exacerbate this instability. These inequities and marginalization are essential in differential access to resources that cause gender-based vulnerability (Naz & Saqib, 2021). The intersection of gender and disaster is particularly evident in Bangladesh, a country regularly dealing with gender difficulties and various natural disasters. Bangladesh's unique geographic situation of extreme population densities overlaid on a low-lying deltaic and coastal landscape interacts with the country's range of environmental and social transitions: issues of democracy, rural-urban divides, poverty, government corruption, and gender equality, as well as problems related to multi-hazard risk, looming effects of climate change, and environmental justice, all of which predispose specific demographics to heightened levels of vulnerability. As a result, the confluence of gender and natural disasters is a rich resource for practical and academic study. It provides a space where these transformations coexist, producing and revealing vulnerability (Juran & Trivedi, 2015).

3. Migration, residency, and mobility

Land abandonment and island nation loss, large-scale population movement, and sweeping changes in cultural traditions are all possible human reactions to the current geohazard circumstances that are already driving environmental change around the planet (Knight et al., 2012). Population displacement is difficult to describe, whether permanent or temporary, domestic or international, forced or voluntary. The reasons for migration vary widely, making it difficult to pinpoint the core causes of population shifts (Mallick & Vogt, 2014). In a broader sense, the five drivers of migration are concerned with the impact of environmental change on human movement. Demographic, political, economic, social, and environmental forces are five drivers that influence migration decisions. Employment possibilities and wage disparities between locations are two economic factors. The number and structure of populations in source areas and the incidence of diseases that affect mortality and morbidity are all demographic factors. Family or cultural expectations, the hunt for educational options, and cultural rituals such as inheritance or marriage are all examples of social drives. Exposure to geohazards and the availability of ecosystem services are two environmental drivers of migration. These five drivers rarely operate in isolation, and movement specifics are determined by their interaction. These drivers apply to both international and domestic migration, emphasizing the importance of human agency in migration decisions, particularly the interaction between family and household characteristics on the one hand and movement barriers and facilitators on the other, in translating drivers into actions (Islam et al., 2016). Female-headed families had more excellent migration rates than male-headed households. According to educational background, there were also differences in rates, with better-educated households sending family members to the next town for temporary shelter. They explain this by saying that more educated people can better comprehend weather forecasts (Penning-Rowsell et al., 2013). While seasonal migration is an adaptation technique in rural regions, more extensive and planned migrations of entire cities necessitate far more resources

which would exceed cities' and communities' capacities. As a result, the role of political and administrative units in adaptation and funding must be addressed. Although migration and relocation are divisive adaptation techniques that frequently cause conflict, the forecast for climate change consequences, such as sea-level rise in the Mekong Delta, Vietnam, suggests that planned movement may become unavoidable (Birkmann, 2011). Understanding mobility characteristics is essential for developing policies and effective adaptation plans. People relocate for several reasons: work, education, religion, and environmental concerns. There is no commonly accepted definition for human movements triggered by climate-related dangers. It refers to population mobility caused by abrupt or gradual changes in weather or climate, especially those caused by geological disasters caused by extreme weather occurrences. The literature uses terms like migration, displacement, and planned relocation (Tan et al., 2022). Each evacuee's coping capacity must be considered. People with high mobility and adequate coping capacity can rescue themselves by picking an appropriate shelter or following the proper evacuation route. Others may perish as a result of the geohazards.

Furthermore, people's mobility is discovered to be significantly related to their age. The elderly had poorer mobility and a negative perception of their health. Because people only sometimes react immediately when they become aware of an emergency, a speedy emergency response is typically determined by age. Because either communicating with neighbors to check a scenario or bringing family members may impair evacuation efficiency, flight behavior is considered. Decisions about which exit to use define evacuation routes and impact evacuation efficiency (Zhang & Zhang, 2014). Transportation network closures during and after geohazard occurrences can significantly impact citizens' mobility and access to essential services. Flooding, for example, can damage the road network and restrict people's movement, including their ability to obtain healthcare services. Other infrastructure failures, such as the collapse of a healthcare facility's infrastructure (e.g., lack of water and electricity), can also play a role. As a result, having a functioning infrastructure network following a geohazard incident is critical (Balomenos et al., 2019).

One of the most challenging difficulties in geohazard-affected areas is population outflow. Population exodus makes it harder to revitalize disaster-affected towns and local economies, leading to a vicious cycle of more population outflow (Kawawaki, 2018). It is critical to have an effective warning system for tsunami-prone areas to alert residents in vulnerable coastal areas to evacuate to designated safe zones at higher elevations (Lin et al., 2014). Previous analyses of population migration resulting from the Great East Japan Earthquake and Tsunami of 2011 captured the scale of population movement that crosses municipal boundaries; however, these macro-level analyses lack information on migration factors such as why residents chose to relocate, which is critical information for the development of recovery policy. On the other hand, completing an individual data analysis is difficult due to the difficulty of organizing adequate surveys that capture information from catastrophe victims who are dispersed over multiple locations after the event. In some nations, such as Indonesia, the extent of tsunami destruction boosted mobility rates in Sumatra across socioeconomic and demographic lines. Still, seismic shocks and volcanic eruptions lowered migration rates and, in the long term, improved the livelihood of local populations (Kawawaki, 2018). Another issue that may arise due to population migration is the increase in construction activities (both residential and common-use infrastructure), which may exacerbate geohazards such as landslides. One of the essential issues in terms of water demand and drought effects in recent decades is the change in rainfall regime

owing to cloud seeding, which may lead to increased precipitation. Unfortunately, the cloud seeding strategy is solely focused on regional water shortages; yet, due to a lack of attention to systematic studies that include landslide hazard evaluation, it may cause irreversible damages in landslide-prone areas (Alimohammadlou et al., 2013).

To assist the millions of people who may be displaced, risk management measures are required. Stakeholders should assist communities in geohazard-prone locations that leave their original site, where geohazards occur regularly and are significant safety threats. They should help with the transition to the new resettlement, which has a high-quality and comprehensive security management system, including full coverage of electronic equipment and daily security patrols, increasing safety (Pan et al., 2021). There are limits to accommodating such dangers, and structural protective measures (such as levees) come with significant maintenance costs, environmental damage, and increased development in risky areas (Hino et al., 2017). In addition, proper land-use rules must also limit urban expansion in zones indicated as potentially vulnerable by the catastrophe assessment research, which may put segments of the population in danger. Additionally, government agencies must establish evacuation plans, post warning signs, and provide clear instructions to the public. Property and business owners could be informed on voluntary measures they can take to preserve their investments if they are in high-risk locations (Pararas-Carayannis, 2021).

4. Education and knowledge

Risk communication relied heavily on public awareness and knowledge of geological hazards (Pan, 2016). Education, especially for local communities around disaster areas, is essential given by the relevant institutions (Rachmawati & Zamroni, 2020). Education programs should be prioritized to encourage a shift in citizens' and authorities' perceptions of the threats posed by significant geohazards and help realize the issues these hazards offer to society. Disseminating geohazard information to appropriate governmental agencies and residents would enable transparent decisions on what to build and how to build it, and were to lessen the vulnerability of existing structures to future disasters (Plag, 2014). Furthermore, properly and quickly transmitting and disseminating warnings and instructive information demands the mass media's commitment and active engagement. Although tremendous success has been achieved in integrating the media in such collaborative efforts, much more needs to be done to improve public awareness of geohazards and maintain long-term civil preparation programs (Pararas-Carayannis, 2014). A unique understanding of geohazards may provide valuable information about people's readiness to adopt preventive measures and identify the critical reasons for present disaster management systems' poor performance levels. To fully comprehend and handle hazard risks, it is vital to investigate the causes of such events by looking at the built environment's susceptibility and how such causes are viewed (Roder et al., 2016).

Education levels are crucial indicators of citizens' income, quality of life, career prospects, and other factors. Education accounts for 20% of the entire variation in social risk. A society's average educational level can reveal its development potential. More education translates to a better ability to respond to, cope with, and recover from natural disasters (Chen et al., 2013). It means that the higher one's level of knowledge, the easier it is to comprehend and interpret early warning and evacuation decisions (Ainuddin & Routray, 2012). Furthermore, lesser levels of expertise may compromise the ability to understand warnings and gain access to recovery information (Martins & Cabral, 2012). If 60% of the population has completed high school or

higher, they may be more prepared to deal with earthquakes (Ainuddin & Routray, 2012). The impact of educational level on the scientific explanation of what an earthquake was most significant in Turkey. The highest level of education was linked to increased knowledge about earthquake risk, followed by the home's location (Tekeli-Yeşil et al., 2011). According to a study conducted in Pakistan, populations with higher educational levels have a more remarkable ability to return to their everyday lifestyles following an earthquake than communities with lower academic levels. People's earthquake education is weak, and most respondents had no idea what to do during and after an earthquake. Most people are still uninformed of the risks associated with potential seismic hazards in the area due to a lack of awareness campaigns, resulting in low community resilience (Ainuddin and Routray, 2012). Furthermore, research in Bangladesh found that higher-educated households had sent family members to a safer location to take temporary shelter in a disaster in their neighborhood. According to this study, the better one's educational level, the greater one's capacity to interpret weather forecasts, save money, and store preventative food, reducing disaster risk (Paul & Routray, 2011).

5. Religion and beliefs

Religious beliefs may influence how people react to geohazards and how they deal with the repercussions. For example, if people perceive threats as "acts of God," it may be easier to bear losses and more challenging to implement adequate preventive measures. However, religiously based place connection influences risk management behavior far less (or not at all) than economic or social factors (Clar, 2019). Religion strongly influences whether people will prepare for disasters. According to a recent study, those with religious views are more likely to qualify for calamities (Bian et al., 2021). Religious beliefs can influence how people perceive disaster risk and how they react to disasters and recover. Studies on the role of religion in disasters have increased in recent years, from a topic of relatively little scholarly interest. According to studies on religion and disasters, religious beliefs can influence how people respond to disasters, how they feel and interpret risk, and how they influence resilience and vulnerability while meeting hazards and suffering disasters (Holmgaard, 2019). Natural disasters are viewed as God's punishment in religious doctrines, particularly in Judaism, Christianity, and Islam. Because of human sin, Islamic leaders frequently say that tragedy is God's punishment. They are referring to a tale in the Holy Qur'an about a non-believer being punished by God through a natural disaster. Many accounts in the Holy Qur'an claim that God punished humanity for rebelling against Him. On the other hand, many verses in the Holy Qur'an advise people to make emergency preparations. "O you who have believed, strive and endure and remain stationed and dread Allah so you may be successful," says Qur'an (Ali 'Imran) 3: 200. Qur'an (An'aam) 6:131 and (Al-Hasyr) 59:18 highlight another requirement for preparation. These passages can be construed to mean that those in catastrophe-prone locations must be ready for disaster (Adiyoso & Kanegae, 2015).

People in underdeveloped countries assess threats based on their cultural and religious beliefs rather than current science. In Indonesia, the belief that God's punishment for human crimes causes natural calamities persists (Adiyoso & Kanegae, 2012). Indonesia is a multicultural and religiously diverse country. Religious and community leaders play critical roles in disaster management in such situations. This is the situation in some parts of Indonesia, where religious or community leaders are the most effective conduits for communication between government scientists or disaster management and the general public. For example, communication has been

more effective through local religious leaders during Sumatra's ongoing Sinabung volcanic crisis However, communication through other community leaders was beneficial during recent problems at the Merapi and Kelud volcanoes in Java (Andreastuti et al., 2017).

Furthermore, because Aceh is an Indonesian province that follows Islamic law, understanding tsunamis will help determine the student's perception of tsunami tragedies. The importance of religion in interpreting natural occurrences is demonstrated by many school children's answers on the cause of tsunamis in schools. The concept that God's retribution causes disasters should be carefully considered while designing disaster risk reduction materials in a country where most Moslems live, such as Indonesia. However, if people are willing to take sufficient precautions, such beliefs will have little impact on successful catastrophe risk reduction. It is critical to build catastrophe knowledge based on religious ideas (Adiyoso & Kanegae, 2012). As a result, religious teaching is one of the most successful ways to communicate a message. It can be an effective risk communication method after and before a disaster (Adiyoso & Kanegae, 2015).

In November 2013, 21 bishops from Manila's Catholic ecclesiastical province wrote to the president to express their opposition to the plans for additional reclamation of Manila Bay. The letter lays out their case's scientific, legal, and moral arguments. First, the bishops mention two consultant geologists who found that the Manila Bay Reclamation Project will bring geological risks and raise the risk of storm surges and liquefaction during earthquakes in their project analysis. Second, they oppose the idea on legal grounds, claiming that a Presidential Proclamation prohibits commercial or residential usage of the Manila Bay area. Third, they claim that Manila Bay is located inside the region of internationally significant wetlands, making it the state's responsibility to protect it from sale or settlement. This synthesis of scientific, legal, and moral foundations with religious teaching exemplifies an epistemic posture that accepts the compatibility of these several modes of reasoning. The legitimate and transparent response of religion to modern science, secular morality, and positive law already includes integrating these grounds (S. Aduna, 2015).

3.2 Links between certain parts of the dynamic population and geohazard risk management

The elements of the dynamic population are essential to the management of geohazard risks. Data on community socioeconomic situations will be critical since it is linked to government help as the primary source of resilience when a community's ability to cope with geohazards is inadequate. The government's financial commitment and allocation will directly impact the tenacity of relief workers and assets, potentially improving authorities' emergency response capabilities in public health care and expertise. As a result, the quantity of government financing available has become vital to addressing a substantial need for assistance. Furthermore, because marginalized people are less able to protect themselves from geohazards, return home or work after a disaster, and access social safety nets before and after a disaster, the socioeconomic situation of communities should be one of the factors examined when evaluating disaster management plans. Understanding mobility characteristics is critical for designing effective policies and adaptation plans. People move for various reasons, including work, education, religion, and environmental concerns. The ability of each evacuee to cope must be considered. People with good mobility and coping skills can save themselves by finding a suitable shelter or following the proper evacuation route. As a result of the geohazards, others may perish.

Communities in geohazard-prone areas should be assisted in abandoning their original location, where geohazards occur frequently and everyday safety dangers are considerable. They should help transfer to the new resettlement, which has a high-quality and comprehensive security management system, including full coverage of electronic equipment and daily security patrols, resulting in increased safety. Because it creates a space where these transitions coexist, producing and disclosing the vulnerability, the intersection of gender and geohazards is a rich resource for practical and academic study. Men's and women's adaptable capacity is governed by their access to capital assets and livelihood activities, and gender influences disaster adaptation. Examples include physical differences, gendered societal roles and connections, employment, and the domestic environment. Levels of education are essential indications of residents' income, quality of life, employment opportunities, and other things. The average educational level of society might reflect its potential for progress. More education means better preparedness to respond to, cope with and recover from natural disasters. It indicates that the more knowledge one has, the easier it is to understand and interpret early warning and evacuation decisions. Lastly, religious beliefs can influence how people respond to catastrophes, how they experience and understand risk, and how religious beliefs exploit resilience and vulnerability when confronted with hazards and disasters. Therefore, religious or community leaders are the most effective conduits for communication between government, scientists, and the general public.

4. CONCLUSIONS

The review shows that geohazards based on a dynamic population approach include socioeconomic status, migration, residency, and mobility; gender and gender relations; education and knowledge; and religions and beliefs. The economic dimension of vulnerability is the propensity for financial loss due to physical asset destruction and business interruption such as services, activities, or product delivery. In contrast, social vulnerability is a complicated and dynamic concept that changes over time and space, making it difficult to represent with a single variable. In a larger sense, the five drivers of migration are concerned with the impact of environmental change on human movement. Five drivers influencing migration decisions are identified: demographic, political, economic, social, and environmental variables. Men's and women's adaptable capacity is governed by their access to capital assets and livelihood activities, and gender influences disaster adaptation. Examples are physical differences, gendered societal roles and connections, employment, and the domestic environment. Levels of education are essential indications of residents' income, quality of life, employment opportunities, and other things. The average educational level of society might reflect its potential for progress. More education means better preparedness to respond to, cope, and recover from natural disasters.

Moreover, religious views can have an impact on how people perceive catastrophe risk, as well as how they respond to and recover from disasters. The management of geohazard risks requires an understanding of those factors. Understanding those factors has several advantages, including

1. assisting the government in its financial commitment and allocation in the event of a disaster,
2. assisting in the construction of effective policies and adaptation plans, and
3. including communities in the management of geohazard risks.

5. ACKNOWLEDGEMENTS

Thanks to Universitas Gadjah Mada for supporting research funding for this study. We also thank Deutscher Akademischer Austauschdienst (DAAD) and Southeast Asian Regional Center for Graduate Study and Research in Agriculture (SEARCA) for giving scholarship funding for one of the authors (Akhmad Zamroni).

6. REFERENCES

Adiyoso, W., & Kanegae, H. (2012). The effect of different disaster education programs on tsunami preparedness among schoolchildren in Aceh, Indonesia. *Disaster Mitigation of Cultural Heritage and Historic Cities*, *6*(1), 165-172.

Adiyoso, W., & Kanegae, H. (2015). The role of Islamic teachings in encouraging people to take tsunami preparedness in Aceh and Yogyakarta Indonesia. In *Recovery from the Indian Ocean Tsunami* (pp. 259-278). Springer, Tokyo.

Agarin, C. J. M., Mascareñas, D. R., Nolos, R., Chan, E., & Senoro, D. B. (2021). Transition metals in freshwater crustaceans, tilapia, and inland water: Hazardous to the population of the small island province. *Toxics, 9*(4), 71.

Ainuddin, S., & Routray, J. K. (2012). Earthquake hazards and community resilience in Baluchistan. *Natural Hazards*, *63*(2), 909-937.

Alimohammadlou, Y., Najafi, A., & Yalcin, A. (2013). Landslide process and impacts: A proposed classification method. *Catena*, *104*, 219-232.

Amini Hosseini, K., & Ghayamghamian, M. R. (2012). A survey of challenges in reducing the impact of geological hazards associated with earthquakes in Iran. *Natural Hazards*, *62*(3), 901-926.

Amini Hosseini, K., Hosseinioon, S., & Pooyan, Z. (2013). An investigation into the socioeconomic aspects of two major earthquakes in Iran. *Disasters*, *37*(3), 516-535.

Andreastuti, S., Budianto, A., & Paripurno, E. T. (2017). Integrating social and physical perspectives of mitigation policy and practice in Indonesia. In *Observing the Volcano World* (pp. 307-320). Springer, Cham.

Asih, A. S., Zamroni, A., Alwi, W., Sagala, S. T., & Putra, A. S. (2022). Assessment of Heavy Metal Concentrations in Seawater in the Coastal Areas around Daerah Istimewa Yogyakarta Province, Indonesia. *The Iraqi Geological Journal*, 14-22.

Balomenos, G. P., Hu, Y., Padgett, J. E., & Shelton, K. (2019). Impact of coastal hazards on residents' spatial accessibility to health services. *Journal of Infrastructure Systems*, *25*(4), 04019028.

Bian, Q., Liang, Y., & Ma, B. (2021). Once Bitten, Twice Shy? Does the Public Adopt More Disaster Preparedness Practices after Experiencing More Disasters?. *Available at SSRN 3978434*.

Birkmann, J. (2011). First-and second-order adaptation to natural hazards and extreme events in the context of climate change. *Natural Hazards*, *58*(2), 811-840.

Chen, W., Cutter, S. L., Emrich, C. T., & Shi, P. (2013). Measuring social vulnerability to natural hazards in the Yangtze River Delta region, China. *International Journal of Disaster Risk Science*, *4*(4), 169-181.

Clar, C. (2019). How demographic developments determine the management of hydrometeorological hazard risks in rural communities: The linkages between demographic and natural hazards research. *Wiley Interdisciplinary Reviews: Water*, *6*(6), e1378.

Contreras, D., Chamorro, A., & Wilkinson, S. (2020). The spatial dimension in the assessment of urban socio-economic vulnerability related to geohazards. *Natural Hazards and Earth System Sciences*, *20*(6), 1663-1687.

D'Amato, G., Holgate, S. T., Pawankar, R., Ledford, D. K., Cecchi, L., Al-Ahmad, M., ... & Annesi-Maesano, I. (2015). Meteorological conditions, climate change, new emerging factors, and asthma and related allergic disorders. A statement of the World Allergy Organization. *World Allergy Organization Journal*, *8*(1), 1-52.

Deschênes, O., & Greenstone, M. (2011). Climate change, mortality, and adaptation: Evidence from annual fluctuations in weather in the US. *American Economic Journal: Applied Economics*, *3*(4), 152-85.

Dikshit, A., Pradhan, B., & Alamri, A. M. (2021). Pathways and challenges of the application of artificial intelligence to geohazards modelling. *Gondwana Research*, *100*, 290-301.

Ding, M., Tang, C., Huang, T., & Gao, Z. (2020). Dynamic vulnerability analysis of mountain settlements exposed to geological hazards: a case study of the upper Min River, China. *Advances in Civil Engineering*, *2020*.

Fatouros, S., & Capetola, T. (2021). International journal of disaster risk reduction examining gendered expectations on women's vulnerability to natural hazards in low to middle income countries: A critical literature review. *International Journal of Disaster Risk Reduction*, 102495.

Forzieri, G., Cescatti, A., e Silva, F. B., & Feyen, L. (2017). Increasing risk over time of weather-related hazards to the European population: a data-driven prognostic study. *The Lancet Planetary Health*, *1*(5), e200-e208.

Frazier, T., Boyden, E. E., & Wood, E. (2020). Socioeconomic implications of national flood insurance policy reform and flood insurance rate map revisions. *Natural Hazards*, *103*(1), 329-346.

Freire, S., Aubrecht, C., & Wegscheider, S. (2013). Advancing tsunami risk assessment by improving spatio-temporal population exposure and evacuation modeling. *Natural Hazards*, *68*(3), 1311-1324.

Gao, Z., Ding, M., Huang, T., & Hu, X. (2021). Geohazard vulnerability assessment in Qiaojia seismic zones, SW China. *International Journal of Disaster Risk Reduction*, *52*, 101928.

Gioia, E., Casareale, C., Colocci, A., Zecchini, F., & Marincioni, F. (2021). Citizens' Perception of Geohazards in Veneto Region (NE Italy) in the Context of Climate Change. *Geosciences*, *11*(10), 424.

Gutiérrez, F., Parise, M., De Waele, J., & Jourde, H. (2014). A review on natural and human-induced geohazards and impacts in karst. *Earth-Science Reviews*, *138*, 61-88.

Hajra, R., Szabo, S., Tessler, Z., Ghosh, T., Matthews, Z., & Foufoula-Georgiou, E. (2017). Unravelling the association between the impact of natural hazards and household poverty: evidence from the Indian Sundarban delta. *Sustainability Science*, *12*(3), 453-464.

Halevi, G., Moed, H., & Bar-Ilan, J. (2017). Suitability of Google Scholar as a source of scientific information and as a source of data for scientific evaluation—Review of the literature. *Journal of Informetrics*, *11*(3), 823-834.

Harzing, A. W., & Alakangas, S. (2016). Google Scholar, Scopus and the Web of Science: a longitudinal and cross-disciplinary comparison. *Scientometrics*, *106*(2), 787-804.

Hidaayatullaah, H. N., & Suprapto, N. (2022). Global Trend of Megathrust Research in The Last Ten Years. *Science of Tsunami Hazards*, *41*(4), 336–351.

Hino, M., Field, C. B., & Mach, K. J. (2017). Managed retreat as a response to natural hazard risk. *Nature Climate Change*, *7*(5), 364-370.

Holmgaard, S. B. (2019). The role of religion in local perceptions of disasters: The case of post-tsunami religious and social change in Samoa. *Environmental Hazards*, *18*(4), 311-325.

Islam, M. R., & Hasan, M. (2016). Climate-induced human displacement: A case study of Cyclone Aila in the south-west coastal region of Bangladesh. *Natural Hazards*, *81*(2), 1051-1071.

Juran, L., & Trivedi, J. (2015). Women, gender norms, and natural disasters in Bangladesh. *Geographical Review*, *105*(4), 601-611.

Kawawaki, Y. (2018). Economic analysis of population migration factors caused by the Great East Japan earthquake and tsunami. *Review of Urban & Regional Development Studies*, *30*(1), 44-65.

Knight, J., & Harrison, S. (2013). The impacts of climate change on terrestrial Earth surface systems. *Nature Climate Change*, *3*(1), 24-29.

Kung, Y. W., & Chen, S. H. (2012). Perception of earthquake risk in Taiwan: Effects of gender and past earthquake experience. *Risk Analysis: An International Journal*, *32*(9), 1535-1546.

Lin, F. C., Sookhanaphibarn, K., Sa-yakanit, V., & Pararas-Carayannis, G. (2014). REMOTE: Reconnaissance & monitoring of tsunami events. *Science of Tsunami Hazards*, *33*(2), 86-111.

Lin, J., Chen, W., Qi, X., & Hou, H. (2021). Risk assessment and its influencing factors analysis of geological hazards in typical mountain environment. *Journal of Cleaner Production*, *309*, 127077.

Liu, B., Han, S., Gong, H., Zhou, Z., & Zhang, D. (2020). Disaster resilience assessment based on the spatial and temporal aggregation effects of earthquake-induced hazards. *Environmental Science and Pollution Research*, *27*(23), 29055-29067.

Mallick, B., & Vogt, J. (2014). Population displacement after cyclone and its consequences: Empirical evidence from coastal Bangladesh. *Natural Hazards*, *73*(2), 191-212.

Martín-Martín, A., Orduña-Malea, E., Harzing, A. W., & López-Cózar, E. D. (2017). Can we use Google Scholar to identify highly-cited documents?. *Journal of Informetrics*, *11*(1), 152-163.

Martins, V. N., & Cabral, P. (2012). Social vulnerability assessment to seismic risk using multicriteria analysis: the case study of Vila Franca do Campo (São Miguel Island, Azores, Portugal). *Natural Hazards*, *62*(2), 385-404.

Miao, C., & Ding, M. (2015). Social vulnerability assessment of geological hazards based on entropy method in Lushan earthquake-stricken area. *Arabian Journal of Geosciences*, *8*(12), 10241-10253.

Mohaghegh, N., Atlasi, R., Alibeik, M. R., Salehi, M., Hojatizadeh, Y., & Bagheri, Z. (2018). The Relationship between Number of Keywords Used in Titles of Articles and Number of Citations to These Articles in Selected Journals Published by Tehran University of Medical Sciences. *Journal of Studies in Library and Information Science*, *9*(22), 17-30.

Naz, F., & Saqib, S. E. (2021). Gender-based differences in flood vulnerability among men and women in the char farming households of Bangladesh. *Natural Hazards*, *106*(1), 655-677.

Nguyen, T. H., Helm, B., Hettiarachchi, H., Caucci, S., & Krebs, P. (2019). The selection of design methods for river water quality monitoring networks: a review. *Environmental Earth Sciences*, *78*(3), 1-17.

Nolos, R. C., Agarin, C. J. M., Domino, M. Y. R., Bonifacio, P. B., Chan, E. B., Mascareñas, D. R., & Senoro, D. B. (2022). Health Risks due to metal concentrations in soil and vegetables from the six municipalities of the Island Province in the Philippines. *International Journal of Environmental Research and Public Health, 19*(3), 1587.

Pan, A. (2016). Study on mobility-disadvantage group'risk perception and coping behaviors of abrupt geological hazards in coastal rural area of China. *Environmental Research*, *148*, 574-581.

Pan, Z., Zhang, Y., Zhou, C., & Zhou, Z. (2021). Effects of individual and community-level environment components on the subjective well-being of poverty alleviation migrants: the case in Guizhou, China. *International Journal of Sustainable Development & World Ecology*, *28*(7), 622-631.

Pappalardo, G., Mineo, S., Carbone, S., Monaco, C., Catalano, D., & Signorello, G. (2021). Preliminary recognition of geohazards at the natural reserve "Lachea Islet and Cyclop Rocks"(Southern Italy). *Sustainability*, *13*(3), 1082.

Pararas-Carayannis, G. (2014). Mass media role in promotion of education, awareness and sustainable preparedness for tsunamis and other marine hazards. *Science of Tsunami Hazards*, *33*(1).

Pararas-Carayannis, G. (2021). Risk assessment of earthquakes, tsunamis and other disasters in China and Taiwan. *Science of Tsunami Hazards*, *40*(4).

Paul, S. K., & Routray, J. K. (2011). Household response to cyclone and induced surge in coastal Bangladesh: coping strategies and explanatory variables. *Natural Hazards*, *57*(2), 477-499.

Penning-Rowsell, E. C., Sultana, P., & Thompson, P. M. (2013). The 'last resort'? Population movement in response to climate-related hazards in Bangladesh. *Environmental Science & Policy*, *27*, S44-S59.

Plag, H. P. (2014). Foreword: Extreme geohazards—A growing threat for a globally interconnected civilization. *Natural Hazards*, *72*(3), 1275-1277.

Poulimenou, S., Stamou, S., Papavlasopoulos, S., & Poulos, M. (2014). Keywords extraction from articles' title for ontological purposes. In *Proceedings of the 2014 international conference on pure mathematics, applied mathematics, computational methods (PMAMCM 2014)* (pp. 120-125).

Prasetya, H. N. E., Aditama, T., Sastrawiguna, G. I., Rizqi, A. F., & Zamroni, A. (2021, June). Analytical landslides prone area by using Sentinel-2 Satellite Imagery and geological data in Google Earth Engine (a case study of Cinomati Street, Bantul Regency, Daerah Istimewa Yogyakarta Province, Indonesia). In *IOP Conference Series: Earth and Environmental Science* (Vol. 782, No. 2, p. 022025). IOP Publishing.

Rachmawati, Y., & Zamroni, A. (2020). How Indonesian Governments Care for Local People's Education in the Mining Area: Experiences from other Countries. *Psychology and Education*, *57*(9), 5924-5934.

Roder, G., Ruljigaljig, T., Lin, C. W., & Tarolli, P. (2016). Natural hazards knowledge and risk perception of Wujie indigenous community in Taiwan. *Natural Hazards*, *81*(1), 641-662.

S. Aduna, D. P. (2015). The reconciliation of religious and secular reasons as a form of epistemic openness: Insights from examples in the Philippines. *The Heythrop Journal*, *56*(3), 441-453.

Snyder, H. (2019). Literature review as a research methodology: An overview and guidelines. *Journal of Business Research*, *104*, 333-339.

Strambo, C., Jahović, B., & Segnestam, L. (2021). Climate change and natural hazards in Bosnia and Herzegovina: a gender equality, social equity and poverty reduction lens.

Suprapto, N., Yanti, V. K., & Hariyono, E. (2022). Global research on tsunami education and tsunami mitigation: A bibliometric analysis. *Science of Tsunami Hazards, 41*(2), 130– 148.

Suprapto, N., Zamroni, A., & Yudianto, E. A. (2017). One Decade of the "LUSI" Mud Volcano: Physical, Chemical, and Geological Dimensions. *Chemistry*, *26*(4), 615-629.

Tan, J., Zhou, K., Peng, L., & Lin, L. (2022). The role of social networks in relocation induced by climate-related hazards: an empirical investigation in China. *Climate and Development*, *14*(1), 1-12.

Tekeli-Yeşil, S., Dedeoğlu, N., Braun-Fahrlaender, C., & Tanner, M. (2011). Earthquake awareness and perception of risk among the residents of Istanbul. *Natural Hazards*, *59*(1), 427-446.

Tomás, R., & Li, Z. (2017). Earth observations for geohazards: Present and future challenges. *Remote Sensing*, *9*(3), 194.

Werg, J., Grothmann, T., & Schmidt, P. (2013). Assessing social capacity and vulnerability of private households to natural hazards–integrating psychological and governance factors. *Natural Hazards and Earth System Sciences*, *13*(6), 1613-1628.

Zamroni, A., Kurniati, A. C., & Prasetya, H. N. E. (2020). The assessment of landslides disaster mitigation in Java Island, Indonesia: a review. *Journal of Geoscience, Engineering, Environment, and Technology*, *5*(3), 129-133.

Zamroni, A., Sugarbo, O., Trisnaning, P. T., Sagala, S. T., & Putra, A. S. (2021). Geochemical Approach for Seawater Intrusion Assessment in the Area around Yogyakarta International Airport, Indonesia. *The Iraqi Geological Journal*, 1-11.

Zamroni, A., Trisnaning, P. T., Prasetya, H. N. E., Sagala, S. T., & Putra, A. S. (2022). Geochemical Characteristics and Evaluation of the Groundwater and Surface Water in Limestone Mining Area around Gunungkidul Regency, Indonesia. *The Iraqi Geological Journal*, 189-198.

Zhang, N., Huang, H., Su, B., & Zhang, H. (2013). Population evacuation analysis: considering dynamic population vulnerability distribution and disaster information dissemination. *Natural Hazards*, *69*(3), 1629-1646.

Zhang, J. J., Yue, D. X., Wang, Y. Q., Du, J., Guo, J. J., Ma, J. H., & Meng, X. M. (2012). Spatial pattern analysis of geohazards and human activities in Bailong River Basin. In *Advanced Materials Research* (Vol. 518, pp. 5822-5829). Trans Tech Publications Ltd.

Zhang, A., Wang, J., Jiang, Y., Chen, Y., & Shi, P. (2018). Spatiotemporal changes of hazard intensity-adjusted population exposure to multiple hazards in Tibet during 1982–2015. *International Journal of Disaster Risk Science*, *9*(4), 541-554.

Zhang, S., & Zhang, L. M. (2014). Human vulnerability to quick shallow landslides along road: fleeing process and modeling. *Landslides*, *11*(6), 1115-1129.

Zientek, L. R., Werner, J. M., Campuzano, M. V., & Nimon, K. (2018). The use of Google Scholar for research and research dissemination. *New Horizons in Adult Education and Human Resource Development*, *30*(1), 39-46.

ISSN 8755-6839

SCIENCE OF TSUNAMI HAZARDS

Journal of Tsunami Society International

Volume 42 Number 3 2023

TSUNAMIS, SEISMIC SEICHES, AND UNDETERMINED WAVES ON NEW ZEALAND LAKES, 1846–2022: A NEW DATABASE, AND OVERVIEW.

John Benn
Department of Conservation
Private Bag 4715
Christchurch Mail Centre 8140
New Zealand
Email: jbenn@doc.govt.nz

ABSTRACT

A new database of tsunamis, seismic seiches and undetermined waves (collectively called lake waves) that occurred on New Zealand lakes between1846-2022 has been compiled and summarized. Based on an extensive literature review, photographic and field evidence, the investigation is the first to collate such information on a national scale. It increases the knowledge of a poorly understood natural hazard that has occurred throughout the country and provides a basis for further research.

Seventy-four lake waves were recorded, implying a much higher occurrence frequency than previously considered. Apart from meteorite impact, lake waves have been generated by all known mechanisms, from local to global scale. Eleven tsunamigenic categories were identified. Most (n = 48; 65%) have been associated with seismic shaking, either directly, or with co seismic processes. Lake waves have been recorded in all types of lakes, ranging from the country's largest to some of the smallest; some of the deepest to shallowest, and from the highest-altitude lake to those around sea level. The greatest wave height (c. 10 m), and run-up elevation (c. 20 m above the lake surface), was associated with the May 1992 Maud Lake tsunami. To date, lake waves have caused minimal property damage or personal injury, although the hazard and risk they present is predicted to increase, in association with intensifying lakeside developments and, possibly, with climate-change effects.

***Keywords*:** lakes, lake waves, New Zealand, seismic seiche, tsunami, undetermined waves.

1. INTRODUCTION

New Zealand is prone to all known natural hazards (e.g., Spenden & Crozier 1984; Owens 2001), owing to its position across the active Australian–Pacific tectonic plate boundary, and its maritime location in the South Pacific Ocean (Figure 1). Yet, no research has been undertaken nationally, examining the historic occurrence of tsunamis, seismic seiches, or other undetermined waves (collectively termed lake waves) on the country's lakes, despite there being nearly 4,000 lakes greater than one hectare there being nearly 4,000 lakes greater than one hectare in area, with the eight largest each being greater than 100 km^2 (Schallenberg et al. 2013).

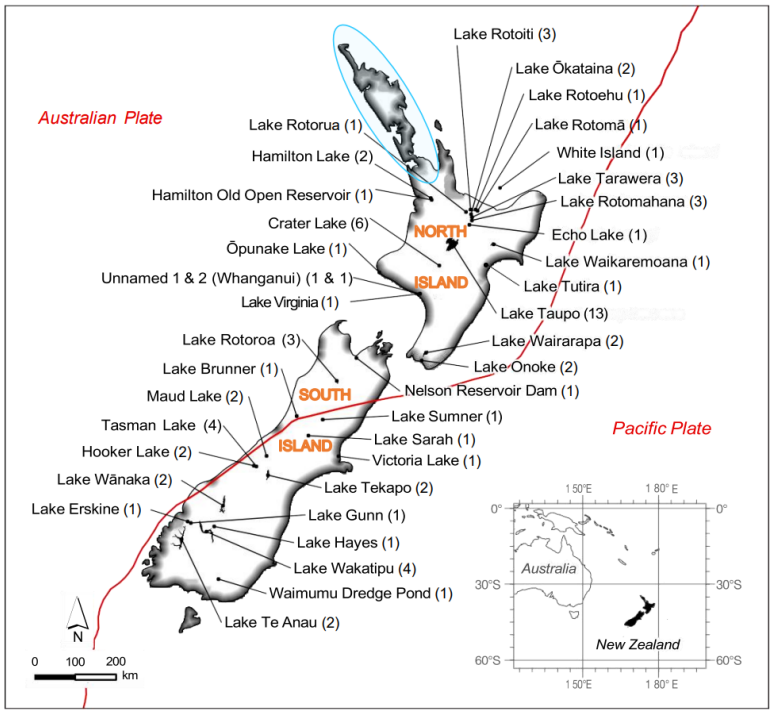

Figure 1. *er of occurrences at each). Red line is the Australian-Pacific tectonic plate boundary. Blue-shaded area shows the Northland and Auckland regions, where no records were found.*

Recent lake wave research has been site-specific and focused on event prediction, based on return-periods of other natural hazards, that could be tsunamigenic (e.g., de Lange et al. 2002; Allen et al. 2009; Clark et al. 2011, Clark et. al 2015; Mackey 2015; de Lange & Moon 2016, Fraser & McMorran 2016; Brambus 2017, Mountjoy et al. 2019; Wang et al. 2020). Regarding historic lake waves, most literature has given them only a passing mention

(excluding those generated by wind-forcing), as it has focused on initial generating mechanisms like seismic shaking (e.g., Hogben 1890; Downes 1995, 2006), or landslides (e.g., Hawley 1984; Hancox et al. 2004), rather than the subsequent lake waves produced. Besides details of four historic lake tsunamis, presented by McSaveney (1992a, b, 1993, 2002), Dykes (2013), and Dykes et al. (2017), most information for such events is found in contemporary newspapers. Contrastingly, research for oceanic tsunamis is extensive and several national databases have been compiled - the most recent being the New Zealand Tsunami Database (Downes et al. 2017; GNS 2023).

To address this knowledge gap, the New Zealand government's Department of Conservation (which administers approximately one third of the country's land area) undertook an investigation to establish baseline information of historic lake waves, including locations, generating mechanisms, wave types, height and run-up elevations, frequency, and damage they have caused to life and property (Benn 2023). This complements predictive modeling and risk analyses recently undertaken by other government and external organizations, as commercial developments, recreation, and tourism activities intensify around many of the country's lake margins. Locations of reported lake waves are shown in Figure 1, with basic details for each event listed in Appendix 1.

2. METHODS

2.1 Information sources

An extensive desktop literature search was undertaken, combined with video/photographic, survey, field, and eye-witness evidence of lake wave occurrence, obtained via communications with others in similar fields of research. The Papers Past website (Papers Past | Newspapers Home (natlib.govt.nz)) provided most information (especially for the period 1846–1930s), as all New Zealand's newspapers have been scanned by the National Library, from each paper's first publication date up until at least 1920, and some major papers, up to the late 1980s. Parliamentary papers/reports/journals, personal letters and diaries, and other historic documents have also been scanned (ongoing and updated regularly). Other information sources included:

a) Earth-science journals,
b) New Zealand Tsunami Database (Downes et al. 2017; GNS 2023),
c) New Zealand Historic Weather Event Catalogue (NIWA 2023),
d) GNS landslide and earthquake reports for specific events,
e) Readily available natural hazard reports (councils and consulting companies),
f) Postgraduate theses,
g) General internet searches,
h) Miscellaneous history books,
i) Personal communications with other New Zealand-based earth scientists.

Words and phrases (and derivatives or combinations of them) such as agitated, disturbance, earthquake, earthquake-wave, landslide (slip/slump/fall), lake (water[s], surface), oscillation, pulsation, ripple, seiche, surge, tidal wave, tsunami, whirlpool, and specific locality names of known, or potential lake wave events, were searched.

2.2 Definitions

Accepted definitions for tsunamis (e.g., Sheppard et al. 1950; CERC 1984; Pararas-Carayannis 2000) and seismic seiches (e.g., Kvale 1955; McGarr 2020) were used. For this investigation, all waves caused by material falling into, or entering lakes and displacing water, were called tsunamis, regardless of the volume of the material involved (e.g., mass movement, small rockfalls). Undetermined waves (or oscillations) were those generated by unidentified processes but were known to have not been generated by wind forcing.

In cases when a generating mechanism like the February 1931 M_S 7.8 Napier earthquake (Downes & Dowrick 2014) produced a series of waves on unconnected lakes, the waves were defined as separate (multiple) lake waves. Conversely, in events such as the May 1992 Mount Fletcher rock avalanche/Maud Glacier ice collapse, which produced a single wave that travelled across multiple, connected lakes, the wave was defined as a single lake wave. In the database (Benn 2023), original reported units of measurement (imperial or metric) were maintained, as were earthquake magnitudes (M_W, M_{WF}, M_L, M_S, etc.) and intensities (MM, R-F) as defined by Downes and Dowrick (2014). Lake types listed in Table 1 are defined by Lowe and Green (1987).

2.3 Validity

For oceanic tsunamis, previous researchers have used a combination of numeric and descriptive methods to rank the validity of occurrence, ranging from the most detailed and reliable, to the vaguest and least reliable reports (e.g., Cox & Morgan 1977; de Lange & Healy 1986; Downes et al. 2017). Based on available evidence, lake wave validity classes for this investigation were defined in descending order as Definite, Probable, and Possible (Table 3, Appendix1). Further analysis may refine these, to align to the five validity classes established by Downes et al. (2017).

3. RESULTS

Seventy-four lake waves have been recorded on 38 lakes throughout New Zealand, between 1846 and 2002 (Figure 1; Appendix 1). Results are summarized in Tables 1–4, below.

Table 1. Lake waves recorded in New Zealand

Lake	Lake Type	Total Number of Waves	Wave Type & Number		
			Tsunami	Seismic Seiche	Undetermined
White Island	Volcanic	1	1		
Rotoroa / Hamilton	Peat	2		2	
Hamilton old open reservoir	Artificial	1		1	
Rotoehu	Volcanic	1	1		
Rotoiti	Volcanic	3	1	2	
Rotomā	Volcanic	1		1	
Rotorua	Volcanic	1		1	
Ōkataina	Volcanic	2		2	
Tarawera	Volcanic	3	1		2
Rotomahana	Volcanic	3	2	1	
Echo	Volcanic	1	1		

Taupo	Volcanic	13	7	4	2
Waikaremoana	Landslide	1		1	
Tūtira	Landslide	1	1		
Crater Lake	Volcanic	6	6		
Ōpunake Lake	Artificial	1	1		
Virginia	Dune	1		1	
Unnamed (1) Whanganui	Dune	1		1	
Unnamed (2) Whanganui	Dune	1		1	
Wairarapa & Onoke	Riverine & Bar	2	2		
Nelson reservoir dam	Artificial	1		1	
Rotoroa	Glacial	3	1		2
Brunner	Glacial	1	1		
Sumner	Glacial	1	1		
Victoria	Artificial	1		1	
Sarah	Glacial	1	1		
Maud & Tekapo	Pro-glacial & Glacial	2	2		
Hooker	Pro-glacial	2	2		
Tasman	Glacial	4	4		
Wānaka	Glacial	2	1	1	
Wakatipu	Glacial	4	1	3	
Erskine	Glacial	1	1		
Gunn	Glacial	1	1		
Hayes	Glacial	1			1
Te Anau	Glacial	2	1		1
Waimumu dredge pond	Artificial	1		1	
Totals		74 (100%)	41 (55%)	25 (34%)	8 (11%)

Notes: 1) Lakes listed from north to south - North Island lakes above red line, South Island lakes below; 2) Connected lakes are listed together, as individual lake wave events have affected the connected lakes simultaneously. Lakes Wairarapa and Onoke are connected via the Ruamahanga River; Maud Lake and Lake Tekapo are connected via the Godley River; 3) Blank spaces = no record.

Table 2. North Island, South Island, and New Zealand sub-totals, from Table 1.

	Wave type and number			
Location	**Tsunami**	**Seismic Seiche**	**Undetermined**	**Total**
North Island	24	18	4	46 (62%)
South Island	17	7	4	28 (38%)
New Zealand	41 (55%)	25 (34%)	8 (11%)	74 (100%)

Table 3. Lake wave association with generating mechanisms. Note that the sum and percentages of waves are greater than 74 and 100%, respectively, as many lake waves were counted more than once, reflecting their association with multiple, simultaneous generating mechanisms.

Lake wave generating mechanism	Number (%) of lake waves associated with generating mechanisms
Seismic shaking	48 (65%)
Mass-movement (sub aerial/subaqueous slides)	18 (24%)
Volcanic/geothermal activity	14 (19%)
Ice-calving/collapse	10 (14%)
Gas-expulsion	6 (8%)
Rainfall	3 (4%)
Avalanche (snow, ice)	3 (4%)
Liquefaction	2 (3%)
Faulting/tilting (lakebed/margins)	1 (1%)
Atmospheric coupling	1 (1%)
Undetermined	6 (8%)

Table 4. Validity of lake wave occurrence.

Validity	Number (%) of lake waves
Definite	48 (65%)
Probable	16 (22%)
Possible	10 (13%)

4. DISCUSSION

4.1 Historic record and validity

It is acknowledged that the list of events recorded may be incomplete and may contain potential inaccuracies, for the following reasons. Many of New Zealand's lakes are remote from populated areas so numerous lake waves may not have been witnessed nor recorded. This concurs with findings by the likes of Kvale (1955), Roberts et al. (2013), and Clark et al. (2015). Similarly, many potential or actual tsunamigenic mechanisms have occurred at night, and again, eyewitness accounts may be absent. Corresponding with a gap of digitized newspapers, comparatively little information was found for the period between the mid-1930s and early 2000s. Searching hard copy newspapers from this digital gap were outside the project's scope, as was searching for lake level data held by numerous organizations, which may have identified more events. However, real-time lake level data for most New Zealand's lakes do not exist, further increasing the possibility of lake waves being undetected. Lake wave research in New Zealand is a relatively recent occurrence, focused on modeling future events rather than documenting those past, so historical information is limited. Also, some records may have been overlooked in the literature search.

Accounts relying solely on historic (especially singular) newspaper reports may not be as accurate as others based on several independent sources of information (Munro & Fowler 2014), so details for some events listed in Tables 1–4 and Appendix 1 may change, as more information is found, and further analysis undertaken. Nonetheless, in similar investigations for oceanic tsunamis, Cox and Morgan (1977), de Lange and Healy (1986), and Downes et al. (2017), noted the importance of historic newspapers as an information source, which holds true for this investigation. Despite the recognized limitations, the events recorded provide a baseline for further research and allow the following initial observations to be made

4.2 Distribution

Seventy-four lake waves have been recorded throughout New Zealand, from White Island's crater lake in the north, to the Waimumu gold-dredge pond in the south. However, no records were found for the Auckland or Northland regions, despite both regions having numerous natural lakes and artificial reservoirs (Figure 1; Table 1). Northland's lack of records is attributed to a possible absence of events and/or observation bias (being sparsely populated), whilst the most likely explanation for Auckland is event absence: Auckland is the most densely populated region in the country, making the probability of observation high, if any events had occurred. Almost two-thirds of lake waves have been recorded from the North Island (n = 46 [62%] in 21 lakes), compared to just over a third (n = 28 [38%] in 17 lakes) for the South Island (Table 2). This is also attributed to observation bias rather than environmental factors, as historically, many North Island lake-margins (such as Lake Taupo, with the highest recorded number of events; n = 13) have had much higher population densities than those of the South Island.

Lake waves have occurred on natural, modified, and artificial lakes, ranging in size from Lake Taupo, New Zealand's largest lake (616 km^2), to some of the smallest, such as Victoria Lake in Christchurch (< 2.0 ha), and in some of the country's deepest lakes, like Lake Te Anau (417 m deep), to some of the shallowest, with several being < 2.0 m deep (e.g., Irwin 1975; Livingston et al. 1986a, b). Lake waves have also occurred in the country's highest altitude lake (Crater Lake, Mount Ruapehu) at c. 2,734 m above sea level (e.g., Allen 1907; *Evening Post* 23 March 1945, p. 6.) and in some of the lowest lying, such as Lake Wairarapa at < 1.0 m above mean sea level (Livingston et al. 1986a).

4.3 Generating mechanisms

Lake waves in New Zealand have been generated by all known mechanisms except for meteorite impact, with eleven categories of tsunamigenic mechanisms identified: In many events, multiple, simultaneous trigger mechanisms were involved (Table 3). Most lake wave events (n = 48; 65%) have been associated with earthquakes, either as a direct consequence of seismic shaking (seismic seiches), or from secondary co seismic effects, like mass-movement, lakebed faulting, and liquefaction (tsunamis). Given New Zealand's high seismicity levels owing to its tectonic position, this result was not unexpected. The lowest earthquake magnitude found to be associated with lake wave generation was M_L 5.3 (1956 and 2022 Taupo tsunami events: Downes & Dowrick 2014; GeoNet 2022), although descriptive accounts for other events suggest it is probable that earthquakes of < M_L 5.3 have generated lake waves. Records show that large-magnitude earthquakes and volcanic eruptions can generate more lake waves over a wider area than other

tsunamigenic mechanisms, which tend to produce an individual wave at a specific site (Figures 2 & 3; Appendix 1). Eighteen lake waves (24%) have been attributed to some form of sub aerial or subaqueous mass-movement (Table 3). However, it is likely at least eight more (11%) were associated with this, in cases where landslides were recorded in the immediate vicinity of a lake wave event, but no reports were found of mass movements directly affecting the lakes. The generating mechanisms for six events (8%) could not be determined.

Geological controls produce broad tsunamigenic variances between the North and South Islands. In the North Island, lake waves have been generated by all mechanisms identified, although those associated with ice-calving/collapse have been restricted to Crater Lake (Mount Ruapehu) - the only North Island lake with a permanent ice field adjacent to it. In the South Island, lake waves have been generated by most mechanisms, except volcanic activity (confined to the North Island) and atmospheric coupling, although the latter remains a possibility.

Lake waves in New Zealand have been generated by local, national, and remote, global-scale mechanisms (Figure 2). As examples, the May 1992 Maud Lake (unofficial, but common name) tsunami was generated by a local event – the Mount Fletcher rock avalanche/Maud Glacier ice-collapse (e.g., McSaveney 2002). On a national scale, Grapes (2000) noted the 1855 Wairarapa earthquake (M_{WF} 8.2, Downes & Dowrick 2014) caused seismic seiching in lakes and rivers between Lake Rotoiti (North Island) and Christchurch (South Island); an approximate range of 690 km (geodesic distance). At a global scale, the 1883 Krakatau eruption (Indonesia) caused a volcano-meteorological (atmospheric) tsunami on Lake Taupo (*The Thames Star* 15 September 1883; de Lange & Healy 1986; Lowe & de Lange 2000), 7, 900 km (geodesic distance) from the source. Similarly, the February 1938, M_W 8.6 Banda Sea earthquake in Indonesia (Okal & Reymond 2003; Cummins et al. 2020), was the apparent source for the seismic seiche reported on Virginia Lake (e.g., *Evening Post* 5 February 1938). Besides these two global-scale examples, all other reported lake waves (97%) were generated by mechanisms originating within New Zealand.

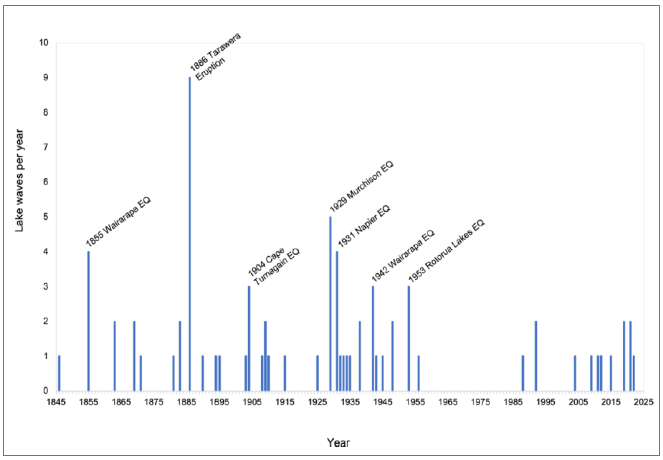

Figure 2. *Lake wave occurrence, 1846–2022 (EQ = Earthquake)*

As illustrated by Figure 2, three or more lake waves generated by earthquakes were recorded. Thetsunamigenic wave generating mechanisms of such earthquakes were dominated by the above listed, large-magnitude geological events, which produced waves on multiple lakes. The 1886 Mount Tarawera eruption is the dominant tsunamigenic event, although this could be misleading, as the 1855 Wairarapa Earthquake most likely generated many more lake waves than the four recorded (see Grapes 2000; Appendix 1). Gaps in the record, especially from the 1930s to early 2000s, correlate with an absence of digitized newspapers, and prior to the early 1900s, many newspapers were not published daily, so some events may not have been reported. Prior to the early/mid 1900's, much of New Zealand was very sparsely populated, making the probability of lake wave observation highly unlikely. The recent cluster of events between 2009–2022, reflects increasing observation, monitoring, and reporting, from several of the South Island's remote glacial and pro-glacial lakes, and the volcanic Lake Taupo in the North Island.

Figure 3. *Hooker Lake tsunami, Southern Alps, New Zealand (looking northwest to the Aroarokaehe Range): 7:00 a.m., October 13, 2021. The tsunami, generated by an avalanche in the Hayter Stream catchment (centre), crossed the 600 m wide lake in approximately two minutes (c ≈ 5.0 m/s or 18 km/h). Time-lapse photograph courtesy of Aubrey Miller (Mountain Research Centre, University of Otago, Dunedin, New Zealand)*

4.4 Wave height and run-up elevation

The greatest lake wave height to have been instrumentally recorded was the c. 3.1 m high tsunami on Tasman Lake, during the February 2011 Tasman Glacier ice-calving event (Dykes 2013; Dykes et al. 2017). However, wave heights presented for the May 1992 Maud Lake tsunami, have ranged from Dore's (1992) estimated > 20 m, to McSaveney's (2002) calculated 10 m (based on valley dimensions and iceberg/debris deposition levels). A tsunami height of c. 10 m appears most credible and comparable to the largest oceanic tsunamis recorded around the New Zealand coast (e.g., de Lange & Healy 1986; Fraser 1998; GNS 2023; NIWA 2023). McSaveney (2002) doubted a tsunami height of > 20 m, noting that icebergs stranded 20 m above the lake represented a combination of wave run-up and iceberg momentum, rather than wave height. If Dore's (1992) estimate were correct, then this would be the highest tsunami (oceanic, lake, or river) recorded during historic times in New Zealand, exceeding the supposed 15 m high landslide-generated tsunami in the Waikari River, during the 1931 Napier (Tait 1977, Donaldson 2016, Donaldson et al. 2019).

Nevertheless, a tsunami run-up height of 20 m above the lake surface is comparable with comparable with modeling results by Clark et al. (2015), and Fraser and McMorran (2016), who calculated tsunami run-up heights of up to 25 m could result from large landslides entering the nearby glacial lakes of Tekapo, Pukaki, and Ohau.

Based on reliable evidence, the 1992 Maud Lake tsunami is most likely the largest terrestrial-based tsunami recorded in New Zealand during historic times, as from its source in Maud Lake, the wave travelled 45 km down the Godley River valley, and discharged c. 7.8 x 10^6 m^3 of water into Lake Tekapo, raising the 87 km^2 lake by c. 90–98 mm (Dore 1992; McSaveney 1993, 2002). At the opposite extreme, detailed surveying by GNS after the small November 2022 Lake Taupo tsunami, showed that relative to the lake's usual high-water mark, the maximum wave run-up elevation was 1.0 m and horizontal inundation distance was 40 m, respectively (GeoNet 2022; Appendix 1).

Reported wave heights for seismic seiches and undetermined waves (mostly based on visual observations), have ranged from as little as c. 12 mm on Victoria Lake (*Christchurch Star* 17 June 1929a, b) in the June 1929 M_S 7.8 Murchison Earthquake (Downes & Dowrick 2014), to 4.5 m at Lake Waikaremoana (*Poverty Bay Herald* 4 February 1931) in the 1931 Napier Earthquake. The upper limit is comparable to modeling results by Wang et. al. (2020), who showed that seismic seiche wave heights in the southern arm of Lake Tekapo during a M_W 8.2 Alpine Fault earthquake could reach c. 4.0 m. Where estimates for seismic seiche and undetermined wave heights are given in Benn (2023), most are less than 2.0 metres.

4.5 Duration

The longest observed period of seismic seiching was on Lake Rotorua, where continuous lake oscillations occurred for just over a month following the June 1886 Mount Tarawera eruption and associated earthquake swarm (Pond & Smith 1886). Another long period of lake oscillating, possibly caused by sub-aqueous mass-movement, occurred continuously for a week in February 1933, on Lake Taupo (e.g., *Auckland Star* 21 February 1933; *Nelson Evening Mail*, 23 February 1933). The longest recorded tsunami durations have been considerably shorter. McSaveney (2002) noted a rapid rise in Lake Tekapo's level from the arrival of Maud Lake tsunami (5.6 h after generation), which then declined exponentially over the next few days. Likewise, almost immediately after the February 2011 Tasman Glacier ice-calving event, Dykes et al. (2017) reported a large, rapid rise in the level of Tasman Lake, which then returned to a lower level around four days after the event (and preceding rainfall input). Where lake wave durations are known, most fall between a few minutes to a few hours (Benn 2023).

4.6 Frequency

It has been generally accepted that lake waves in New Zealand are rare, low-frequency events. When discussing large-scale rock avalanches in the Southern Alps, Hawley (1984) stated: *"A remote, but real possibility exists that one of these may fall into a lake (natural or "Hydro") and create waves of damaging proportions"*. More recently, Clark et al. (2015) stated: *"There have been relatively few reported occurrences of tsunami and seiche waves on lakes in New Zealand, but this is probably due to a short written history (since ~ AD 1840), rather than a real absence of record"*. Similar statements by Painter (2004), Clark et al. (2011), Ward et al. (2015),

Mackey (2015), Dykes et al. (2017), and Mountjoy et al. (2019) are challenged here, as 74 lake waves over a 176-year period shows their occurrence in New Zealand has been far more frequent than previously considered. For example, the New Zealand Tsunami Database (GNS 2023) lists 128 tsunami events but only six of those are lake tsunamis.

Figure 2 shows the historic frequency distribution of lake wave occurrence. The frequency of tsunamis, especially in the South Island's glacial lakes, could increase in the future with predicted climate change increasing the frequency of landslides, avalanches, and ice-calving events around lake margins in the Southern Alps, as glaciers rapidly retreat. Warren and Kirkbride (1998) examined ice-contact lakes in the Southern Alps, noting that climate change had altered glacier behavior, which in turn, initiated ice-calving events. McSaveney (2002) reported on rock falls and rock avalanches in the Southern Alps, noting that over centuries, climatic warming and glacier-thinning had unloaded the toes of some exceptionally steep slopes, which had likely increased the frequency of catastrophic rock collapses (albeit, a small increase), and that: *"Glacier recession, however, has increased the number of lakes in the Southern Alps, and heightened the risk of down-stream flooding"*. However, Allen et al. (2011) examined possible climate change impacts on rock avalanches and other landslides in the Southern Alps and concluded that it was not yet possible to distinguish the influence of atmospheric warming from the *"… simultaneous effects of weather, erosion, seismicity, and uplift along an active plate margin"*.

4.7 Personal injury and near misses

The only reported case of personal injury caused by lake waves, was in the August 1904 Lake Rotomahana seismic seiche (M_S 6.8 Cape Turnagain earthquake, Downes & Dowrick 2014), where a tour-boat guide badly injured his hand as he tried to hold a boat against the jetty whilst the lake was seiching (*Poverty Bay Herald* 17 August 1904; Downes 2006). Nonetheless, there have been several cases of people being swept away or knocked over by lake waves, or they have been in small watercraft when waves struck. Examples include an unnamed lake at Whanganui (January 1855), Lake Wakatipu (April 1871), Lake Tarawera (June 1886), Waimumu dredge pond (March 1909), Lake Taupo (March 1910; March 1956), Lake Brunner (June 1929), Lake Waikaremoana (February 1931), Lake Wairarapa (June 1942), Echo Lake (May 1948), Lake Te Anau (June 1988), and Tasman Lake (February 2011).

4.8 Property and structural damage

Lake waves have caused minimal damage to private property or public infrastructure, primarily because most of the major events have occurred in both sparsely populated, and sparsely developed locations, at the time of occurrence. The most significant structural damage recorded, occurred near the outlet of Lake Rotoroa (South Island) during the 1929 Murchison earthquake, where a tsunami destroyed both the Gowan River bridge and lakeside jetty, and severely damaged the Lake Rotoroa Hotel (e.g., *Nelson Evening Mail* 19 June 1929). Lesser damage has included the washing-out of small sections of the vehicle access route to Godley Hut during the May 1992 Maud Lake tsunami (McSaveney 2002). On several occasions, small watercraft have been washed away from boatsheds, jetties, and moorings, as at Lake Tarawera (June 1886), Lake Taupo (March 1910, November 2022), Lake Sumner (March 1929), Lake Brunner (June 1929), Lake Waikaremoana (February 1931), and Lake Te Anau (June 1988).

4.9 Environmental damage

The most significant environmental damage caused by a lake wave, was around the margins of Maud Lake and in the Godley River valley during the May 1992 Maud Lake tsunami. Dore (1992) and McSaveney (1992a, b; 1993, 2002) described masses of ice and debris being deposited up to 20 m above the lake and widespread severe scouring of vegetation and sediment from the Godley River valley, many kilometers downstream of Maud Lake. The November 2022 Lake Taupo tsunami caused shoreline erosion (undercutting) at several localities around the lakeshore and deposited silt, pumice, and driftwood, up to 40 m inland from the from the lake's normal high-water level (GeoNet 2022).

5. CONCLUSION

The most comprehensive database of historic lake waves in New Zealand has now been compiled, which has helped improve the understanding of these natural hazards. Furthermore, a baseline for further historical research has been established. Major findings were that lake waves have occurred at a much higher frequency than previously considered and have been generated by all known mechanisms (except meteorite impact); most being generated by, or associated with, seismic shaking. Lake wave magnitudes have ranged from barely detectable to catastrophic, and although lake waves have caused minimal damage historically, the hazard and risk they pose are expected to increase, with intensifying lakeside development and climate change effects. These findings, in conjunction with further research, may have implications for future lakeside planning and management.

ACKNOWLEDGEMENTS

Thanks are extended to the following contributors. The Department of Conservation (Eastern South Island Region, Christchurch) funded the project. Don Neale and Marie-Louise Grandiek (Department of Conservation) and two anonymous reviewers offered constructive comments on the draft manuscript. Aubrey Miller (Mountain Research Centre, University of Otago, Dunedin) provided the photograph of the 2021 Hooker Lake tsunami (Figure 3).

REFERENCES

Allen, G.F. 1907: Ruapehu and the other mountains of the Tongariro group. In: *Evening Star, 25 May 1907*: 11.

Allen, S.K.; Schneider, D.; Owens, I.F. 2009: First approaches towards modelling glacial hazards in the Mount Cook region of New Zealand's Southern Alps. *Natural Hazards and Earth System Sciences 9*: 481–499.

Allen, S.K.; Cox, S.C.; Owens I.F. 2011: Rock avalanches and other landslides in the central Southern Alps of New Zealand: a regional study considering possible climate change impacts. *Landslides 8*: 33–48.

Auckland Star. 1933: *"Bosom Throbs"*. Lake Taupo waters. Strange movement ceases. Level rose every 4 minutes. *Auckland Star*, *21 February 1933*: 8.

Benn, J.L. 2023. Tsunamis, seismic seiches and undetermined wave events on New Zealand lakes, 1846-2022: a review. New Zealand Government. Department of Conservation, Wellington, New Zealand. *Science for Conservation 338*. 55 p. https://www.doc.govt.nz/globalassets/documents/science-and-technical/sfc338entire.pdf

Brambus, O. 2017: The analysis of glacial retreat of selected mountain regions of New Zealand and natural hazards from GLOFs. Diploma thesis (Geography and Geoecology). Charles University. Prague. 146 p.

CERC. 1984. Shore protection manual, Vol. 1. Department of the Army, Waterways Experiment Station, Corps of Engineers, Coastal Engineering Research Center (CERC). Washington D.C.

Christchurch Star. 1929a: Sway was from east to west: Mr. H.F. Skey says it was a severe one. *Christchurch Star, 17 June 1929*: 1.

Christchurch Star. 1929b: Greater than Arthur's Pass earthquake: Shocks too severe to be registered at the Observatory. *Christchurch Star, 17 June 1929*: 10.

Clark, K.; Hancox, G.; Forsyth, P.J.; Power, W.; Strong, D.; Lukovic, B. 2011: Identification of potential tsunamis and seiche sources, their size and distribution on Lakes Te Anau and Manapouri. Institute of Geological and Nuclear Sciences (GNS), Lower Hutt, New Zealand. *GNS Science Consultancy Report* 2011/96. 74 p.

Clark, K.; Upton, P.; Carey, J.; Rosser, B.; Strong, D. 2015: Tsunami and seiche scoping study for Lakes Tekapo, Pukaki, Ohau, Alexandrina and Ruataniwha. Institute of Geological and Nuclear Sciences (GNS), Lower Hutt, New Zealand. *GNS Science Report* R15/39. 82 p.

Cox, D.C.; Morgan, J. 1977: Local tsunamis and possible local tsunamis in Hawaii. Hawaii Institute of Geophysics. Honolulu. 124 p.

Cummins, P.R.; Pranantyo, I.R.; Pownall, J.M.; Griffin, J.D.; Meilano, I.; Zhao, S. 2020: Earthquakes and tsunamis caused by low-angle normal faulting in the Banda Sea, Indonesia. *Nature Geoscience 13*: 312–318.

de Lange, W.P.; Healy, T.R. 1986. New Zealand tsunamis 1840–1982: *New Zealand Journal of Geology and Geophysics 29(1)*: 115–134.

de Lange, W.P.; Magill, C.R.; Nairn, I.A.; Hodgson, K.A. 2002: Tsunami generated by pyroclastic flows entering Lake Tarawera. Conference presentation. *Eos, Transactions of the American Geophysical Union 83(22)*: Supplement – Conference abstracts.

de Lange; W.P.; Moon, V. 2016: Volcanic generation of tsunamis: Two New Zealand palaeo-events. In: Lamarche, G. et al. (Eds). Submarine mass movements and their consequences. *Advances in Natural and Technological Hazards Research, 41*: 559–567.

Donaldson, G.M. 2016: 1931 Waikari River tsunami: New Zealand's largest historical tsunami. Unpublished BSc thesis, University of New South Wales. 65 p.

Donaldson, G.M; Goff, J.; Chagué, C.; Gadd, P.; Fierro, D. 2019: 1931 Waikari River tsunami: New Zealand's largest historical tsunami. *Sedimentary Geology 383*: 148–158.

Dore, J.F. 1992: Mackenzie District Council Civil Defence Officer's report – Mt Fletcher rockfall and consequence: Godley Valley 2–3 May 1992. Mackenzie District Council, Fairlie. File Ref. j/rpt/cd-fletch. 1 p.

Downes, G.L. 1995: Atlas of isoseismal maps of New Zealand earthquakes. Institute of Geological and Nuclear Sciences, Lower Hutt, New Zealand. *GNS Science Monograph 11*. 304 p.

Downes, G.L. 2006: The 1904 Ms 6.6, Mw 7.0–7.2 Cape Turnagain, New Zealand earthquake. *Bulletin of the New Zealand Society for Earthquake Engineering 28(4)*: 183–207.

Downes, G.L.; Barberopoulou, A.; Cochran, U.; Clark, K.; Scheele, F. 2017: The New Zealand tsunami database: Historical and modern records. *Seismological Research Letters 88(2A)*: 342–353.

Downes, G.L.; Dowrick, D.J. 2014: Atlas of isoseismal maps of New Zealand earthquakes: 1843-2003. Second edition (revised). Institute of Geological and Nuclear Sciences, Lower Hutt, New Zealand (GNS). *GNS Science Monograph* 25. 769 p.

Dykes, R.C. 2013: A multi—parameter study of iceberg calving and the retreat of *Haupapa*/Tasman Glacier, South Island, New Zealand. PhD thesis (Geography). Massey University, Palmerston North, New Zealand. 273 p.

Dykes, R.C.; Brook, M.S.; Lube, G. 2017: A major ice-calving event at the Tasman Glacier terminus, Southern Alps, 22 February 2011. *Journal of the Royal Society of New Zealand 47(4)*: 336–343.

Evening Post. 1938: Sign of earthquake: Lake gives demonstration. *Evening Post, 5 February 1938*: 10.

Evening Post. 1945: More intense: Ruapehu's activity. *Evening Post, 23 March 1945*: 6.

Fraser, R.J. 1998: Historical tsunami database for New Zealand. Unpublished MSc thesis (Earth Sciences). University of Waikato, Hamilton, New Zealand. 86 p.

Fraser, J.; McMorran, T. 2016: MacKenzie lakes – landslide tsunami investigation. Report for Environment Canterbury. Golder Associates (Christchurch). Report No. 1546369_7407_002_R_Rev1. 35 p.

GeoNet. 2022. Taupo earthquake update. 14 December 2022. GeoNet News. Institute of Geological and Nuclear Sciences (GNS), Lower Hutt, New Zealand. https://www.geonet.org.nz/news/LuzOzDmQcQUUmdeiL67oX

GNS. 2023: New Zealand Tsunami Database: Historical and modern records. Institute of Geological and Nuclear Sciences (GNS), Lower Hutt, New Zealand. https://data.gns.cri.nz/tsunami/index. html

Grapes, R. 2000: The day the earth shifted. *New Zealand Geographic 46*. https://www.nzgeo.com/stories/the-day-the-earth-shifted/

Hancox, G.T.; Dellow, G.; McSaveney, M.; Scott, B.; Villarmor, P. 2004: Reconnaissance studies of landslides caused by the M_L 5.4 Lake Rotoehu earthquake and swarm of July 2004. Institute of Geological and Nuclear Sciences (GNS), Lower Hutt, New Zealand. *GNS Science Report* 2004/24. 21 p.

Hawley, J. 1984: Slope instability in New Zealand. In: Spenden I.; Crozier, M.J. (Eds). 1984. Natural hazards in New Zealand. Chapter 11: 88–133. Complied for the New Zealand National Commission for UNESCO, 1984. 500 p.

Hogben, G. 1890: The determination of the origin of the earthquake of 5th December 1881, felt at Christchurch and other places. Article LIV. *Transactions and Proceedings of the New Zealand Institute 23*: 465–470.

Irwin, J. 1975: Checklist of New Zealand lakes. New Zealand Oceanographic Institute, Wellington, New Zealand. *New Zealand Oceanographic Institute Memoir 74*. 161 p.

Kvale, A. 1955: Seismic seiches in Norway and England during the Assam earthquake of August 15, 1950. *Bulletin of the Seismological Society of America, 45(2)*: 93–113.

Livingston, M.E.; Biggs, B.J.; Gifford, J.S. 1986a: Inventory of New Zealand lakes; Part I - North Island. National Water and Soil Conservation Authority, Ministry of Works and Development. Wellington, New Zealand. 200 p.

Livingston, M.E.; Biggs, B.J.; Gifford, J.S. 1986b: Inventory of New Zealand lakes; Part II - South Island. National Water and Soil Conservation Authority, Ministry of Works and Development. Wellington, New Zealand. 193 p.

Lowe, D.J.; Green, J.D. 1987: Origins and development of the lakes. In: Viner, A.B. (Ed). Inland waters of New Zealand. New Zealand Department of Scientific and Industrial Research, Wellington, New Zealand. *Bulletin 241*: 1–64.

Lowe, D.J.; de Lange, W.P. 2000: Volcano-meteorological tsunamis, the c. AD 200 Taupo eruption (New Zealand) and the possibility of a global tsunami. *The Holocene 10(3)*: 410–407.

Mackey, B. 2015: Seismic hazard in the Queenstown Lakes District – August 2015. Otago Regional Council, Dunedin, New Zealand. 89 p.

McGarr, A. 2020: Seismic seiches. In: Gupta, H. (Ed). Encyclopedia of Solid Earth Geophysics. *Encyclopedia of Earth Science* Series.

McSaveney, M.J. 1992a: The Mt Fletcher rock avalanche of 2 May 1992: Immediate Report. Geology and Geophysics. Department of Scientific and Industrial Research, Christchurch, New Zealand. 20 p.

McSaveney, M.J. 1992b: The Mt Fletcher rock avalanche of May 2, and again on September 16. *New Zealand Alpine Journal 45*: 99–103.

McSaveney, M.J. 1993: Rock avalanches of 2 May and 16 September 1992, Mt Fletcher, New Zealand. *Landslide News 7*: 2–4.

McSaveney, M.J. 2002: Recent rockfalls and rock avalanches in Mt Cook National Park, New Zealand. Geological Society of America. *Reviews in Engineering Geology 15*: 35–70.

Mountjoy, J.; Wang, X.; Woelz, S.; Fitzsimmons, S.; Howarth, S.; Howarth, J.D.; Orpin, A.R.; Power, W. 2019: Tsunami hazard from lacustrine mass wasting in Lake Tekapo, New Zealand. In: Linton, D.G. et al. (eds). 2019. Subaqueous mass movements. Geological Society, London. *Special Publications 477*: 413–426.

Munro, D.; Fowler, A. 2014: Testing the credibility of historical newspaper reporting of extreme climate and weather events. *New Zealand Geographer, 70*: 153–164.

Nelson Evening Mail. 1929: *"Like a tipping basin"*: Lake Rotoroa - Flow in stream reversed. *Nelson Evening Mail, 19 June 1929*: 7.

Nelson Evening Mail. 1933: Taupo's behaviour; Curious movement. Explanation by Professor Speight. *Nelson Evening Mail,* 23 February 1933: 6.

NIWA. 2023*:* New Zealand Historic Weather Events Catalogue. National Institute for Water and Atmospheric Research (NIWA), Wellington, New Zealand. https://hwe.niwa.co.nz/event/July_2004_Bay_of_Plenty_Flooding_and_Landslides

Okal, E.A.; Reymond, D. 2003. The mechanism of great Banda Sea earthquake of 1 February 1938: applying the method of preliminary determination of focal mechanism to a historical event. *Earth and Planetary Science Letters 216*: 1–15.

Owens, I.F. 2001: Chapter 23: Natural Hazards. In: Sturman, A; Spoken-Smith, R. (Eds). The physical environment – a New Zealand perspective: 427–446. Oxford University Press, Melbourne.

Painter, D. 2004: Chapter 45: Managing water-related risks. In: Harding, J.; Mosley, P.; Pearson, C.; Sorrell, B. 2004 (Eds). Freshwaters of New Zealand. New Zealand Hydrological Society and New Zealand Limnological Society. 702 p.

Papers Past. 2022. National Library of New Zealand, Wellington, New Zealand. Papers Past | Newspapers Home (natlib.govt.nz)

Pararas-Carayannis, G. 2000. Tsunami glossary. International Tsunami Information Centre; Intergovernmental Oceanographic Commission (of UNESCO); International Co-ordination Group of the Tsunami Warning System in the Pacific. Honolulu, Hawaii. 20 p. http://www.drgeorgepc.com/TsunamiGlossary.pdf

Pond, J.A.; Smith, S.P. 1886: Observations on the eruption of Mount Tarawera, Bay of Plenty, New Zealand, 10 June 1886. Article XLIV. *Transactions and Proceedings of the New Zealand Institute 19*: 342–371.

Poverty Bay Herald. 1904: The recent earthquake. *Poverty Bay Herald, 17 August 1904*: 3.

Poverty Bay Herald. 1931: Anxiety in Australia - avalanche of enquiries. *Poverty Bay Herald, 4 February 1931*: 12.

Roberts, N.J.; McKillop, R.J.; Lawrence, M.S.; Psutka, J.F.; Clague; J.J.; Brideau, M-A.; Ward, B.C. 2013: Impacts of the 2007 landslide-generated tsunami in Chehalis Lake, Canada. Conference paper. The Second World Landslide Forum. In: *Landslide Science and Practice:* 133–140. Springer (Berlin).

Schallenberg, M.; de Winton, M.D.; Verberg, P.; Kelly, D.J.; Hamill, K.D., Hamilton, D.P. 2013: Ecosystem services of lakes. In: Dymond, J.D. (Ed). 2013. Ecosystem services in New Zealand – conditions and trends: 203–225. Manaaki Whenua/Landcare Research Press. Lincoln, New Zealand. 539 p.

Sheppard, F.P.; Macdonald, G.A.; Cox, D.C. 1950. The tsunami of April 1,1946. *Bulletin of the Scripps Institution of Oceanography 5(6)*: 391-527.

Spenden, I.; Crozier, M.J. (Eds). 1984: Natural hazards in New Zealand: New Zealand National Commission for UNESCO, Wellington, New Zealand. 500 p.

Tait, S.U. 1977: Waikari Station 1840 to 1940. Hawkes Bay Regional Council (HBRC) Report No. AM15-16, HBRC Plan No. 4571.

Thames Star. 1883: Untitled. *Thames Star, 15 September 1883*: 2.

Wang, X.; Holden, C.; Power, W.; Lui, Y.; Mountjoy, J. 2020: Seiche effects in Lake Tekapo, New Zealand, in an Mw 8.2 Alpine Fault earthquake. *Pure Applied Geophysics*. 8 October 2020. 16 p.

Ward, H.; Morrow, F.; Ferguson, R. 2015: Taupo District flood hazard study: Lake Taupo foreshore. Report for the Waikato Regional Council and Taupo District Council. Opus International Consultants, Wellington, New Zealand. 112 p.

Warren, C.R.; Kirkbride, M.P. 1998: Temperature and bathymetry of ice-contact lakes in Mount Cook National Park, New Zealand. *New Zealand Journal of Geology and Geophysics 41(2)*: 133–143.

ISSN 8755-6839

SCIENCE OF TSUNAMI HAZARDS

Journal of Tsunami Society International

Volume 42 Number 3 2023

PROFILE OF TSUNAMI EARLY WARNING SYSTEM FOR DISABILITIES: A MANIFESTATION OF THE INDONESIAN'S NATIONAL CONGRESS IN DISASTER MANAGEMENT

Binar Kurnia Prahani[*1], Hanandita Veda Saphira[1], Shelly Andari[1], Wagino[1], Madlazim[1], Eko Hariyono[1], Saiyidah Mahtari[2],

[1] Universitas Negeri Surabaya, Surabaya 60231, INDONESIA
[2] Universitas Lambung Mangkurat, Banjarmasin 70123, INDONESIA
Email: binarprahani@unesa.ac.id

ABSTRACT

The advancement of technology is projected to result in the creation of efficient tsunami detection early warning systems to aid individuals, especially those disabilities-friendly, in raising their consciousness and preparing for the worst-case disaster scenarios before they occur. This qualitative descriptive study uses data-gathering procedures based on the library research method. The numerous TEWS has been developed as an effort to recover, rehabilitate, and reconstruct and are carried out in such a way as to anticipate and prepare residents to be more alert and alert to the occurrence of tsunami. IoT based on IMU devices can be utilized as TEWS sensors with minimum limitation. IDSL information concerning elevation is highly correlated with the BIG forecast information. The Android-based received a response time of fewer than five seconds to start receiving with retrieving the tsunami and earthquake data. In conclusion, the EWS needs to be developed along with professional sign-language translators in all catastrophe knowledge as required by the National Regulation on the fundamental rights of individuals with disabilities as part of disclosing information for deaf citizens. Hence, recommendations for further research are needed to develop the TEWS integrated with VBEWS, ViBEWS, ViSEWS, and sign language.

Keywords: *Disabilities, Sign Language, Tsunami, Warning Systems.*

1. INTRODUCTION

Indonesia is one of the countries with tsunami potential because it is located on the path of meeting plates in the sea, so a large earthquake with a shallow depth will potentially cause a tsunami. Tsunami waves are mechanical waves that have a propagation speed proportional to the density of the propagation medium. In addition, tsunami waves include longitudinal waves whose vibration direction parallels their propagation. Tsunami will vibrate harmoniously in an area with an intense sea surface with a large wavelength and speed (Matsumoto et al., 2021). The energy of a tsunami wave is always constant, so when a wave enters a shallow area, its wavelength and speed will be smaller, while its amplitude will be more significant. This process can be formulated as $v=,-gd$. (Bolin et al., 2023). Where v is the speed of the wave, g is the acceleration due to gravity, and d is the depth of the sea surface (Prahani et al., 2022). However, tsunami can be triggered by temporal el Niño and other climatic anomalies (Pararas-Carayannis & Zoll, 2017)

The tsunami waves are among the occurrences of nature, leading to one of the most devastating tragedies on Earth. However, in 2004 the Aceh tsunami was one of the biggest disasters in Indonesia (Robbe-Saule et al., 2020). Indian Ocean earthquake and tsunami its epicenter is located off the west coast of Sumatra, Indonesia (Jihad et al., 2023; Syamsidik et al., 2021; Tursina et al., 2021). The earthquake was 9.1–9.3 on the moment magnitude scale and IX on the Mercalli intensity scale. The number of victims due to the Aceh tsunami reached 167,000 people, both dead and missing. In addition, no less than 500,000 people were left homeless (Fathiah et al., 2019; Riswandi, 2023; Samphantharak, 2019). The death toll does not include tsunami victims in other regions. Other than that, Multiple devastating tsunamis and earthquakes have been recorded in the Eastern Mediterranean region throughout the last three centuries (Pararas-Carayannis, 2011). Figure 1 is a tsunami Hazard in Indonesia by Australia-Indonesia Facility for Disaster Reduction (AIFDR). A tsunami calamity is likely to strike practically every area of Indonesia.

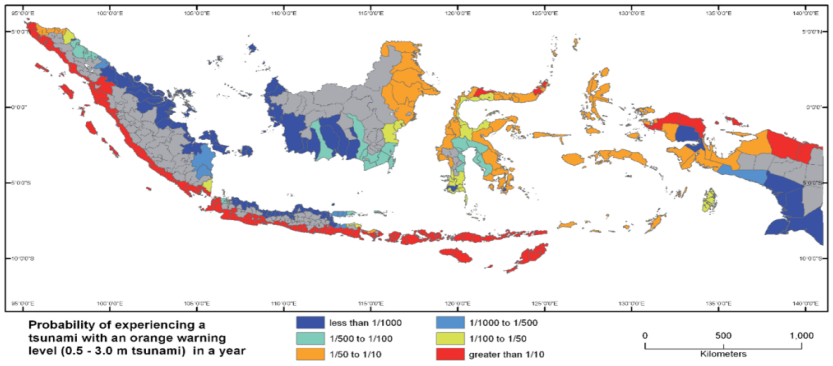

Figure 1. Tsunami Hazard in Indonesia by AIFDR (Source: Horspool et al., 2013)

In the context of the unique needs of the disabilities, efforts to recover, rehabilitate, and reconstruct are carried out in such a way as to anticipate and prepare residents to be more alert and alert to the occurrence of the tsunami (Fathiah et al., 2019; Goto et al., 2021). As one of the disaster mitigation efforts, the National Disaster Management Agency (NDMA), together with the Indonesian Deaf Welfare Movement (IDWFM), held a National Congress of Indonesian Sign Language in Disaster Management. However, Law Number 24 of 2007 concerning Disaster Management states that disability groups are protected groups in disaster events (as objects). However, they can also become actors (subjects) in Disaster Management through the capacity building of these groups. Efforts to pay attention to those with special needs are covered in the Head Regulation of the National Disaster Management Agency Number 14 of 2014 concerning Handling, Protection, and Participation of Persons with Disabilities in Disaster Management.

The advancement of technology is projected to result in the creation of efficient tsunami detection early warning systems to aid individuals, especially those disabilities-friendly, in raising their consciousness and preparing for the worst-case disaster scenarios before they occur. In line with this, the preparedness of families with disabilities children in the face of disasters; it was seen that the preparedness plan category was not ready (37.8%), the knowledge category was ready (42.2%), the resource mobilization category was not ready (82.2%), the tsunami disaster preparedness index value is 57% (ready category), the disaster warning category was not ready (46.7%) (Riviwanto et al., 2021). Governments in local areas must give persons with disabilities preferential attention (Fuady et al., 2021; Riviwanto et al., 2021). This study will summarize the development of a tsunami early warning system (TEWS) for disability groups so that from this study can be concluded the advantages, limitations, and updates that can be applied as an effort to realize the goals of the National Congress by NDMA so that parties to develop an inclusive early warning system, especially paying attention to the disabilities community. This congress is an important milestone because the disabled community, who have sign language, are willing to come together to agree on how they can contribute to disaster relief with their wealth of sign language (Schniedewind et al., 2020).

2. METHODS

This qualitative descriptive study uses data-gathering procedures based on the library research method. The first library research is collected. Then, the article was reduced to the most relevant topic of TEWS for disabilities group. This research produces descriptive analysis in a series of written sentences. According to Sugiyono (2017), the stages of analysis for qualitative research are generally depicted in Figure 2.

Qualitative data analysis includes four stages (Suliyanah et al., 2021), namely (1) Data collection is obtaining data from various trusted sources to obtain the required information that supports the ability of research objectives; (2) Data reduction is sorting out important things focused on the needs of the author to facilitate obtaining the desired data in line with the research objectives (Shafi et al., 2020; Sovacool et al., 2018); (3) Presentation of data is the exposure of research data which is generally in the form of short descriptions, charts, relationships between subjects, and so on for qualitative research types (Bauer & Scheim, 2019); (4) Conclusion and verification are the final results obtained after conducting a series of previous processes to attract new findings for the study's purpose.

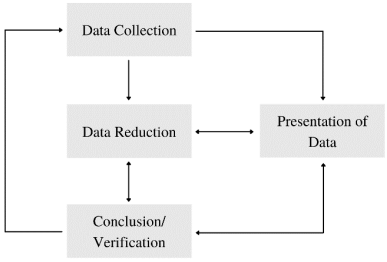

Figure 2. Stages of Qualitative Data Analysis in General (Sugiyono, 2017)

3. RESULTS AND DISCUSSION

3A. TEWS Based on IoT and Underwater Sensors

Tsunami mitigation is often accomplished by placing buoys along the shore, although this detection method has limits. Determining the sea level compared to specific guidance, whereas altimetry observation needs to be done continuously and correctly, usually carries out tsunami pulse observation on the shore. Furthermore, traditional markers are more extensive and more costly to use. Underwater Wireless Sensor Networks, in broad terms, may be utilized to collect and preserve information about broad geographical areas and transfer it to a headquarters for information processing and EW creation (Ding et al., 2021; Gola & Gupta, 2020; Jin et al., 2019). UWSNs are employed in a variety of programs, and the Internet of Underwater Things (IoT) is a framework that enables the identification and forecasting of occurrences that may lead to emergencies (Bhattacharya et al., 2022, 2022; Kotis et al., 2023; Mohsan et al., 2022), see in Figure 3.

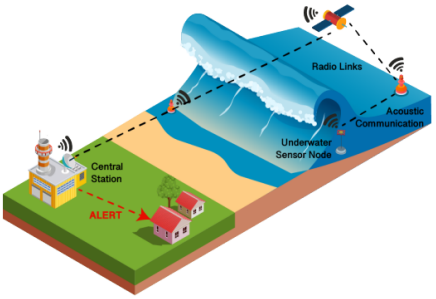

Figure 3. Integrating of TEWS based on IoT and Underwater Sensor (Source: Esposito et al., 2022)

In the context of Early Warning (EW), IoT solutions may be highly successful in data gathering, transmission, and disaster forecasting while being affordable. As a result, Wireless Sensor Networks, Cloud solutions, Machine Learning, and other Internet of Things components should be employed while implementing or integrating existing Early Warning Systems (EWS) (Esposito et al., 2022). Further research studies the uses of blockchain-enabled IoT, such as in Figure 4.

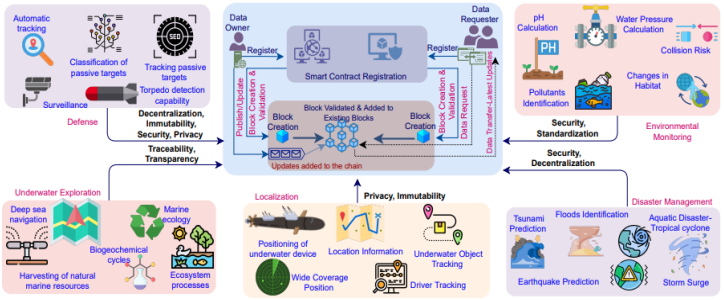

Figure 4. Blockchain-enabled IoT (Source: Bhattacharya et al., 2022)

IoT enables us to save numerous lives through emergency preparedness. As a result, the IoT allows for the connectivity of many devices; the IoT-empowered disaster preparedness system is utilized for EWS by applying data analysis and computational capabilities (Sharma et al., 2021). Although undersea investigation contributes significantly to nations' economies, research into the implementation of rising technologies like blockchain for the IoT is still in the early stages. Furthermore, due to their compact size and low construction and upkeep costs, IoT-based Inertial Measurement Unit (IMU) devices can be utilized as TEWS sensors (Suryanto et al., 2020). However, Anping Port in Taiwan found that low-cost IMUs had a good capacity for measuring the height of waves with both frequency and amplitude as relatively precise parameters (Huang et al., 2016).

3B. Inexpensive Device for Sea Level

IDSL research by Novianto et al. (2021) information concerning elevation is highly correlated with the BIG forecast information. The typical frequency of present-day information gaps is three to five minutes long, primarily due to transmission or transmission network interruption (Yunarto & Sari, 2018). IDSL is also equipped with CCTV to visually recognize the water lines as an indicator of a tsunami, as in Figure 6. However, previous research developed a Pacific TWS (PTWS) based on sea level Gauges (Pararas-Carayannis, 2015) as in Figure 5. PTWS provide an evaluation of both tsunami or earthquake in the Pacific Ocean Basin (Toulkeridis et al., 2022).

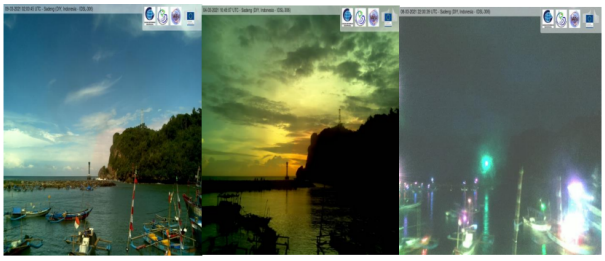

Figure 5. IDSL CCTV Image Comparison (Source: Novianto et al., 2021)

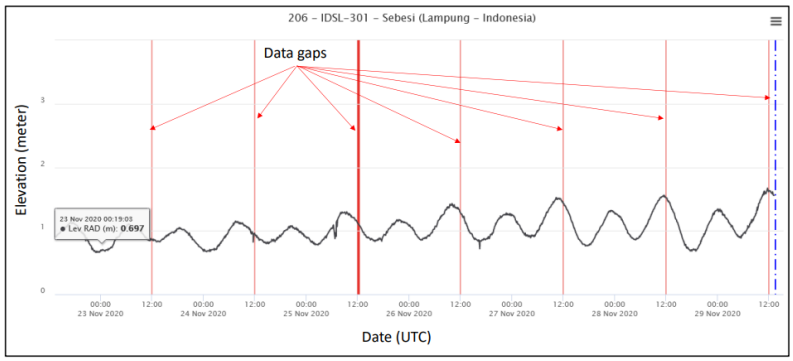

Figure 6. The Data Gaps During Rest Time of IDSL (Source: Husrin et al., 2022)

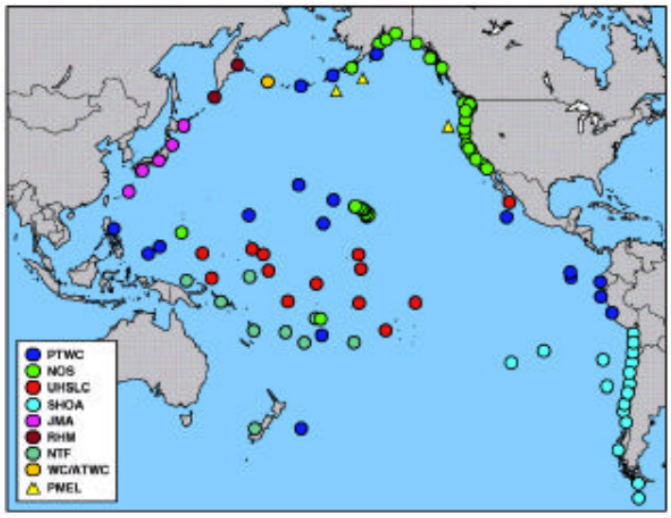

Figure 7. TWS Sea Level Gauges (Source: Pararas-Carayannis**, 2015**)

Inconsistencies are missing data caused by a long delay time, a weak transmission system, or a communication breakdown. During the measurement process, poor connectivity and connection loss were caused by the operational handling of the equipment and the level of quality connectivity (internet) facilities. The only factor that may affect IDSL performance is the high delay time that occurs on occasion (Husrin et al., 2022). This mainly happened between 30 seconds and 5 minutes. Considering operational management, the amount of data breaches for IDSL was less than 9% (Husrin et al., 2021). The IDSL alert system is adequate for providing EW of wave abnormalities. However, it gets frequently disrupted by local occurrences, including vibrations from ships corroborated by CCTV photos in Figure 6 and 7. However, the development of IDSL is on high reliability as TEWS.

3C. Mobile-Based TEWS

Digitalization of technology with the help of mobile-phone applications has become very dominant in connectivity between people in various parts of the world. The digital world has become "critical" to today's society, but perhaps more should be addressed to realize its democratizing possibilities (Brody et al., 2018; Hantrais et al., 2021). Mobile-phone application at pace and scale, its general application in some sectors prompted legal, social, and security problems, along with increasing threats for underprivileged groups (Budd et al., 2020; Gallouj et al., 2015; Marabelli et al., 2021; Mumtaz et al., 2021). Several developments of TEWS are integrating mobile-based due to its practice of public awareness. Rais et al. (2022) developed android-based TEWS, such as in Figure 8.

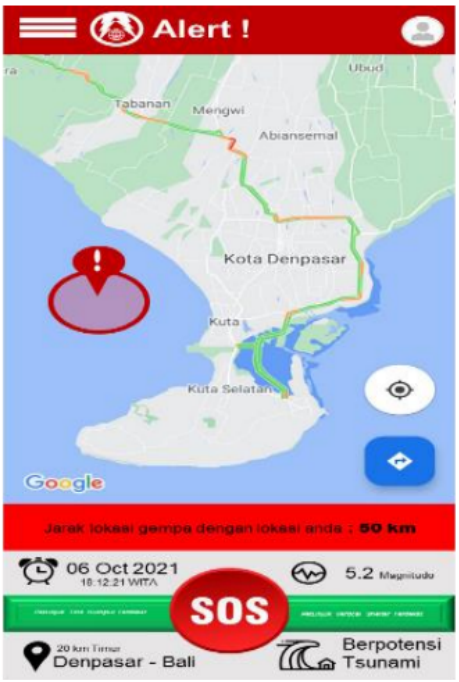

Figure 8. Android-based TEWS (Source: Rais et al., 2022)

The Android-based received a response time of fewer than five seconds to start receiving with retrieving the tsunami and earthquake data from the Meteorology Climatology and Geophysics Council webpage to trigger an early warning in users' Android-based. Furthermore, engineers upgrade the technology to distribute tsunami and earthquake information and provide evacuation direction guidance and survivor detecting functions to reduce catastrophe risk (Chamola et al., 2021; Lindell et al., 2021). However, due to the high volume of user activity, this function may have the opportunity to be interrupted.

Figure 9. Integrated EWS of Lampung (Source: Imamura et al., 2019)

Furthermore, Imamura et al. (2019) developed a mobile-based named "Integrated EWS of Lampung" in Figure 9. This application consists of six menus: 1) mitigation, 2) emergency number, 3) EWS, 4) evacuation point, 5) evacuation signs, and 6) post-earthquake. This application is effective in giving alerts and knowledge as EWS. As a promising EWS, the "Integrated EWS of Lampung" can be developed for national purposes, such as in Figure 9. In line with this, the research by Berawi et al. (2021) developing *'SaveMyLife'* as a mobile-based help rescue in order to victims prioritized (Infants, elderly people, pregnant women, and other defined groups have relied extensively on physical facilities such as buildings, mode of transport, and ecological systems to ensure their life by providing shelter, nourishment, potable water, as well as access to energy), and technology utilized. Figure 10 is the development of *'SaveMyLife.'*

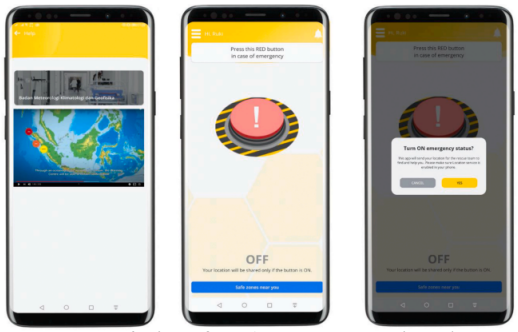

Figure 10. '*SaveMyLife'* interface (Source: Berawi et al., 2021)

Various TEWS algorithms exist to provide educated tsunami source characterization for quick, limited notification. The mechanism by which this critical information is disseminated is an ignored part of TEWS (Davidson, 2022; de Silva, 2021). Current procedures are primarily focused on when an alarm is sent from a warning center; however, that notice goes through many groups and departments before reaching concerned populations (Williamson & Allen, 2023). However, there is a lack of attention from parties with authority in providing EWS, especially regarding warning of danger and emergency disasters that can reach the Deaf. Deaf people are almost entirely unable to recognize the distress warning signals issued by the Voice-Based Early Warning System (VBEWS).

The equipment for the EWS recommended by the study of Munandar et al. (2019) to complement the VB-EWS is Visual-Based Early Warning System Equipment (VisEWS) and Shock Vibration-Based Early Warning System Equipment (VibEWS). VisEWS is applied by using a hazard light placed where the Deaf can easily see it. Whereas VibEWS is applied by using devices such as smart bracelets or smart watches, or intelligent rings worn by deaf people when they are individually in public facilities, such as in hospital inpatient rooms or hotel rooms. Otherwise, the EWS offers professional sign-language translators in all catastrophe knowledge as required by the National Regulation on the fundamental rights of individuals who have disabilities as part of the disclosure of information for deaf citizens (Fauziyah & Jannah, 2022; Hansson et al., 2020).

4. CONCLUSIONS

The numerous TEWS has been developed as an effort to recover, rehabilitate, and reconstruct and are carried out in such a way as to anticipate and prepare residents to be more alert and alert to the occurrence of tsunami. IoT based on IMU devices can be utilized as TEWS sensors with minimum limitation. IDSL information concerning elevation is highly correlated with the BIG forecast information. The Android-based received a response time of fewer than five seconds to start receiving with retrieving the tsunami and earthquake data from the Meteorology Climatology and Geophysics Council webpage to trigger an early warning in users' Android-based. However, there is a lack of attention from parties with authority in providing EWS, especially regarding warning of danger and emergency disasters that can reach the Deaf. In conclusion, the EWS needs to be developed along with professional sign-language translators in all catastrophe knowledge as

required by the National Regulation on the fundamental rights of individuals who have disabilities as part of the disclosure of information for deaf citizens. Hence, recommendations for further research are needed to develop the TEWS integrated with VBEWS, ViBEWS, ViSEWS, and sign language.

ACKNOWLEDGEMENTS

This research is part of collaborative research in 2023 which is fully supported by the Directorate of the Institute for Research and Community Service, Universitas Negeri Surabaya, Indonesia.

REFERENCES

Bauer, G. R., & Scheim, A. I. (2019). Methods for analytic inter-categorical intersectionality in quantitative research: Discrimination as a mediator of health inequalities. *Social Science and Medicine*, *226*, 236–245. https://doi.org/10.1016/j.socscimed.2018.12.015

Berawi, M. A., Leviäkangas, P., Siahaan, S. A. O., Hafidza, A., Sari, M., Miraj, P., Harwahyu, R., & Saroji, G. (2021). Increasing disaster victim survival rate: SaveMyLife Mobile Application development. *International Journal of Disaster Risk Reduction*, *60*, 1-14. https://doi.org/10.1016/j.ijdrr.2021.102290

Bhattacharya, S., Victor, N., Chengoden, R., Ramalingam, M., Selvi, G. C., Maddikunta, P. K. R., Donta, P. K., Dustdar, S., Jhaveri, R. H., & Gadekallu, T. R. (2022). Blockchain for the internet of underwater things: State-of-the-art applications, challenges, and future directions. *Sustainability (Switzerland)*, *14*(23), 1–21. https://doi.org/10.3390/su142315659

Bolin, H., Yueping, Y., Renjiang, L., Peng, Z., Zhen, Q., Yang, L., Shulou, C., Qiuwang, L., & Kaikai, X. (2023). Three-dimensional experimental investigation on hazard reduction of landslide-generated impulse waves in the Baihetan reservoir, China. *Landslides*, 1-19. https://doi.org/10.1007/s10346-023-02068-w

Brody, H., Hodson, R., Batty, E., Haines, N., Fernandes, W., Duncan, K., Bruni, N., Jones, R., Hughes, R., Pearson, H., & Hodson, R. (2018). Digital revolution. *Nature Outlook, 563*(7733), 1–2.

Budd, J., Miller, B. S., Manning, E. M., Lampos, V., Zhuang, M., Edelstein, M., Rees, G., Emery, V. C., Stevens, M. M., Keegan, N., Short, M. J., Pillay, D., Manley, E., Cox, I. J., Heymann, D., Johnson, A. M., & McKendry, R. A. (2020). Digital technologies in the public health response to COVID-19. *Nature Medicine*, *26*(8), 1183–1192. https://doi.org/10.1038/s41591-020-1011-4

Chamola, V., Hassija, V., Gupta, S., Goyal, A., Guizani, M., & Sikdar, B. (2021). Disaster and pandemic management using machine learning: A survey. *IEEE Internet of Things Journal*, *8*(21), 16047–16071. https://doi.org/10.1109/JIOT.2020.3044966

Davidson, A. (2022). Social and Technical sustainability of a tsunami early warning system (tews) -a case study of Patong, Thailand. *SSRN Electronic Journal*, 1–34.

de Silva, M. K. K. K. (2021). Strategies for internet-enabled and gender-sensitive tsunami early warning. *Australasian Journal of Disaster and Trauma Studies*, *25*(1), 17–34.

Ding, Q., Zhu, R., Liu, H., & Ma, M. (2021). An overview of machine learning-based energy-efficient routing algorithms in wireless sensor networks. *Electronics (Switzerland)*, *10*(13), 1–24. https://doi.org/10.3390/electronics10131539

Esposito, M., Palma, L., Belli, A., Sabbatini, L., & Pierleoni, P. (2022). Recent advances in Internet of Things solutions for early warning systems: A review. *Sensors*, *22*(6), 1-39. https://doi.org/10.3390/s22062124

Fathiah, A., Afrizal, & Jendrius. (2019). Bencana alam dan konflik agraria: Suatu kajian literatur. *Talenta Conference Series: Local Wisdom, Social, and Arts (LWSA)*, *2*(1), 1–5. https://doi.org/10.32734/lwsa.v2i1.581

Fauziyah, S., & Jannah, L. M. (2022). Access to disclosure of disaster information for deaf people through a sign language interpreter. *IJDS Indonesian Journal of Disability Studies*, *9*(1), 137–152. https://doi.org/10.21776/ub.ijds.2022.009.01.11

Fuady, M., Munadi, R., & Fuady, M. A. K. (2021). Disaster mitigation in Indonesia: Between plans and reality. *IOP Conference Series: Materials Science and Engineering*, *1087*(1), 1-9. https://doi.org/10.1088/1757-899x/1087/1/012011

Gallouj, F., Weber, K. M., Stare, M., & Rubalcaba, L. (2015). The futures of the service economy in Europe: A foresight analysis. *Technological Forecasting and Social Change*, *94*, 80–96. https://doi.org/10.1016/j.techfore.2014.06.009

Gola, K. K., & Gupta, B. (2020). Underwater sensor networks: "Comparative analysis on applications, deployment, and routing techniques." *IET Communications*, *14*(17), 2859–2870. https://doi.org/10.1049/iet-com.2019.1171

Goto, K., Ishizawa, T., Ebina, Y., Imamura, F., Sato, S., & Udo, K. (2021). Ten years after the 2011 Tohoku-oki earthquake and tsunami: Geological and environmental effects and implications for disaster policy changes. *Earth-Science Reviews*, *212*, 1-25. https://doi.org/10.1016/j.earscirev.2020.103417

Hansson, S., Orru, K., Siibak, A., Bäck, A., Krüger, M., Gabel, F., & Morsut, C. (2020). Communication-related vulnerability to disasters: A heuristic framework. *International Journal of Disaster Risk Reduction*, *51*, 1-19. https://doi.org/10.1016/j.ijdrr.2020.101931

Hantrais, L., Allin, P., Kritikos, M., Sogomonjan, M., Anand, P. B., Livingstone, S., Williams, M., & Innes, M. (2021). COVID-19 and the digital revolution. *Contemporary Social Science*, *16*(2), 256–270. https://doi.org/10.1080/21582041.2020.1833234

Horspool, N., Pranantyo, I. R., Griffin, J., Latief, H., Natawidjaja, D., Kongko, W., Cipta, A., Bustaman, Anugrah, S. D., & Thio, H. K. (2013). A national tsunami hazard assessment for Indonesia. *Australian-Indonesia Facility for Disaster Reduction*, *January* 1–32.

Huang, Y. L., Kuo, C. Y., Shih, C. H., Lin, L. C., Chiang, K. W., & Cheng, K. C. (2016). Monitoring high-frequency ocean signals using low-cost GNSS/IMU buoys. *International Archives of the Photogrammetry, Remote Sensing and Spatial Information Sciences - ISPRS Archives*, *41*, 1127–1134. https://doi.org/10.5194/isprsarchives-XLI-B8-1127-2016

Husrin, S., Annunziato, A., Prasetya, G. S., & Hidayat, R. (2022). IDSL for Tsunami Early Warning System in Indonesia. *IOP Conference Series: Earth and Environmental Science*, *1117*(1), 1-10. https://doi.org/10.1088/1755-1315/1117/1/012028

Husrin, S., Novianto, D., Bramawanto, R., Setiawan, A., Nugroho, D., Permana, S. M., Sufyan, A., Sarnanda, S., Sianturi, D. S. A., Mulyadi, U., Daniel, D., Suhelmi, I. R., & Purnama, M. S. B. (2021). Analisa kinerja IDSL/PUMMA untuk peringatan dini tsunami di pangandaran. *Jurnal Kelautan Nasional*, *16*(2), 87-96. https://doi.org/10.15578/jkn.v16i2.9846

Imamura, F., Boret, S. P., Suppasri, A., & Muhari, A. (2019). Recent occurrences of serious tsunami damage and the future challenges of tsunami disaster risk reduction. *Progress in Disaster Science*, *1*, 1–3. https://doi.org/10.1016/j.pdisas.2019.100009

Jihad, A., Muksin, U., Syamsidik, S., Ramli, M., Banyunegoro, V. H., Simanjuntak, A. V. H., & Rusdin, A. A. (2023). Tsunami evacuation sites in the northern Sumatra (Indonesia) were determined based on the updated tsunami numerical simulations. *Progress in Disaster Science*, *18*, 1-14. https://doi.org/10.1016/j.pdisas.2023.100286

Jin, Z., Zhao, Q., & Su, Y. (2019). RCAR: A Reinforcement-learning-based routing protocol for congestion-avoided underwater acoustic sensor networks. *IEEE Sensors Journal*, *19*(22), 10881–10891. https://doi.org/10.1109/JSEN.2019.2932126

Kotis, K., Stavrinos, S., & Kalloniatis, C. (2023). Review on semantic modeling and simulation of cybersecurity and interoperability on the internet of underwater things. *Future Internet*, *15*(1), 1-29. https://doi.org/10.3390/fi15010011

Lindell, M. K., Bostrom, A., Goltz, J. D., & Prater, C. S. (2021). Evaluating hazard awareness brochures: Assessing the textual, graphical, and numerical features of tsunami evacuation products. *International Journal of Disaster Risk Reduction*, *61*, 1-23. https://doi.org/10.1016/j.ijdrr.2021.102361

Marabelli, M., Vaast, E., & Li, J. L. (2021). Preventing the digital scars of COVID-19. *European Journal of Information Systems*, *30*(2), 176–192. https://doi.org/10.1080/0960085X.2020.1863752

Matsumoto, H., Araki, E., Kimura, T., Fujie, G., Shiraishi, K., Tonegawa, T., Obana, K., Arai, R., Kaiho, Y., Nakamura, Y., Yokobiki, T., Kodaira, S., Takahashi, N., Ellwood, R., Yartsev, V., & Karrenbach, M. (2021). Detection of hydroacoustic signals on a fiber-optic submarine cable. *Scientific Reports*, *11*(1), 1–12. https://doi.org/10.1038/s41598-021-82093-8

Mohsan, S. A. H., Mazinani, A., Othman, N. Q. H., & Amjad, H. (2022). Towards the internet of underwater things: a comprehensive survey. *Earth Science Informatics*, *15*(2), 735–764. https://doi.org/10.1007/s12145-021-00762-8

Mumtaz, M., Hussain, N., Baqar, Z., Anwar, S., & Bilal, M. (2021). Deciphering the impact of novel coronavirus pandemic on agricultural sustainability, food security, and socio-economic sectors—a review. *Environmental Science and Pollution Research*, *28*(36), 49410–49424. https://doi.org/10.1007/s11356-021-15728-y

Munandar, A., Silvia, D., & Wenas, J. R. (2019). Analisis efektifitas sound basedearly warning system dalam rangka pegurangan risiko bencana bagi kaum tuli di indonesia. *MIMBAR : Jurnal Penelitian Sosial Dan Politik*, *8*(1), 17-29. https://doi.org/10.32663/jpsp.v8i1.772

Novianto, D., Husrin, S., Nugroho, D., Bramawanto, R., Setiawan, A., Permana, S. M., Sufyan, A., Sianturi, D. S. A., Daniel, D., Ridlo Suhelmi, I., & Fauzah, S. (2021). IDSL (Inexpensive Device for Sea Level) performance analysis for tews (Tsunami Early Warning System) in Sadeng fisheries port. *IOP Conference Series: Earth and Environmental Science*, *860*(1), 1-10. https://doi.org/10.1088/1755-1315/860/1/012101

Pararas-Carayannis, G. (2011). The earthquake and tsunami of July 21, 365 AD in the Eastern Mediterranean Sea - Review of impact on the ancient world - Assessment of recurrence and future impact. *Science of Tsunami Hazards*, *30*(4), 253–292.

Pararas-Carayannis, G. (2015). Brief historical review of its establishment and institutional support. *Science of Tsunami Hazards*, *34*(2), 101–143.

Pararas-Carayannis, G., & Zoll, P. (2017). Incipient evaluation of temporal el nino and other climatic anomalies in triggering earthquakes and tsunamis – case study: The earthquake and tsunami of 16th april 2016 in Ecuador. *Science of Tsunami Hazards*, *27*(2), 69–85.

Prahani, B. K., Alfarizy, Y., Madlazim, M., Hariyono, E., Mahtari, S., & Wibowo, F. C. (2022). Analyze the mechanism of tsunami based on the scopus database. *Science of Tsunami Hazards*, *41*(3), 175–195.

Rais, A. M., Priyambodo Nur, A. N., & Tricahyaningati, D. (2022). Android real-time earthquake & tsunami warning alert system based on open data from the Indonesia government agency of geophysics. *IOP Conference Series: Earth and Environmental Science*, *1095*(1), 1-11. https://doi.org/10.1088/1755-1315/1095/1/012008

Riswandi, R. (2023). Dampak program pembangunan perumahan dan karakteristik demografi terhadap keputusan pengungsi meninggalkan barak : Studi kasus tsunami 2004. *JPED (Jurnal Perspektif Ekonomi Darussalam)*, 30–42.

Riviwanto, M., Darwel, D., Dwiyanti, D., & Juanda, J. (2021). The preparedness level of families with disabilities and children in facing the earthquake and tsunami disaster in Padang, west Sumatra. *International Journal of Disaster Management*, *4*(1), 61-90. https://doi.org/10.24815/ijdm.v4i1.19323

Robbe-Saule, M., Morize, C., Henaff, R., Bertho, Y., Sauret, A., & Gondret, P. (2020). Experimental investigation of tsunami waves generated by granular collapse into water. *Journal of Fluid Mechanics*, *907,* 1-11. https://doi.org/10.1017/jfm.2020.807

Samphantharak, K. (2019). Natural disaster and economic development in Southeast Asia. *SSRN Electronic Journal*, 1–15. https://doi.org/10.2139/ssrn.3388396

Schniedewind, E., Lindsay, R., & Snow, S. (2020). Ask, and ye shall not receive: Interpreter-related access barriers reported by deaf users of American sign language. *Disability and Health Journal*, *13*(4), 1-33. https://doi.org/10.1016/j.dhjo.2020.100932

Shafi, M., Liu, J., & Ren, W. (2020). Impact of COVID-19 pandemic on micro, small, and medium-sized Enterprises operating in Pakistan. *Research in Globalization*, *2,* 1-18. https://doi.org/10.1016/j.resglo.2020.100018

Sharma, K., Anand, D., Sabharwal, M., Tiwari, P. K., Cheikhrouhou, O., & Frikha, T. (2021). A disaster management framework using internet of things-based interconnected devices. *Mathematical Problems in Engineering*, 1–10. https://doi.org/10.1155/2021/9916440

Sovacool, B. K., Axsen, J., & Sorrell, S. (2018). Promoting novelty, rigor, and style in energy social science: Towards codes of practice for appropriate methods and research design. *Energy Research and Social Science*, *45*, 12–42. https://doi.org/10.1016/j.erss.2018.07.007

Sugiyono, S. (2017). *Metode penelitian kuantitatif, kualitatif, dan R&D*. Alfabeta.

Suliyanah, S., Deta, U. A., Kurniawan, F. K., Lestari, N. A., Yantidewi, M., Jauhariyah, M. N. R., & Prahani, B. K. (2021). Literature review on the use of educational physics games in improving learning outcomes. *Journal of Physics: Conference Series*, *1805*(1), 1-9. https://doi.org/10.1088/1742-6596/1805/1/012038

Suryanto, W., Supriyanto, Hartantyo, E., Juhana, T., Budiarjo, Handaru, A. S., & Satriani, J. (2020). IMU (inertial measurement unit) device for internet of things based disaster early warning system: Applications and innovation. *IOP Conference Series: Earth and Environmental Science*, *451*(1), 1-8. https://doi.org/10.1088/1755-1315/451/1/012015

Syamsidik, S., Oktari, R. S., Nugroho, A., Fahmi, M., Suppasri, A., Munadi, K., & Amra, R. (2021). Fifteen years of the 2004 Indian Ocean tsunami in Aceh-Indonesia: Mitigation, preparedness, and challenges for a long-term disaster recovery process. *International Journal of Disaster Risk Reduction*, *54*, 1-12. https://doi.org/10.1016/j.ijdrr.2021.102052

Toulkeridis, T., Martinez, N., Barrantes, G., Rentería, W., Barragan-Aroca, G., Simón-Baile, D., Palacios, I., Salazar, R., Salcedo-Hurtado, E. de J., & Pararas-Carayannis, G. (2022). Impact and response in central and south america due to the tsunami generated by the submarine eruption of hunga tonga-hunga ha'apai volcano. *Science of Tsunami Hazards*, *41*(1), 1–38.

Tursina, Syamsidik, Kato, S., & Afifuddin, M. (2021). Coupling sea-level rise with tsunamis: Projected adverse impact of future tsunamis on Banda Aceh city, Indonesia. *International Journal of Disaster Risk Reduction*, *55*(7), 1-20. https://doi.org/10.1016/j.ijdrr.2021.102084

Williamson, A., & Allen, R. M. (2023). Improving the efficacy of tsunami warnings along the west coast of the united states. *Pure and Applied Geophysics*, *180*(5), 1661–1678. https://doi.org/10.1007/s00024-023-03277-z

Yunarto, Y., & Sari, A. M. (2018). Analysis of community tsunami evacuation time: An overview. *IOP Conference Series: Earth and Environmental Science*, *118*(1), 1-10. https://doi.org/10.1088/1755-1315/118/1/012033

ISSN 8755-6839

SCIENCE OF **TSUNAMI HAZARDS**

Journal of Tsunami Society International

Volume 42 Number 3 2023

THE 26 DECEMBER 2004 EARTHQUAKE IN INDONESIA - FUTURE EARTHQUAKES AND TSUNAMIS IN THE SUMATRA-ANDAMAN MEGATHRUST REGION

George Pararas-Carayannis
Tsunami Society International

Future major earthquakes in the Sumatra-Andaman megathrust region can be expected to generate destructive tsunamis that will result in great losses of life and property in countries bordering the Andaman Sea Basin, Sumatra and the Indian Ocean. Megathrust earthquakes with moment magnitutes of Mw=9 or more, similar to the Mw=9.2+ of 26 December 2004, at convergent tectonic plate boundaries closer to the oceanic trench west of Sumatra, can be expected to generate very destuctive tsunamis, along populated coastal areas of Indonesia, but also to other countries bordering the Indian Ocean. In spite of the better understanding of the risks and of the protective measures that have been implemented since 2004, the destructiveness of future events is expected to be significant in the Andaman Sea basin, coastal areas of Sumatra and countries bordering the Indian Ocean. In order to estimate the recurrence frequency of future tsunami-generating earthquakes in the Sumatra-Andaman megathrust region similar to the 2004 event, the present study examines briefly existing geodynamic processes in the north and west of the Island of Sumatra, as well as past and recent tsunami generating earthquakes in the vicinity of the Andaman Sea Basin, including the Andaman and Nicobar groups of islands. Specifically examined is the Andaman fault system, recently prolonged through the Sumatra zone (the Sumatra fault), which has been reactivated due to the lateral escape of the Sumatra forearc sliver plate, and as a result of the oblique convergence and subduction with the Indo-Australian plate to the south. The present study reviews and analyzes the active mechanisms for different tectonic zones in this Sumatra-Andaman megathrust region, and provides an assessment of the potential for future destructive tsunamis, based mainly on the recent historic record, on active tectonic forces, and on evaluation of recurrence frequency.

Keywords: *tsunami; Sumatra-Andaman megathrust, tsunami vulnerability of India, Indonesia, Thailand, Bangladesh, Pakistan; historical tsunami records, Indian Ocean.*

1. INTRODUCTION

As in the past, tectonic subduction and thrust faulting along the Sumatra-Andaman megathrust region can be expected to generate large magnitude destructive earthquakes and tsunamis in the future, similar to the 26 December 2004 which had an estimated moment magnitude of Mw=9.1 later revised to Mw=9.3. With this revision this became the second largest earthquake in recent history after the Mw=9.2 Prince William Sound, Alaska earthquake of 28 March 1964, and the Mw=9.5 Valdivia, Chile of 22 May 1960. Although relatively infrequent, future Sumatra-Andaman megathrust earthquakes will result in great losses of life and property in countries bordering the Andaman Sea Basin, the Andaman and Nicobar groups of islands, eastern Sumatra and other countries in the Indian Ocean. The present paper reviews thoroughly the 26 December 2004 earthquake and tsunami, and estimates the reccurrence of a similar disaster in the future. Such a future event is expected because the Sumatra-Andaman megathrust region is a portion of the collision zone of subduction megathrust plate boundary. The Sunda-Java trench further southeast, also accommodates the convergence between the Indo-Australia and Sunda plates and is expected to generate large earthquakes and volcanic activity in the future. This convergence is responsible for the intense seismicity in both Sumatra and Java and further east on the great Sunda tectonic arc.

The present study presents a brief overview of historical earthquakes and tsunamis in the Andaman Sea, including the Andaman and Nicobar group of islands, all comprising the Sumatra-Andaman megathrust. Furthermore, the study analyzes the active mechanisms of the different tectonic zones in this region, and particularly provides a detailed account of the impact of the 26 December 2004 tsunami in regions bordering the Indian Ocean, as well an assessment of the potential for future destructive events, based mainly on the historic record, on active tectonic forces.

Specifically examined in this review is the Andaman fault system, recently prolonged through the Sumatra zone (the Sumatra fault), which has been reactivated due to the lateral escape of the Sumatra forearc sliver plate, and as a result of the oblique convergence and subduction with the Indo-Australian plate. Thus, the present study reviews and analyzes the active mechanisms for different tectonic zones in the Sumatra megathrust region, which includes earthquakes and tsunamis in the vicinity of the Andaman Sea Basin, and the islands of the Andaman and Nicobar group. Additionally provided is an assessment of the potential future destructive tsunamis in the Sumatra-Andaman megathrust region, based mainly on the recent historic record, on active tectonic forces, and on evaluation of recurrence frequencies as estimated, based on older and more recent studies (Berninghausen, 1966; Pararas-Carayannis, 1978, 2000, 2001a,b, c, 2003, 2005a,b, c, d, 2006a,b, 2007a,b; Bilham, EtAl. 2005; Ishii EtAl 2005, 2007; Krüger & Ohrnberger 2005; Rastogi & Jaiswal, 2006; Hutchings & Mooney 2021).

Finally included are brief descriptions of recent historical destructive tsunamis, and of expected future events. Subsequent studies will examine future potential tsunami generation in other Indian Ocean regions in the Inland Red Sea, the Arabian Sea, the Java Sea, the Persian Gulf, the Sea of Zanj, the Java Sea, the Bali Sea, the Flores Sea, the Timor Sea, the Celebes Sea, the Sea of Arafora, the Makassar Strait between Borneo and Sumatra, and the Malacca Straight between Malaysia and Sumatra.

2. MAIN SOURCES OF TSUNAMIGENIC EARTHQUAKES IN THE SUMATRA – ANDAMAN MEGATHRUST REGION

Complex on-going seismotectonic processes in the Indian Ocean are mainly the direct result of the Indian and Australian blocks moving northward at a rate ranging from 59 to 68 mm/year as shown in Fig. 1, and colliding with the Eurasian continent. There are several regions where large earthquakes have occurred in the past and destructive tsunamis were generated. The same regions can be expected to generate destructive tsunamis in the future that will adversely impact countries bordering the Indian Ocean. As stated in previous publications the main regions that are identified as more critical for future tsunami generation are: 1) The Andaman Sea Basin, 2) The Northern and Eastern Segments of the Great Sunda Tectonic Arc, 3) The Makran Subduction Zone in the Northern Arabian Sea, 4) The Karachi and deltaic Indus region and the Owens Fault Zone, 5) The Kutch Grabben region, and 6) The Chagos Archipelago.

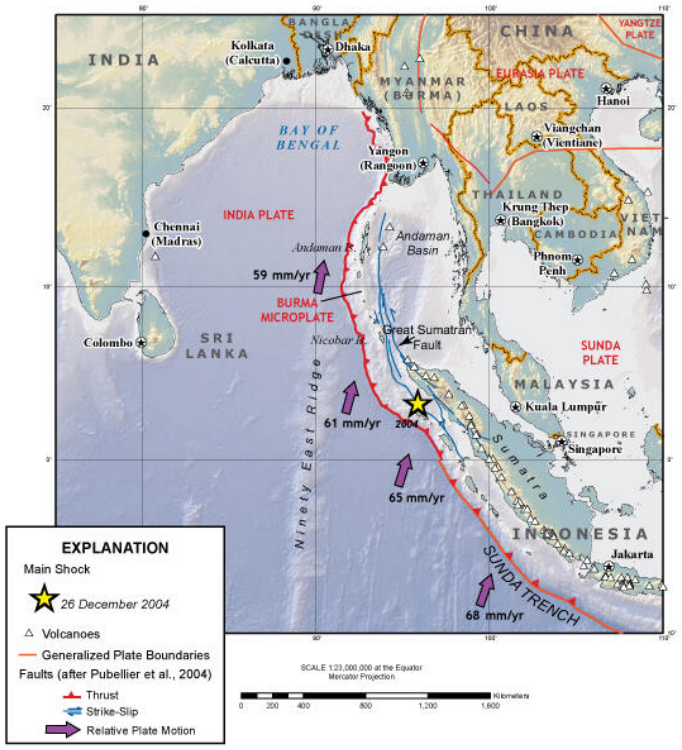

Fig. 1. Tectonic base map of the Sumatra subduction zone showing major faults and relative motion between the India and Sunda plates. Star marks the location of the main shock of the December 26, 2004 earthquake (USGS map)

Fig. 2 portrays an expanded view of the December 26, 2004 earthquake's tsunami generating area and its orientation paralleling the Sunda Trench along Northern Sumatra.

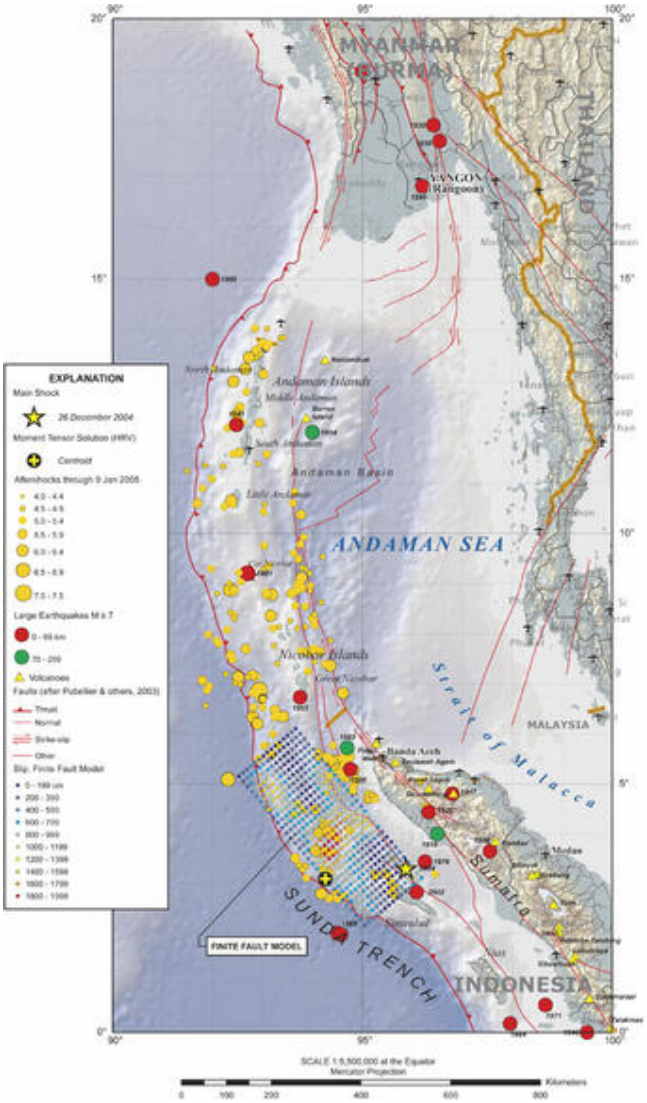

Fig. 2 Base map of the Sumatra subduction zone showing seismicity associated with the 2004 Sumatra-Andaman earthquake. (Figure based on info from the USGS Earthquake Hazards Program)

Fig. 3 is another illustration showing the local tsunami intensity and magnitudes of large earthquakes such as the 1994 and 2006 Java events, of the 2005 and 2007 Sumatra events, of the 1964 Alaska and 2004 Sumatra events, and of the 1960 Chile event. As shown the 2004 Sumatra earthquake had a moment magnitude of Mw=9.1, and a local tsunami intensity very close to that of the 1964 great Alaska earthquake (Pararas-Carayannis, 1967), both being even greater than that of the 1960 tsunami in Chile - the latter however being the strongest recorded earthquake which had a moment magnitude slightly greater than Mw=9.5.

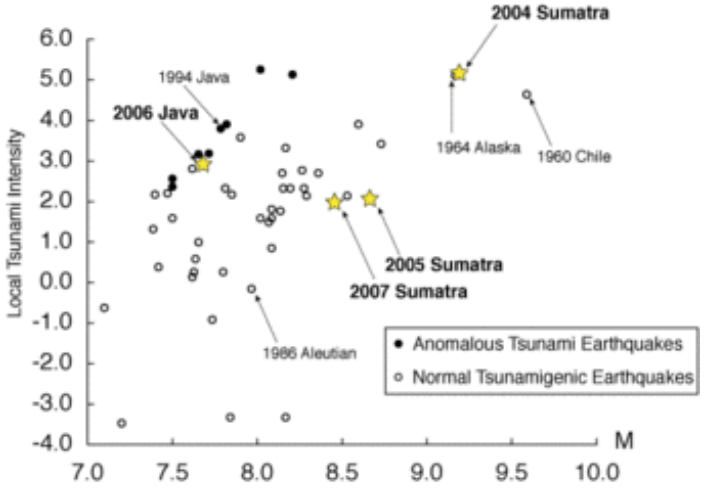

Fig. 3 Earthquake magnitude versus local tsunami intensity for subduction zone earthquakes from 1896-2005(Public Domain. Visit Media to see details)

The second largest earthquake of the 20th Century, and the largest ever recorded in the northern hemisphere, occurred in Alaska on 27 March 1964 (3/27/64, 05:36:14.0 p.m., local time; 3/28/64 03:36:14.0 GMT). This earthquake had a moment magnitude Mw=9.2 and caused extensive damage in Alaska. Local tsunami waves triggered by this earthquake were destructive in Prince William Sound, Valdez Bay, other areas of Alaska in the eastern Aleutian Islands, in Western Canada, Oregon, California and the Hawaiian islands January 2005 (Pararas-Carayannis G, 1967).

The present study reviews only the seismicity of the Sumatra-Andaman megathrust region, and the potential for future tsunami generation in this region of the Great Sunda Arc. Subsequent studies will address individualy the potential of other regions of the Indian Ocean, such as the Makran Subduction Zone in the Northern Arabian Sea, the Karachi and deltaic Indus region and the Owens Fault Zone, the Kutch Grabben region, and the Chagos Archipelago. The next section outlines briefly the 26 December 2004 Sumatra-Andaman earthquake and the tsunami that was generated.

3. THE GREAT EARTHQUAKE OF 26 DECEMBER 2004 ON THE SUMATRA-ANDAMAN MEGATHRUST

On Sunday, 26 December 2004, the greatest earthquake in 40 years occurred about 150 kilometers off the west coast of northern Sumatra Island in Indonesia. The earthquake generated a disastrous tsunami that caused destruction in 11 countries bordering the Indian Ocean. This great tsunamigenic earthquake occurred on Sunday, 26 December 2004, at 00:58:50 UTC (6:58:50 a.m. local time). The epicenter was at 3.298 N, 95.779 E and its focal depth was very shallow (much less than 33 km - possibly about 10km).The quake was widely felt in Sumatra, the Nicobar and Andaman Islands, Malaysia, Myanmar, Singapore, Thailand, Bangladesh and India.

According to the U.S. Geological Survey (USGS NEIC (WDCS-D)), the moment magnitude of the earthquake was Mw=9.1. Such magnitude would make this earthquake to be the third largest in the world in the twentieth century. However, on the basis of subsequent analysis of additional seismograms from around the world, scientists at Northwestern University determined the earthquake's magnitude to be Mw=9.3 and not 9.0 or 9.1, as originally estimated. Therefore, the calculated energy release was 1.13 X 10 (raised to the 30 power) dynes-cm, or three times larger than originally thought. The revised estimate makes this earthquake to be the second largest ever instrumentally recorded. The largest earthquake ever recorded, which measured 9.5, was in Chile on May 22, 1960.

The region where the great earthquake occurred on 26 December 2004, marks the seismic boundary formed by the movement of the Indo-Australian plate as it collides with the Burma subplate, which is part of the Eurasian plate. However, the Indo-Australian tectonic plate may not be as coherent as previously believed. According to recent studies reported in the Earth and Planetary Science Letters (vol 133), it apears that the two plates have separated many million years ago and that the Australian plate is rotating in a counterclockwise direction, putting stress in the southern segment of the India plate.

For millions of years the India tectonic plate has drifted and moved in a north/northeast direction, colliding with the Eurasian tectonic plate and forming the Himalayan mountains. As a result of such migration and collision with both the Eurasian and the Australian tectonic plates, the Indian plate's eastern boundary is a diffuse zone of seismicity and deformation, characterized by extensive faulting and numerous large earthquakes. See USGS graphic Fig. 4 below showing the migration of the Indian tectonic plate, and Fig. 5 showing the seismicity of Southern Asia.

Previous major earthquakes have occurred further north, in the Andaman Sea and further South along the Sumatra, Java and Sunda sections of one of the earth's greatest fault zones, a subduction zone known as the Sunda Trench. This great trench extends for about 3,400 miles (5,500 kms) from Myanmar (Burma) south past Sumatra and Java and east toward Australia and the Lesser Sunda Islands, ending up near Timor. Slippage and plate subduction make this region highly seismic. The volcanoes of Krakatau, Tambora and Toba, well known for their violent eruptions, are byproducts of such tectonic interactions.

The epicenter of the 26 December 2004 earthquake was near the triple point junction of three tectonic plates where major earthquakes and tsunamis have occurred in the past.

Previous major earthquakes have occurred further north, in the Andaman Sea and further South along the Sumatra, Java and Sunda sections of one of the earth's greatest fault zones, a subduction zone known as the Sunda Trench. This great trench extends for about 3,400 miles (5,500 kms) from Myanmar (Burma) south past Sumatra and Java and east toward Australia and the Lesser Sunda Islands, ending up near Timor. Slippage and plate subduction make this entire region highly seismic. The volcanoes of Krakatau, Tambora and Toba, well known for their violent eruptions, are byproducts of such tectonic interactions.

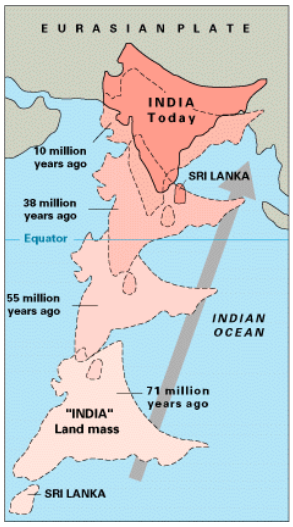

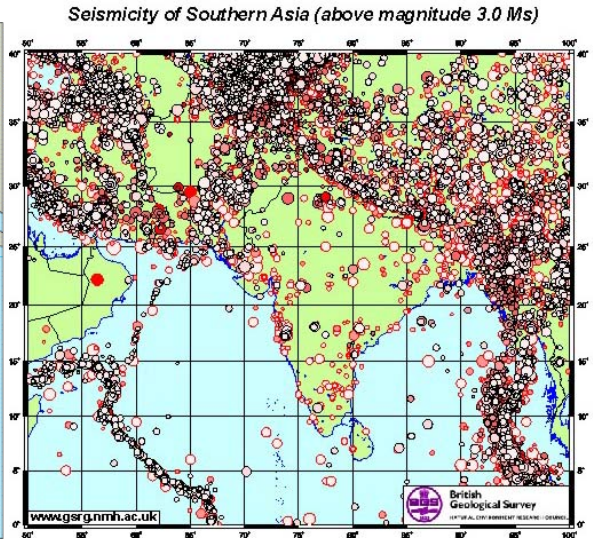

Fig. 4 Northward movement of India *Fig. 5 Seismicity of Southern Asia*

Previous major earthquakes have occurred further north, in the Andaman Sea and further South along the Sumatra, Java and Sunda sections of one of the earth's greatest fault zones, a subduction zone known as the Sunda Trench. This great trench extends for about 3,400 miles (5,500 kms) from Myanmar (Burma) south past Sumatra and Java and east toward Australia and the Lesser Sunda Islands, ending up near Timor. Slippage and plate subduction make this region highly seismic. The volcanoes of Krakatau, Tambora and Toba, well known for their violent eruptions, are byproducts of such tectonic interactions.

In addition to the Sunda Trench, the Sumatra fault is responsible for seismic activity on the Island of Sumatra. This is a strike-slip type of fault which extends along the entire length of the island. The Burma plate encompasses the northwest portion of the island of Sumatra as well as the Andaman and the Nicobar Islands, which separate the Andaman Sea from the Indian Ocean. Further to the east, a divergent boundary separates the Burma plate from the Sunda plate. More specifically, in the region off the west coast of northern Sumatra, the India plate is moving in a northeastward direction at about 5 to 5.5 cm per year relative to the Burma plate.

The 26 December 2004 earthquake was followed by numerous strong aftershocks. As of 1 January, 2005, there were about 84 aftershocks with magnitudes ranging from 5.0 to 7.0 in the region of Northern Sumatra and the Nicobar and Andaman Islands. Twenty six (26) of these - including the largest- occurred on 26 December 2004, the same day as the main earthquake. Since 1 January 2005, many more aftershocks have followed continued for several weeks and months. Some of the major aftershocks occurred in the vicinity of the epicenter of a past earthquake which had occurred on 26 June 1941 and some in the area near the Nicobar Islands where the 1881 earthquake had occurred. The distribution of afteshocls suggests that the earthquake resulted by the sudden slip of these two plates and that there was a slip as well as an upward thrust of the Burma plate along this boundary.

3.1 Chronological Sequence of Major Aftershocks Along the West Coast of Northern Sumatra and in the Nicobar and Andaman Island Region Following the Major Earthquake of 26 December 2004

The distribution of the larger aftershocks indicated that the two tectonic plates (the India plate and the Burma subplate) slipped for about 1,200 km along their boundary. The aftershocks extended from northern Sumatra (approximately 3 degrees North Latitude) to the Andaman Islands (approximately 14 degrees North). Therefore, the length of the overall rupture is estimated to be about 1,200 km. However, the slippage does not appear to have been continuous. It appears that it occurred in two phases along two sections of the great fault that parallels the Sunda Trench. The rupture started near the epicenter off the western coast of North Sumatra and progressed - at a fast rate - northward to the Andaman islands along a preexisting major fault. For the first 500-600 km the orientation of the rupture (the quake's strike) was appoximately 320-330 degrees. Subsequently the rupture continued - at a much slower rate in an approximate North-South direction - for another 500-600 km along another segment of the northern Sunda fault system. This is probably the same segment that ruptured during the 1941 Andaman Islands earthquake - which also generated a destructive tsunami.

It has been estimated that this megathrust faulting along the India and Burma boundary has resulted in a shift that averaged about 15 meters with maximum slip being 20 meters. The vertical upward movement of the sea floor may have been several meters - possibly as much as 5 meters or more in some places. At some of the islands there may have been subsidence while at others there was upthrusting.

3.2 The Great Tsunami of 26 December 2004 in the Indian Ocean

The great earthquake of December 26, 2004 was extremely damaging and resulted in many deaths. However, most of the destruction and deaths were caused by the catastrophic tsunami waves it generated. Massive tsunami waves wiped out entire coastal areas across southeastern Asia, Sri Lanka, India, Thailand, Myanmar and islands in the Andaman Sea and the Maldives in the Indian Ocean.

The tsunami waves caused considerable destruction and killed people more than 2,000 kilometers away, in the Seychelles and in Somalia. As of February 10, 2005, the global death toll

was raised to 226,566 and continued to rise. The demographics in this part of the world are not very good, so the final number of deaths cannot be established with certainty.. There are many remote islands in the Nicobar, Andaman, Maldives and off the African coasts, so there were many unreported deaths.

In total, the large tsunami struck 11 of the nations that border the Indian Ocean, and it was a complete surprise for the people living there, but not for the scientists who are aware of the tectonic interactions in the region. Many seismic networks recorded the massive earthquake, but there was no tide gauges or other wave sensors to provide confirmation as to whether a tsunami had been generated. There was no established communications network or organizational infastructure to pass a warning of any kind to the people coastlines. At the time, there was no Tsunami Warning System for the Indian Ocean as there was for the Pacific. The Pacific Tsunami Warning Center in Honolulu had no way of providing warning information to the region. Part of the problem was that most of the countries in the region had underestimated their potential tsunami threat from the Northern end of the Sunda Trench. Review of historical records would have revealed that a very destructive tsunami occurred in 1941, in the same general area. This particular tsunami killed more than 5,000 people on the eastern coast of India, but it was mistaken for a "storm surge". Thousands more must have gotten killed elsewhere in the islands of the Bay of Bengal in 1941, but there has been no sufficient documentation. Unfortunately, no Regional Tsunami Warning System, Preparedness Program, or effective Communications Plan existed at that time for this part of the world.

3.3 Tsunami Generating Area of the 2004 Earthquake on the Sumatra-Andaman megathrust

Based on the plate tectonics of the convergence zone that has formed the SundaTrench and on the earthquake's aftershock distribution, the tsunami generating area is believed to be a somewhat irregular, broken up ellipsoid which changes from a Northwest-Southeast orientation of about 330 degrees in the lower section to an almost North - South 360 degrees orientation in the upper section.

The major axis of this ellipsoid is estimated to be approximately 1,200 km and its minor axis to be about 180 km. It is believed that this ellipsoid type of block movement occurred along an oblique but very shallow subduction angle, and that the Burma subplate was thrusted upward by several meters (by as much as 5 meters in some places) with an oblique lateral movement of as much as 15 meters and possibly as much as 20 meters along the southern tsunami generating region. Also, the earthquake's relatively slow slippage along the 1,200 kms long rupture added additional energy to tsunami generation.

A preliminary estimate of the Tsunami Generating Area in Fig. 6 is a modified USGS map showing the earthquake epicenter, the distribution of initial major afteshocks, and the interaction of major tectonic plates along the Sunda Trench. A personal communication received by the author in early 2005 from Indonesia indicated that at Simeulue, an island close to the epicenter off the coast of Northern Sumatra, there was only vertical displacement but no tsunami. Surprisingly, residents of beach communities claimed that no tsunami waves were observed, no deaths from the tsunami were reported, but that the island

rose and was now several kilometers longer. No information was provided on how much the island rose, but preliminary data indicated that it may have been as much as 5 meters.

The reason that the tsunami did not cause deaths and destruction on Simeulu Island is because the amount of crustal uplift was greater than the height of the waves. Additional eyewitness accounts or observations helped clarify that this was indeed was the case. A preliminary estimate was that the tsunami generating area involved about 280-300,000 square kilometers of the ocean floor. This estimate was verified as more data on aftershock distribution became available and when tsunami travel times to operating tide gauge stations in the Bay of Bengal were obtained. Also, based on reports of subsequent field
surveys and subsequently collected data, helped determine the net underea crustal displacements on the islands off Sumatra and in the Nicobar and Andaman Islands, and a more accurate determination of the catastrophic tsunami generation of the 26 December 2004 earthquake.

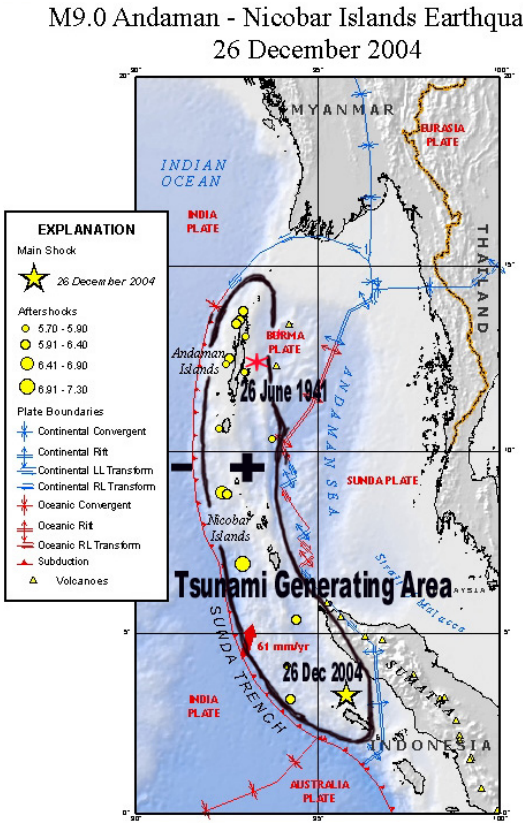

Fig. 6 Generating area of the 26 December 2004 Tsunami

These results have implications as to why Sri Lanka to the West of the tsunami generation area, suffered such a great impact, destruction and loss of lives.

3.4 THE TSUNAMI OF 26 DECEMBER 2004

3.4.1 Evaluation of Tsunami Reccurrence in the Region

Indonesia is surrounded by four major tectonic plates, the Pacific, the Eurasian, the Australian and the Philippine plates. All these major tectonic plates and their subplates are presently active. Major earthquakes and tsunamis can be expected in the semi-enclosed seas and along the Indian Ocean side of Indonesia. Major earthquakes in the semi-enclosed seas can generate destructive local tsunamis in the Sulu, Banda and Java Seas. Major earthquakes along the Sunda Trench can generate tsunamis that can be destructive not only in Indonesia but to other countries bordering the Indian Ocean.

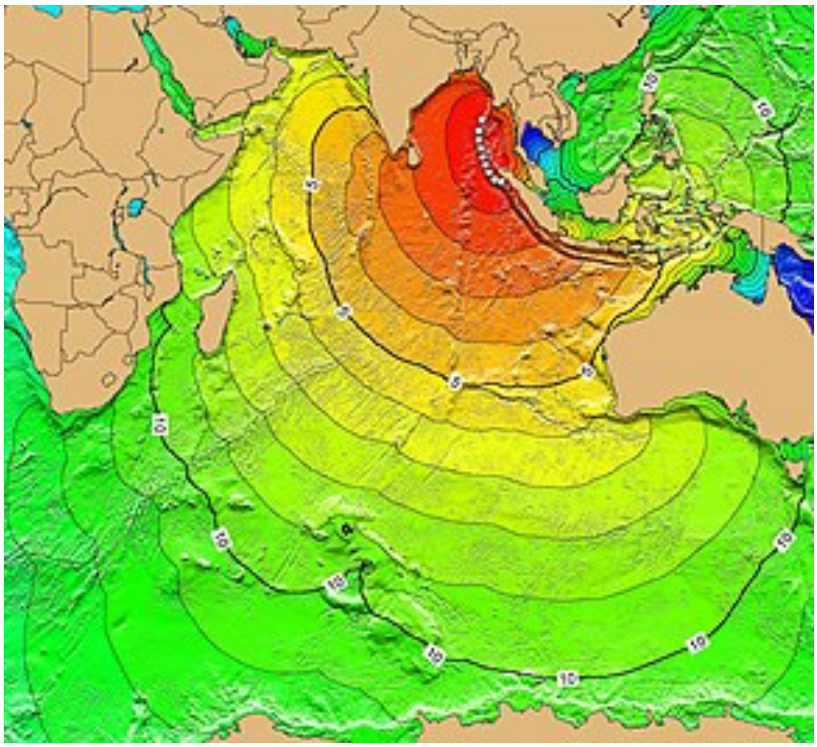

Fig. 7 Wave Refraction Map and Travel Times of the 2004 Tsunami in the Indian Ocean (Wikipedia)

In the immediate vicinity off Northern Sumatra, most of the stress and energy that had accumulated were released by the crustal movement that caused the 26 December 2004 earthquake. The subduction of the India tectonic plate underneath the Burma plate caused upward thrusting of an extensive block and generated the destructive tsunami. There was significant slip and rupture for about 600 km and possibly a less significant slip for another 400 km along the Nicobar and Andaman Islands (see Fig 8). Thus, it is unlikely that another major earthquake will occur in the immediate region off Northern Sumatra for a while, but stress has started building up again. Also, it is quite possible that not all of the energy was released in the Nicobar and Andaman section of the Sunda Trench by the 26 December 2004 earthquake - in which case the next major earthquake could occur there sooner than one closer to Northern Sumatra.

Fig. 8 Map of the Nicobar and Andaman Islands

Although the danger of another major tsunami has passed trmporarily in the region small local tsunamis could possibly be generated by smaller magnitude earthquakes. Aftershocks from such events can be expected to last for months in the region, but they would diminish in strength with the passage of time. Most of the aftershocks from subsequent to the 2004 earthquakes will result from the continuous gravitational adjustments of the crustal material that was moved during major earthquakes and the continuing stress to the North. Such aftershocks represent nature's way of restoring stability and temporary equlibrium. It is unlikely that a destructive tsunami will occur again soon in the same region, however caution is advised for the coastal residents in Northern Sumatra and in the Nicobar and Andaman islands. In fact, strong shaking of the ground in

an earthquake is nature's warning that a tsunami may be imminent.

Furthermore - and though stress in the region off Northern Sumatra has been released by the 26 December 2004 earthquake, this does not necessarily mean that another earthquake further north or further south cannot occur. In the North, a repeat of the 1881 Nicobar Islands or of the 1941 Andaman Islands earthquakes and tsunamis can be expected in the future - although it is difficult to say how soon (see Fig. 9 below). Such events seem to occur on the average of every 50 years so a strong, destructive earthquake is long overdue.

Further to the South, the movement of the tectonic plates added stress along other tectonic boundaries. A repeat of earthquakes and tsunamis along the Sunda Trench off the central region of Western Sumatra, as in 1833 (magnitude 8.7) and 1861, is very possible in the future (see Fig. 9). Such earthquakes and tsunamis can be expected every hundred years or so. In fact, the 26 December 2004 earthquake occurred along the section that did not rupture during the 1861 earthquake. It took approximately 144 years to occur. However, this does not mean that it will take that long for the next destructive tsunami to occur again off central or northern Sumatra. Destructive tsunamis are possible in the next 20 years or less. A repeat of the 1833 earthquake could generate a devastating tsunami. This section of the Sunda megathrust is one of the more likely sources of a destructive tsunamis in the region.

Malaysia - Despite Malaysia's proximity to the tsunami generating area, the impact of tsunami was not as severe as in other countries in the region or countries thousands of kilometers away. Malaysia was partly sheltered by Sumatra and the tsunami waves attenuated somewhat in the Straits of Malacca. However, there were numerous deaths and destruction reported. The country's worst affected areas were the northern coastal areas and the outlying islands. Hardest hit were Penang, Kedah, Perak, Selangor and Langkawi. It was reported that the red flag warning system used by lifeguards on beaches in some resort areas in Penang helped reduce fatalities there. Houses in fishing villages along coastal areas were damaged in Batu Maung and Bayan Lepas in Penang. Coastal areas in Peninsular Malaysia and 13 villages in Kuala Muda, Kedah and Kuala Triang in Langkawi Island were also affected. About a quarter of the boats anchored in Rebak and Telaga harbour in Langkawi were damaged. The number of deaths was reported as 67 or 68 with 52 in Penang, 10 in Kedah, 3 in Perak and 1 in Selangor. Another 6 were missing and presumed to be dead.

Myanmar - The mainland of Myanmar was somewhat sheltered from the full impact of the tsunami by the numerous offshore islands. Also the approximate North-South orientation of the tsunami generating area resulted in waves of lesser amplitude traveling northward. Still the tsunami caused numerous deaths and destruction in Myanmar. Reportedly 90 people were killed, but eyewitnesses estimated that more than 600 people died. 788 buildings were reported as damaged or destroyed, and 30,000 people were displaced.

Andaman and Nicobar Islands – The 2004 tsunami hit hard the Andaman and Nicobar group, which comprises of a total of 572 islands of which 38 were significantly inhabited. The waves

literally washed away some of these islands, and there were reports that the island of Trinket had split in two. The Great Nicobar and Car Nicobar were the worst hit among all the southern Nicobar Islands because of their proximity to the earthquake's epicenter and relative low topography. The maximum tsunami wave reached a height of 15 meters. According to reports one fifth of the population of the Nicobar Islands were killed, injured or missing. Chowra Island lost two thirds of its population of 1,500. The official death toll was 812, but about 7,000 were reported as missing. However the unofficial death toll (including those missing and presumed dead) is estimated to have been about 7,000 or greater. Previous major tsunamigenic earthquakes in 1881 and 1941 impacted severely both the Andaman and the Nicobar group of islands (Fig. 9). On 30 December 2004, four days after the great 2004 earthquake, the Barren volcano on Barren Island - located 135 kilometers (80 miles) northeast of the capital Port Blair - erupted.

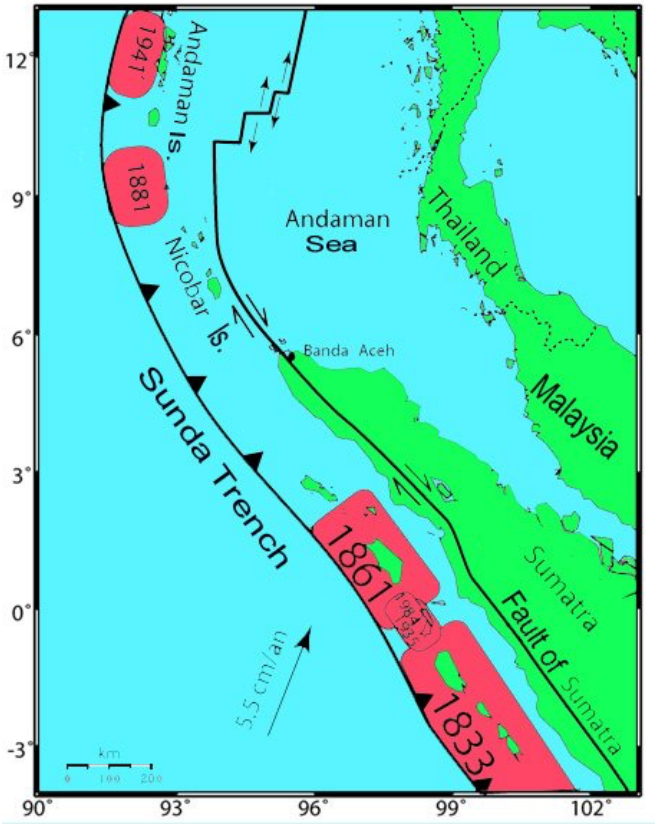

Fig. 9 Historical Earthquakes and Tsunami Generation areas of the 1941 and 1881 and of the 1861 and 1833 Earthquakes

Other seismic regions further South and East of Sumatra have the potential of generating destructive tsunamis even sooner. As in 1977, a major tsunami could be generated in the eastern section of the Sunda Trench that would affect not only Indonesia, but the northern and northwestern coasts of Australia.

Also impacted greatly by the 2004 tsunami was the Peninsula of Acep Meulaboh in Northern Sumatra - one of the hardest hit by the tsunami areas (Fig. 10).

Fig. 10 Peninsula of Acep Meulaboh in Northern Sumatra - one of the hardest hit by the tsunami areas.

3.4.2 Effects of the 26 December 2004 Tsunami in the Bay of Bengal and in the Indian Ocean

Waves of up to 10.5 meters in height struck Northern Sumatra, the Nicobar and Andaman Islands, Thailand, Sri Lanka, India. Destructive waves also struck the Maldives, Somalia, Kenya and the islands off the African coast. The tsunami was recorded by tide gauge stations not only in the Indian Ocean, but in the Pacific as well. In Manzanillo, Mexico, the tide gauge recorded a wave of 2.6 meters.

Eighteen (18) countries bordering the Indian Ocean were affected by the 2004 tsunami. These were: Indonesia, Thailand, India, Sri-Lanka, Malaysia, Myanmar, Bangladesh, Maldives, Reunion Island (French), Seychelles, Madagascar, Mauritius, Somalia, Tanzania, Kenya, Oman, South Africa and Australia.

Death Toll - The 2004 tsunami had its greatest impact and casualties in Indonesia, Thailand, India, Shri-Lanka, Malaysia, Myanmar, Maldives and Somalia. Eleven (11) countries reported deaths, some in tens of thousands.The reported death toll has been as 226,566. However, this is an underestimate as thousands more were reported as missing and many more may have been killed in remote islands. More than 1.5 million people were left homeless around the region.

The following is a brief summary compiled from numerous government, U.N., and media sources:

INDONESIA - Tsunami waves of the 2004 tsunami up to ten meters swamped the smaller outlying islands of Sumatra as well as its northern and western coastal areas - about 100 km (60 mi) from the earthquake epicenter. Hardesh hit was the northern Aceh province. Nearly all the casualties and damage took place within this province. Very heavy damage occurred as far South as Tapatkuan. The waves also propagated around the northern tip of Sumatra into the Straits of Malacca and struck coastal settlements along the northeast coast as far east as Lhokseumawe.

According to official reports (Ministry of Health) 166,320 people were killed, 127,774 were missing and 655,000 people were displaced in Northern Sumatra. A total of 110 bridges were destroyed, 5 seaports and 2 airports sustained considerable damage, and 82% of all roads were severely damaged. However the death toll was probably much higher. The following is a summary of the 2004 tsunami impact in Northern Sumatra:

Banda Aceh - The tsunami waves completely destroyed the city of Banda Aceh's infrastructure and killed thousands of its inhabitants. Banda Aceh is the capital of the Aceh province. in Northern Sumatra. Fig. 11 is a satellite image of Banda Aceh peninsula taken on 2 Jan 2005.

Fig. 11 Another Satellite image of Banda Aceh taken on 2 Jan 2005

Leupung - The tsunami completely obliterated Leupung, a town in the district (Kabupaten/Kota) of Aceh Besar, close to the city of Banda Aceh. Most of the town's 10,000 inhabitants perished. It is estimated that only two to seven hundred people survived.

Gleebruk - The waves completely destroyed Gleebruk, a village in the district (Kabupaten/Kota) of Aceh Besar just to the southwest of Banda Aceh.

Teunom - The tsunami hit hard Teunom, a town of 18,000 people in the Aceh Barat (West Aceh) district of the Province of Aceh. According to official estimates about 8,000 people lost their lives.

Calang - The waves completely devastated Calang, the capital of the district. Only about 30 per cent of the town's population survived. Prior to the tsunami the town's population was estimated to be between 9,000 and 12,000.

Meulaboh - A series of seven waves killed about 40,000 people and destroyed port facilities and most parts of Meulaboh, a town with a population of 120,000. About 50,000 people were left homeless.

Simeulue Island - Tsunami waves of about 5 meters in height struck the island. Although Simeulue was close to the earthquake's epicenter, suprisingly none of the island's 70,000 inhabitants were killed by the waves. Only five people died as a result of the earthquake which destroyed about 90% of all buildings along the coast. Apparently, the island rose which accounts for the lower wave heights that were observed. Also, villagers on the island had an awareness of the dangers of tsunamis, emphasized by traditions memoralizing a destructive tsunami in 1907 that had killed thousands of people.

Nias Island - The island was severely impacted by the tunami which killed many people and severely damaged all existing infrastructure. Original official accounts gave the number of dead at 122, but these appear to be underestimates. According to unconfirmed sources the waves killed 600 people and the final death toll may ecxeed 1,000.

THAILAND – The tsunami struck six provinces in West Thailand causing great damage and deaths. Figure 12 is a map of Thailand, showing in red the areas and coastal areas that which were impacted. The first of the tsunami waves reached the resort of Phi Phi island. The arrival of the tsunami was heralded by a recession of the water, which exposed the sea bottom for considerable distance, including previously submerged rocks. According to eyewitness reports, the first wave arrived at about 10:30 am local time and it was about 4 meters high. The second wave arrived about 2.5 minutes later and it was 7 meters. The third wave was about 11 meters. The waves destroyed all beachfront hotels, bungalows and other structures at Phi Phi, hurling boats and other floating objects. All electricity and phone lines were cut. The highest reported wave was 11.6 meters at Khao-Lak beach (Fig. 14). Thai Government sources initially reported 5,313 deaths, 8,457 injuries and 4,499 missing, including more than 1,000 foreign tourists. Many of the missing were presumed to have died. Most probably the death toll was higher than what it was initially reported. Fig. 13 is a photo of tsunami destruction at Thailand's Khao Lak Beach.

Fig. 12 Inundation of the 2004 tsunami in Thailand

Fig. 13 Tsunami destruction at Thailand's Khao Lak Beach

INDIA

The estimated number of casualties in India was reported at 16,000, with at least 6,000 more as missing. Then death toll was probably underestimated. Along India's southeastern coast, several villages were swept away, and thousands of fishermen at sea were missing. On the western coast of India' mainland, hardest hit was the state of Tamil Nadu. Many tourist hotels in India had to be evacuated. The following is a brief description of some of the 2004 tsunami impact on coastal regions of India.

Andhra Pradesh - There was significant loss of life and destruction. The affected districts were Krishna, Prakasam, Nellore, Guntur, West Godavari and East Godavari.

Kerala - The tsunami killed many people (official toll 168) and caused extensive destruction particularly at Kollam (131 dead), Alappuzha (32) and Ernakulam (5) were also affected.

Pondicherry - In the Union territory of Pondicherry, the affected districts were Pondicherry (107 dead), Karaikal (453 dead). The latest official toll was 560. An estimated 30,000 people were rendered homeless.

Tamil Nadu - The tsunami had a great impact on the state of Tamil Nadu on India's mainland with entire coastal villages destroyed. According to official reports the overall death toll in the state was 7,793. The Nagapattinam district had 5,525 casualties. The latest reported death toll at Velankanni was 1,500. Kanyakumari district has had 808 deaths, Cuddalore district 599, the state capital Chennai 206 and Kancheepuram district 124. The death tolls in other districts were Pudukkottai (15), Ramanathapuram (6), Tirunelveli (4), Thoothukudi (3), Tiruvallur (28), Thanjavur (22), Tiruvarur (10) and Viluppuram (47). The death toll may be significantly higher as many are still missing. The nuclear power plant at Kalpakkam was shut down after seawater rushed into a pump station. No radiation leak or damage to the reactor was reported.

SRI-LANKA

The first of the tsunami waves took a little over two hours to reach Sri-Lanka. A clock on the western side of Sri Lanka at Colombo stopped at 9:20 in the morning, so the tsunami travel time to Colombo (first wave) must have been about 2 hours and 20 minutes. Sri-Lanka's south and east coasts were hardest hit. More than 50,000 people lost their lives - mostly children and the elderly. Most of them (more than 1,200) were in the eastern district of Batticaloa.

At Trincomalee in the northeast, the tsunami reached more than 2 km (1.25 mi) inland killing about 800 people. In the neighboring Amparai district alone, more than 5,000 people died. The naval base at Trincomalee was reported to be submerged. About 3,000 more people died in Mullaitivu and Vadamaradchi East. A train, known as the "Sea Queen", while traveling between Colombo and Galle, with 1,600 passengers on board, was struck and derailed by the tsunami. Only about 300 of the passengers survived. More than one and a half million people were displaced in Shri-Lanka and the death toll is expected to rise.

MALDIVES

The waves flooded two-thirds of Male, the capital. Hardest hit were the outlying low-level atolls. Some other low-lying islands were completely submerged, including some where major resorts were located. Preliminary reports stated that the tsunami killed 82, that 26 were missing, and that there was extensive destruction. However, communications with remote islands were down and the death toll must have been higher than what was reported. Thirteen islands were abandoned because all buildings were destroyed and the fresh water supply was contaminated by seawater.

SOMALIA

The tsunami waves traveled a distance of 4,500 km (2,800 miles) and struck Somalia on Africa's east coast. The height of the tsunami waves was unknown. Hardest hit was the semi-autonomous Puntland area, particularly the region between Hafun in the Bari region and Garacad in the Mudug region. The narrow and low-lying peninsula of Hafun, 1,150km (715 miles) northeast of Mogadishu, was particularly devastated.

The waves caused devastation in the Puntland area, striking the town mosque of Brava and destroying the villages of Beyla, Garacad, Muduy and Nugaal. Other coastal areas including Lower Juba were also affected. At Kulub and Hurdiye, all the fishing boats were either lost or destroyed.

According to a UN report 1,180 homes and 2,400 boats were destroyed. The main bridge, which connects Hafun to the mainland, was washed away. Te flooding rendered freshwater wells and reservoirs unusable. A total of 298 people lost their lives and 50,000 more were displaced. The final death toll is expected to rise as there are many more missing.

AUSTRALIA

No casualties were reported. The tsunami caused minor flooding along the northwestern coast and surging activity was reported along Western Australia. At Geraldton, 425 km north of Perth, several boats were ripped from their moorings. At Busselton, 325 km south of Perth, a father and son in a boat were washed out to sea, but were subsequently rescued. Swimmers at Christmas Island were sucked 150m out to sea by the tsunami. Subsequently they were carried safely back to shore.

BANGLADESH

The tsunami's impact was relatively mild. The waves killed two children and capsized a tourist boat.

KENYA

There was minor damage. One person was report

3.4.3 Lessons Learned from the 26 December 2004 Tsunami in the Indian Ocean

There were many lessons already learned from this tragic event in Southeast Asia. Indeed a bitter lesson has been already learned - that great earthquakes and destructive tsunamis do occur in this region of the Indian Ocean and will occur again in the near future. The magnitude of the 2004 tsunami disaster could have been mitigated with a proper disaster preparedness plan and a functioning early warning system. A warning perhaps could not have been of much help in the immediate tsunami generating area of Sumatra and the Nicobar and Andaman Islands and Northern Sumatra, because the tsunami waves reached the shore very quickly. However the strong shaking by the earthquake should have been nature's warning for the local residents that a tsunami was imminent and they should have run to higher ground to save their lives. A simple program of public education and awareness of the potential hazards could have saved many lives in the immediate area.

For the more distant coastlines of India, Shri-Lanka, and other locations in the Bay of Bengal and the Indian Ocean, there was ample time to issue a warning - if only an early warning system existed for this region of the world and if there was a way of communicating the information to the coastal residents of threatened areas. No such warning system existed at that time. It was reported that in many areas where there was extensive losses of lives, when the water withdrew before the arrival of the tsunami, the local residents went to the shore to collect stranded fish, instead of running to higher ground. People were totally unaware of the imminent danger. A simple educational program on hazard awareness could have prevented the extensive losses of lives - particularly of children. One third of those that perished were children.

The Tsunami Warning System - which operates in the Pacific Region - did not have at that time the capability of extending a warning to countries bordering the Indian Ocean. Although the magnitude and location of the earthquake were quickly determined, there were no wave sensors in the area to confirm the generation of a tsunami. Although both Indonesia and Thailand were members of the Pacific Tsunami Warning System network, they did not at that time operate wave sensors on the western coasts of their islands and territories.

Also India and Shri Lanka were not members of the International Tsunami Warning System in the Pacific and up to that disaster they had not shown interest in joining any regional early warning system. An erroneous belief persisted that tsunamis do not occur frequently enough to warrantee participation into a regional tsunami warning system. Local government authorities in the region did not even have a plan for disseminating warning information to the threatened coastlines - even if a warning had been provided. There was not even a basic educational plan for disaster preparedness. However, since 2004 countries bordering the Indian Ocean have initiated programs that will reduce similar tragedies and losses in the future. It should be obvious that such programs are necessary to prevent similar tragedies in the future.

4. THE ANDAMAN SEA BASIN

The Andaman Sea Basin (see Fig. 1) is is a forearc sliver plate and a seismically active region at the southeastern end of the Alpine-Himalayan belt. Its seismicity is extensively covered in the scientific literature (Sinvhal et al.1978; Verma et al. 1978). The seimotectonic history of the region indicates that an extensional feature developed along a
leaky transform segment of the megashear zone - the Andaman fault - between the Indo-Australian domain and the Sunda-Indochina block (Uyeda and Kanamori, 1979; Taylor and Karner, 1983). This old shear zone acted as a western strike slip guide for the extrusion of the Indochina block 50-20 My ago, (Tapponnier et al., 1986) - and in response to the indentation of the Indian tectonic plate into the Eurasian block. Collision of Indochina with the Sunda and Australian blocks stopped this crustal extrusion process. Subsequently, the Andaman fault system, recently prolonged through the Sumatra zone (the Sumatra fault), reactivated due to the lateral escape of the Sumatra forearc sliver plate, and as a result of the oblique convergence and subduction with the Indo-Australian plate.

4.1 Potential for Large Earthquakes and Tsunamis in the Andaman Sea in the Future.

Most of the earthquakes along the eastern Andaman fault system involve lateral movements, as this represents an elongated extension of the strike-slip type of the great Sumatra faulting which extends along the entire length of the island. Earthquakes along this eastern region of the basin do not generate significant tsunamis. However, the western side of the sliver plate is an extension of the northern Sunda Arc boundary, which can break – as the 26 December 2004 and the 1941 events demonstrated - and generate destructive tsunamis. Furthermore, the region where the 2004 earthquake occurred was a seismic gap region where great stress had accumulated over the years. When this earthquake occurred, the Indian plate subducted the Burma plate and moved in a northeast direction. This movement caused further dynamic transfer and loading of stress to both the Australian and Burma plates, immediately to the south, on the other side of the triple junction point near Padang (Pararas-Carayannis, 2005, 2006, 2007). The following is a cursory evaluation of potential future earthquakes and of tsunami generation in the Andaman Sea basin. Fig. 1 showed the Andaman Sea Basin and the northern section of the Indonesian Island of Sumatra, as well as the southwestern coast of Thailand.

The present study reviews previous studies and expands on an analysis of potential future destructive earthquakes and the projected tsunami generation from this region of the Andaman Sea. Fig. 4 showed the northward movement of the Indian and Australian blocks and the collision with Asia. Fig. 5 showed the seismicity of southern Asia and the partial distribution of earthquake epicenters with Ms magnitude above 3 in the northern Indian Ocean. Active subduction and sinistral crustal movements in the Andaman Sea Basin, have caused many minor and intermediate earthquakes, a few major events, and only one known earthquake with magnitude greater than 8. The historical record indicates that on 2 April 1762, an earthquake with a moment magnitude estimated to be between 8.5–8.8 M_w
at the Arakan Coast off Myanmar generated the earliest known tsunami in the Bay of Bengal (Rastogi & Jaiswal, 2006).

According to a study at the Australian National University of the fault model for this 1762 Arakan earthquake (Cummins, 2007), its rupture had length of 700 km, NS, a width of 125 km along the eastern coast of the northern Bay of Bengal, and a slip of 10 m. In brief, the author chose parameters to reproduce roughly the observed subsidence and uplift associated with this earthquake with the fault's upper edge coincident with the deformation front, thus estimating the maximum offshore heights of the generated tsunami, recognizing though that the onshore run-up could be much greater, and finally concluding that giant tsunamigenic earthquakes have occurred in the past off the coast of Myanmar and will occur again in the future. Fig. 14 below pertains to the earthquake tsunami generating area of the 1762 Arakan event and of the maximum offshore tsunami height in meters.

Specifically, on October 1847, an earthquake near the Great Nicobar Island generated a tsunami, but no details are available. On 31 December 1881 a magnitude 7.9 earthquake near Car Nicobar, generated yet another tsunami in the Bay of Bengal. Its height recorded at Chennai was one meter.

During an eighty year period from 1900 to 1980, a total of 348 earthquakes were recorded in the area bounded by 7.0 N to 22.0 N and 88.0 E to 100 E. These earthquakes ranged in magnitude from 3.3 to 8.5 (Bapat, 1982), but only five of these had magnitudes equal to or greater than 7.1 and generated tsunamis (Murty and Bapat, 1999). For the shorter period from 1916 to 1975, only three of the earthquakes had magnitudes greater than 7.2 and generated significant tsunamis. (Verma et al., 1978).

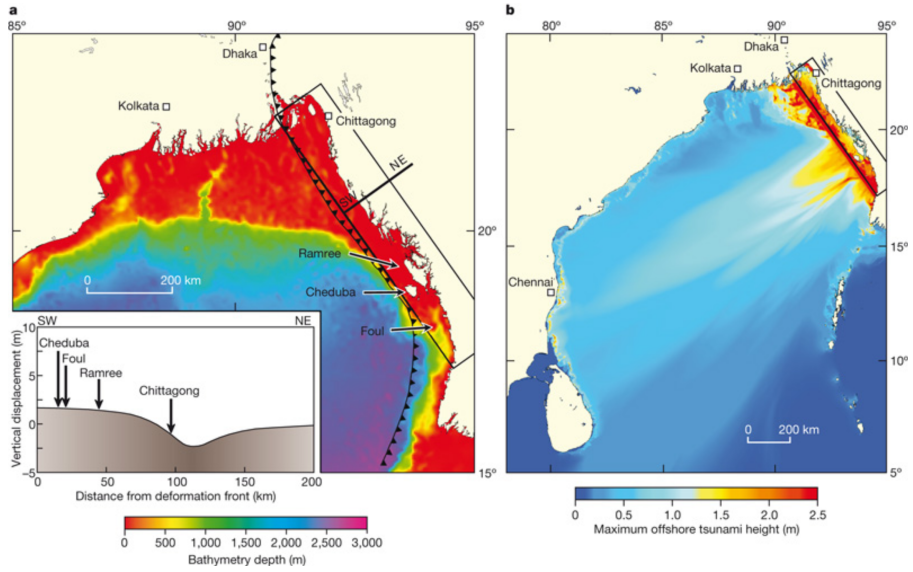

Fig. 14. Models for the 1762 Arakan earthquake and tsunami (after Cummins, 2007)

Until the great earthquake of 26 December 2004 (Pararas-Carayannis 2005; Ishii EtAl 2005, 2007; Krüger & Ohrnberger 2005; Rastogi & Jaiswal, 2006; Hutchings & Mooney 2021), only the earthquake of 26 June 1941 had been the strongest ever recorded in the
vicinity of the Andaman and Nicobar Islands (Fig. 15) in generating a destructive tsunami. Two other earthquakes on 23 August 1936 and 17 May 1955, with magnitudes 7.3 and 7.25, respectively, did not generate tsunamis of any significance.

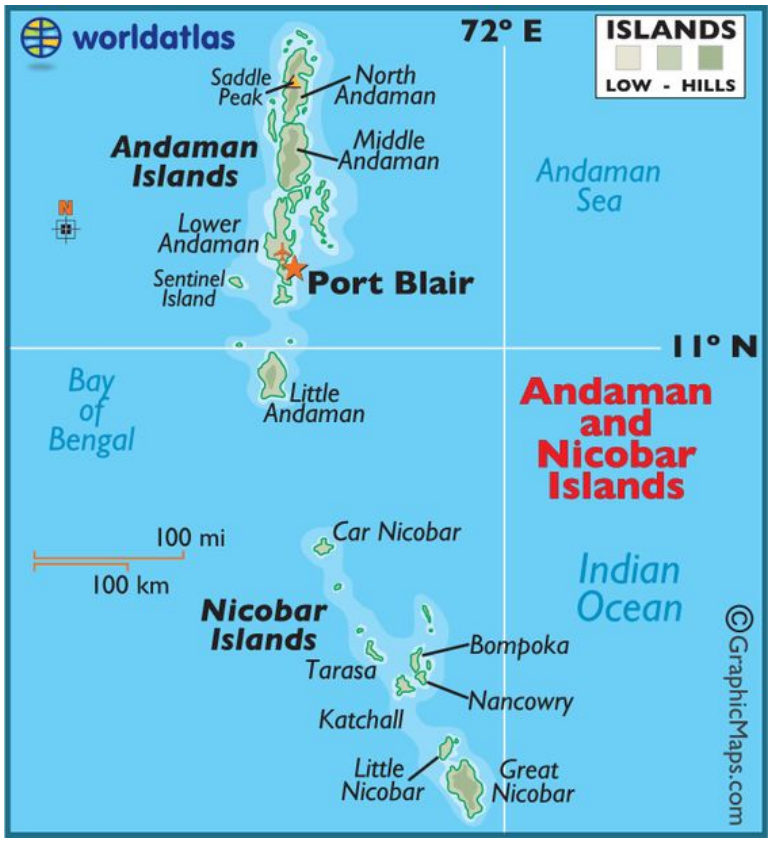

Fig. 15. World Atlas map of the Andaman and Nicobar Islands, North of Sumatra are the two main island groups separating the Bay of Bengal and the Andaman Sea (image of GraphicMaps.com)

Based on the statistical information, it can be concluded that most of the earthquakes in the Andaman Sea Basin, even those with magnitudes greater than 7.1, do not usually generate significant tsunamis. The possible reason for the low number of tsunamis is that most of the

earthquakes in the Andaman Sea are mainly associated with strike-slip type of faulting that involves lateral crustal movements. The exception was the 26 December 2004 earthquake which, not only ruptured the Great Sunda Arc along the northern Sumatra region but also ruptured the same segment in the Andaman Sea as that in 1941. A possible explanation for the extreme tsunami generated in the Andaman segment on 26 December 2004 is that this event had a different mechanism and involved both thrust and bookshelf faulting within the compacted sediments of the Andaman Sea segment of the Great Sunda Arc (Pararas-Carayannis, 2005).

In view of the above historical record, it can be reasonably concluded that large earthquakes along the northern end of the Great Sunda subduction boundary in the Andaman Sea do not occur frequently. However, events with magnitudes greater than 7.1
have the potential of generating local destructive tsunamis. Finally, earthquakes with magnitude 8.0 or greater, associated with "dip-slip" types of vertical crustal displacements along thrust faults, have the potential of generating very destructive tsunamis. Reccurence of such larger magnitude events may be expected in the future, although rather infrequently.

5. FUTURE TSUNAMIGENIC EVENTS ALONG THE NORTHERN AND EASTERN SEGMENTS OF THE GREAT SUNDA TECTONIC ARC

The tectonic arc and the great trench formed by movement of the Indian and Australian tectonic plates and collisions on the eastern boundary have created a zone of subduction known as the great Sunda Arc. This zone extends for about 3,400 miles (5,500 kms) south from Myanmar, past Sumatra and Java and east toward Australia and the Lesser Sunda Islands, ending up near Timor. Fig. 16 is a map of the subduction zone of the great Sunda tectonic arc on the Indian Ocean. Also shown are major fault zones along the Island of Sumatra and on Celebes Island in the Banda Sea, and future potential tsunami generation in the marginal seas of the Indian Ocean, can be expected in the future.

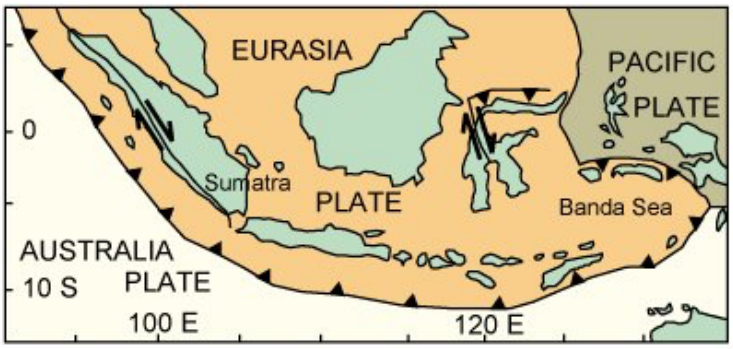

Fig. 16. Map of the subduction zone of the great Sunda tectonic arc in the Indian Ocean, and on major land fault zones along Sumatra and on Celebes Island in the Banda Sea.

In brief, the Sunda Arc is an island-arc structure of about 17,000 islands spread out along a belt of intense volcanic and seismic activity. Such tectonic features characterize the region with a deep oceanic trench on the Indian Ocean side, a geanticline belt and volcanic inner arc, and several marginal basins. This region of the Indian Ocean has about 400 volcanoes, of which about 100 are active. The best known of these volcanoes is Krakatau in the Sunda Strait, between Java and Sumatra. The 1883 explosion and collapse of this volcano generated an enormous tsunami that killed close to 37,00 people (Pararas-Carayannis, 2003). Also, other volcanoes such as Tambora have the potential of generating catastrophic tsunamis that could have an impact on the islands and countries bordering the Andaman Sea

The Sunda Arc comprises of two distinct zones of subduction North of Sumatra (Fig. 17). In the eastern part, further south which is relatively old (more than 100 million years), oceanic lithosphere subducts offshore from Java.

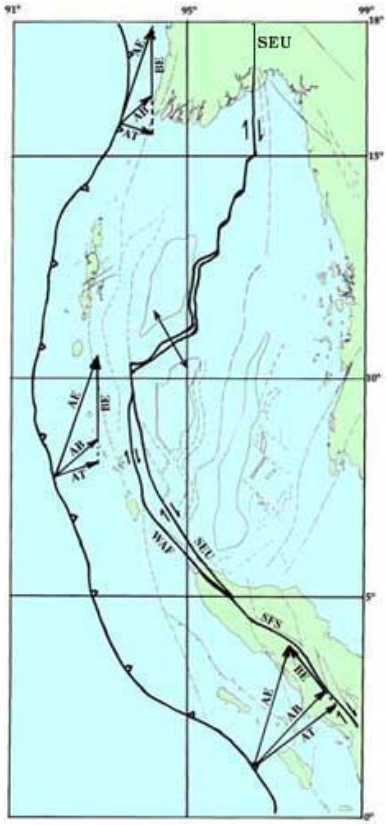

Fig. 17. Subduction zone and directionality of crustal movements of major faults along the northern segment of the Great Sunda tectonic arc near northern Sumatra and the Andaman and Nicobar Islands further North.

The younger (40 million years) northwest segments of the Arc mark the boundaries formed by the movement of the Indo-Australian plate as it collides with the Burma sub-plate, which is part of the Eurasian plate. A divergent boundary separates the Burma plate from the Sunda plate. The Burma sub-plate encompasses the northwest portion of the island of Sumatra as well as the group of the Andaman and the Nicobar Islands (Fig. 17).

In the region off the west coast of northern Sumatra, the India plate is moving in a northeastward direction at about 5 to 5.5 cm per year relative to the Burma plate. Because of this migration and collision with both the Eurasian and the Australian tectonic plates, the India plate's eastern boundary has become a diffuse zone of seismicity and deformation, characterized by extensive thrust faulting and numerous large earthquakes that can generate destructive tsunamis in the future that could affect the Andaman and Nicobar islands and countries bordering the Andaman Sea.

5.1 Potential for Future Tsunami Generation in the Andaman Sea and along the Northern and Eastern Segments of the Great Sunda Tectonic Arc.

Major and great earthquakes and tsunamis occur in the Andaman Sea and further south along the Sumatra, Java and Lesser Sunda segments of the great Sunda Arc. As shown in Fig. 18 of the northern segment of the great Sunda tectonic arc, the 12 September 2007 earthquake occurred offshore.

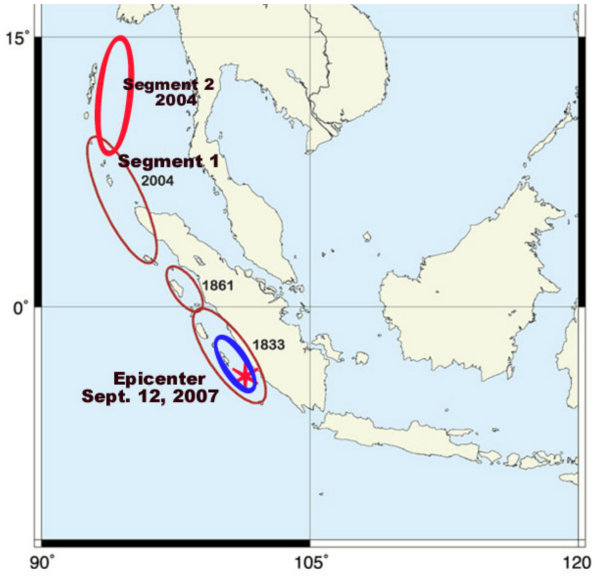

Fig. 18. Estimated dimensions of the tsunami generating source areas off the coast of the island of Sumatra and the Andaman Sea associated with the earthquakes of 1833, 1861, 2004, 2005 and 2007 (Pararas-Carayannis, 2005) https://www.drgeorgepc.com/Tsunami1833Indonesia.html

Following is a review of studies of the different segments of the Great Sunda Tectonic Arc (Newcom & McCann, 1987). Also included is a summary of the seismic history and tectonics of the Sunda Arc with accounts and illustrations of past historical earthquakes (Fig. 18), which most likely will occur again in the future and may have an impact on islands and countries bordering the Andaman Sea.

Shown in Fig. 18 are major earthquakes which occurred in 2004 (on two segments 1&2) which generated tsunami events near the Andaman and the Nicobar Islands but also impacted the countries bordering the Andaman Sea Basin. Earthquakes in 1861, 1833 and 12 September 2007 generated destructive tsunami waves which, because of source orientation toward the south-west, had very little or no impact in the Andaman Sea Basin.

Apparently along the Northern and Easten segments of the Great Sunda megathrust (Fig. 19), destructive earthquakes and tsunamis can be expected to recur at least every hundred years, or even more frequenly in the near future, as each earthquake results in seismic stress tranference on adjacent tectonic blocks. Examples of such seismic stress transference is that caused by the 30 March 2005 and the 12 September 2007 tsunamigenic earthquakes shown above in Fig. 18.

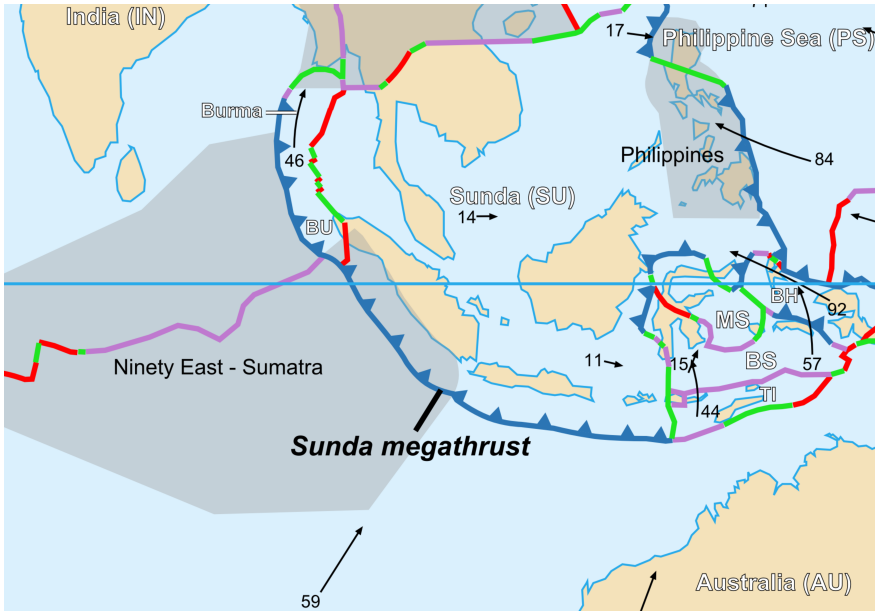

Fig.19. The Sunda megathrust and other subduction zones in adjacent seas of the Indian Ocean where future tsunamigenic earthquakes can be expected..

5.2 Sumatra Segment Tectonics – Past and Future Earthquakes and Tsunami

To summarize, the northern segment of the Great Sunda arc is one of the most seismically active regions in the world. The northern segment and its extension into the Andaman Sea is a region where large earthquakes and tsunamis can be expected frequently in the future. As the 26 December 2004 event demonstrated, tsunamis originating from this region can impact severely islands and countries bordering the entire Indian Ocean and the Andaman Sea (Pararas-Carayannis, 2005).

Because of seismic stress tranference, tsunamigenic earthquakes can be expected to occur in sequence, as the earthquake 28 March 2005, with revised moment-magnitude Mw=8.6 Mw, demonstated on the Sunda megathrust (see Fig. 18 above) near the Nias-Simeulue Island chain, paralleling the west coast of northern Sumatra. This earthquake generated a destructive tsunami of 3.0 meters (9.8 feet), and 915 to 1,314 people on the island of Nias lost their lives injuring also 1,146 people. This event occurred only three months after the great 25 December 2004 earthquake off the coast of northern Sumatra.

Also, the historic record shows that large earthquakes with magnitude greater than seven struck the offshore islands of Western Sumatra in 1881, 1935, 2000, and 2002. Earthquakes with magnitude greater than M=8 struck the same region in 1797, 1833, 1861, 2004, 2005, and as recently as on 12 September 2007, as shown in Fig. 18 (Pararas-Carayannis, 2007). Subduction of the India and Australian plates beneath the Burma plate was the cause, and this process will apparently continue in the near future. The following is a brief summary of some of the events cited above and of their expected recurrences in approximately the same areas, as in the past. Based on the history of past destructive earthquake and tsunami events, future large earthquakes are expected to occur in the region, which will generate destructive tunamis that will impact not only Sumatra and other areas of the Indian Ocean, but also the islands and countries bordering the Andaman Sea Following is a brief review of some of the historical earthquake and tsunami events in this region of Sumatra that could also affect the countries bordering the Andaman Sea, although to a lesser extent because of the southwest orientation of tsunami sources along the Sunda megathrust. Following is a brief discussion of major past events in the Andaman Sea, and adjacent Seas which had a far-reaching impact in coastal commuities in countries bordering the entire Indian Ocean.

The 25 November 1833 Earthquake and Tsunami - This was a significant Sumatra earthquake with a moment magnitude of 8.8 to 9.2 M_w which occurred on 25 November 1833 (see Fig. 9). Destructive tsunami waves struck mainly the southerwestern coast of the island. There are no reliable records of the loss of life, with the casualties being described only as “numerous”. The magnitude of this event has been estimated using records of uplift taken from coral microattolls (Natawidjaja EtAl, 2006; Rastogi & Jaiswal, 2006; (Pararas-Carayannis, 2005c - http://drgeorgepc.com/Tsunami1833Indonesia.html).

The 1861 Sumatra Earthquake and Tsunami. This Sumatra earthquake of 16 February 1861 (see Fig. 9), was one of a series of events on the Sunda megathrust which generated a tsunami off the west coast of the island and caused several thousands of deaths. It was the last in a sequences of earthquakes that ruptured adjacent parts of the Sumatran

segment of the Sunda megathrust. The earthquake was felt as far away as the Malay peninsula and the eastern part of Java (Newcomb & McCann, 1987). A future reccurence of a large magnitude earthquake on this segment of the Sunda megathrust is expected to also generate a tsunami which will affect the islands in the Andaman Sea, but not to the same extend because of the orientation of the fault zone and the tsunami maximum wave propagation towards the South-West of the Indian Ocean.

The 31 December 1881 Car Nicobar Earthquake and Tsunami. On 31 December 1881 (see Fig. 9) a submarine earthquake beneath the Andaman Islands generated a tsunami with a maximum crest height of 0.8 meters, which was recorded by tide gauges surrounding the Bay of Bengal. Very little is known about its rupture parameters or location. Modeling study of the tsunami indicates that it was generated by a $M_w = 7.9 \pm 0.1$ rupture on the India/Andaman plate boundary and that there was an uplift of 10–60 cm of the island of Car Nicobar (Ortiz & Bilham, 2003). Specifically, the referenced study concluded that the rupture consisted of two segments. The northern 40-km-long segment was separated from the southern 150-km-long segment by a 100-km region corresponding to the westward projection of the West Andaman spreading center. Also stated was that the main rupture of this earthquake occurred between 8.5°N and 10°N, had a total area of 150 km × 60 km, a dipping 20°E, and a mean slip of 2.7 m. The recurrence time for 1881-type of events was estimated to be about 114–200 years, based on the basis of inferred GPS convergence rates and inferred plate closure vectors, although slip partitioning in the region may extend this estimate by as much as 30%, a rather long period of time.

The 28 March 2005 Nias-Simeuele Earthquake and Tsunami. The Nias–Simeulue earthquake occurred on 28 March 2005 off the west coast of northern Sumatra in Indonesia (Fig. 19). The event caused panic in the Northern Sumatra region, which had already been devastated by the massive tsunami waves of 26 December 2004, but this earthquake generated a relatively smaller tsunami damage, although at least 915 people were killed, mostly on the island of Nias.

The earthquake had a focal depth of 30 kilometers (19 miles) and a moment magnitude of 8.6. It was the third most powerful earthquake since 1965 in Indonesia. What was surprising about this event was that it occured in less than three months after the great earthquake of 26 December 2004 and in close proximity. For two great earthquakes to occur so close to each other in time and space was very unusual. The affected area was 200 kilometres (120 mi) west of Sibolga, Sumatra, approximately halfway between the islands of Nias and Simeulue, or 1,400 kilometres (870 mi) northwest of Jakarta. Usually, when a great earthquake occurs, most of the stress is relieved and another great earthquake may not occur for many years in the same region. However, this is not always the case, as dynamic stress loading can accelerate the occurrence of another earthquake along an adjacent seismic zone. Sometimes the opposite occurs and the release of energy on one segment, may also release stress on an adjacent seismic fault. In this case it appears that the process
was accelerated rather than delayed. Both of the recent earthquakes had their epicenters near the triple junction point where the Indian, Australian and Burma tectonic plates meet. Triple junction points of tectonic plates, particularly in areas of active subduction, are some of the most seismic areas of the world - capable of causing great earthquakes and tsunamis (Pararas-Carayannis, 2005d). The 1960 Great Chilean Earthquake and Tsunami originated near such a triple point tectonic junction.

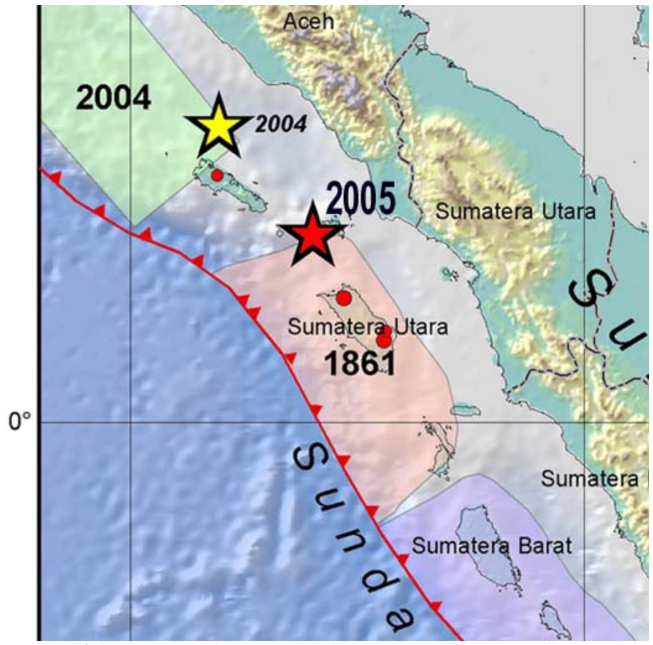

Fig. 19. Epicenter of the 28 March 2005 Earthquake in relation to the epicenter of the 26 December 2004 and the region affected by the 1861 earthquake (Modified USGS graphic)

The 17 July 2006 Earthquake and Tsunami - Fig. 20 below shows the epicenter of a more recent 12 July 2006 earthquake and the area of its tsunami generation.

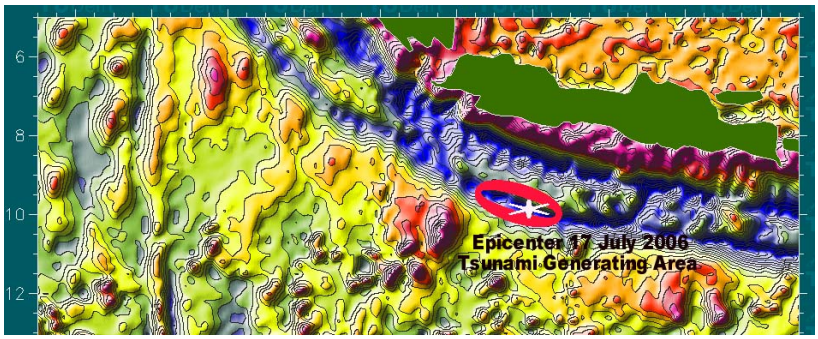

Fig. 20 Epicenter of the 12 July 2006 earthquake and the area of tsunami generation

5.3 Summary of Expected Future Tsunamigenic Earthquakes Along the Northern and Eastern Segments of the Great Sunda Tectonic Arc

To summarize, the tectonic regime of the great Sunda tctonic arc is complex and characterized by geomorphologically evident active faulting and syntaxis which accomodate the continuous morthward translation and collision of the Indian plate into the Eurasian plate. This is the northwestern segment of the Sunda subduction system, where the Indian Plate subducts beneath the Sunda plate in a nearly arc-parallel direction. The entire segment ruptured during the 26 December 2004 great Andaman-Sumatra earthquake. This thrust-dominated plate boundary and the extrusion of crust in its eastern side results in highly oblique strike-slip dominated boundaries which extend through Myanmar (Bates & Jackson 1987; Wang EtAl. 2014; Booth EtAl. 2009), and thus it is expected to have a impact on the seismicity, not only of the Andaman Sea, but also along the Great Sunda Arc. However this process is extremely slow, so it is thus difficult to predict or forecast the interactions and reccurence periods of both earthquake and tsunami events in the region.

When the 26 December 2004 earthquake occurred, the Indian plate subducted the Burma plate which moved in a northeast direction. This movement caused dynamic transfer and loading of stress not only to the North but also to both the Australian and Burma plates, immediately to the south, on the other side of the triple junction point. As a result of such load transfer, the Australian plate also moved in relation to the Burma plate and probably rotated somewhat in a counterclockwise direction, causing the subsequent great earthquake of 28 March 2005. However, the block that moved was relatively small. It is very difficult to forecast on whether this movement will continue and will stress load another segment of the great Sunda fault to the north and thus cause another earthquake and tsunami soon. However, another great earthquake similar to that of 1833 (magnitude 8.7) along the south coast of the western Sumatra, will eventually occur. That particular earthquake generated a great tsunami. The waves may have been as much as 10 to 15 meters on the western coast of Sumatra. Luckily, most of the energy from that tsunami was directed towards the unpopulated regions of the southwest Indian Ocean. When such an event will occur again, cannot be predicted with any certainty. The only thing known with certainty is that it will occur in this region. Thus, a Coulomb stress transfer analysis, based on rupture parameters and the geometric distribution of aftershocks for both the 26 December 2004 and the 28 March 2005 events, would help establish the space-time evolution of stresses and perhaps help determine both static and dynamic modifications that could possibly trigger future tsunami events along known faults in the region that may have an impact along northern Sumatra and in the Andaman Sea. Most of the energy from such tsunami will be directed towards the unpopulated regions of the southwest Indian Ocean. When such an event will occur again, is difficult to predict. The only thing known with certainty is that it will occur in this region near Sumatra. Thus, a Coulomb stress transfer analysis, based on rupture parameters and the geometric distribution of aftershocks for both the 26 December 2004 and the 28 March 2005 events, would help establish the space-time evolution of stresses and help determine both static and dynamic modifications in this region. In summary, major earthquakes can be expected to occur further southeast along the central coast of Sumatra in the next few years. Any such major earthquake with magnitude greater than 7 could generate a tsunami in the region, but its impact in the

Andaman Sea is not expected to be significant. Also, Talang volcano on Sumatra could experience a major eruption in the distant future.

In conclusion, because of load transfer, the Australian plate moved in relation to the Burma plate and probably rotated somewhat in a counterclockwise direction, causing the great earthquake of 28 March 2005. In fact, the 2005 earthquake had occurred in the same region as the 1861 earthquake (see Fig. 18). The block that moved was relatively small in comparison, thus the tsunami that was generated was not very destructive. However, following the great earthquakes of 2004 and 2005, it appears that there was additional significant transference of tectonic stress further south/southeast to the central region of Western Sumatra. The latest great earthquake (magnitude 8.2) of September 12, 2007 (see Fig. 18) and the other two events and aftershocks (and later a fourth event) occurred even further south/southeast and within the segment that ruptured when a great (estimated magnitude Mw=8.7) earthquake occurred in 1833 (Pararas-Carayannis, 2007). Apparently, the September 12, 2007 earthquake (Fig. 18) had a smaller magnitude and length of rupture than the 1833 event, which had generated a much greater tsunami. The shorter rupture (estimated roughly at about 200 km), and the smaller magnitude, was the probable reasons for the smaller 2007 tsunami. Fortunately, the energy release by two other earthquakes, which occurred subsequently in sequence, helped release gradually the tectonic stress along this segment. This may have contributed to the relatively smaller tsunami that was observed in Padang and elsewhere. This did not occur when the 1833 earthquake had struck the same region. All the energy of the 8.7 earthquake in 1833 was released at once and the rupture zone may have been as much as 300 km long, or even more. The effects of the 1833 tsunami in the region were probably great but poorly documented.

It remains to be seen if the earthquake of September 12, 2007 resulted not only from partial subduction but also from counterclockwise rotation of the Australian plate. Such rotation, with diminished vertical uplift, could account for the smaller 2007 tsunami. Further field studies of uplift and lateral motions on the offshore islands would confirm if the mechanism of the 2007 event was different from the one that generated the 1833 tsunami. Field studies on Sipora, North Pagai and South Pagai Islands of the outer-arc ridge of the great Sunda Arc, indicate that the great 1933 earthquake resulted in vertical uplift of up to 2.3 meters. Such extensive vertical uplift generated the greater tsunami. The uplift caused by the September 12, 2007 earthquake may have been much less than that of 1833.

In brief, destructive tsunamis can be generated from earthquakes originating anywhere along this northern segment of the tectonic boundary of the Sunda megathrust. Earthquakes and tsunamis similar to the 2007, 2005, 2004 and 1833 events can be expected every hundred years - or even more frequently - in this northern segment. This particular section of the megathrust along the western coast of the northern, central and southern Sumatra is one of the more likely sources of destructive tsunamis in the region in the future. Fig. 20 (see also Fig. 2) graphically illustrates the active ongoing processes of subduction West and North of the Island of Sumatra and extending to the Nicobar and Andaman Islands to southern Myanmar and Thailand.

A repeat of a single large earthquake with the same rupture and source dimensions as those of the 1833 or 2004 events, could generate devastating tsunamis that could affect Sumatra and other distant regions of the Indian Ocean such as Thailand, Sri Lanka, India, the Maldives, the Arabian Peninsula and northern Africa and somewhat the Andaman Sea region. Also, the northern segments of the great Sunda arc are source regions of tsunamis that can be particularly destructive in the Bay of Bengal, as well. The primary reason is the geographical orientation of this segment of the seismic zone and the directivity of maximum tsunami energy peopagation. Most of the energy of tsunamis generated further east along the coasts of Java or the Lesser Sunda Islands would tend to focus toward southern Africa and Australia and are not expected to be as significant in terms of destruction.

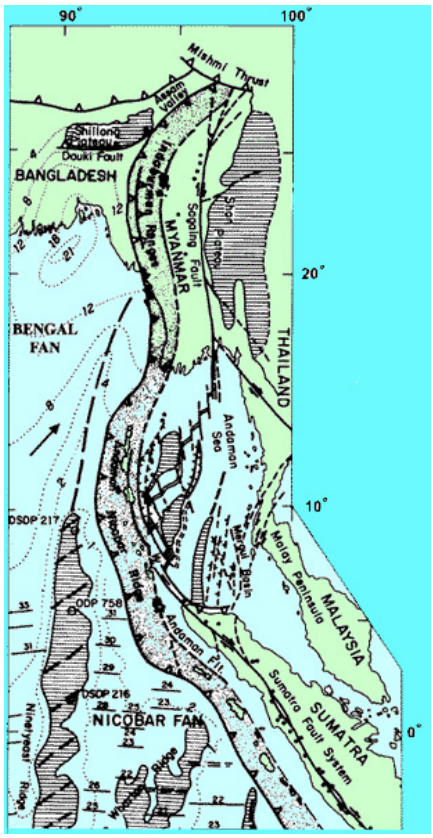

Fig. 20 Subduction zone West and North of the Island of Sumatra, of the land section of the Sumatra Fault System, and its NNW extension to Nicobar and Andaman Islands South of Myanmar.

5.4 The tectonic regime of the Andaman Sea and of Myanbar (Burma) - – Past and Expected Future Tsunami Generation

Fig. 20 illustrates the zone of subduction zone West of the Island of Sumatra, the land section of the Sumatra Fault System and its NNW extension to Nicobar and Andaman Islands South of Myanmar, as well as the secondary faults and offsets north of Sumatra near the Thailand border.

5.5 The Tectonic Regime of the Lesser Sunda Islands Segment – Past and Expected Future Tsunami Generation

The tectonic regime of the Great Sunda tectonic arc further southeast of the Andaman Sea region is also complex, active, and characterized by geomorphologically evident active faulting. In this region of the East Java Trench the rate of subduction is about 50 mm/yr. As previously stated, on August 19, 1977 a great earthquake with a moment magnitude Mw=8.3, westward of Sumba Island, generated a destructive tsunami which had observed run-up heights of up to 5.8 meters (19 ft) and a maximum run-up height of 15 meters at a certain location. This earthquake was the largest outer-rise earthquake ever recorded in Indonesia and its aftershocks along the trench extended for about 130 kilometres (81 mi) eastward and 110 kilometres (68 mi) westward from the epicenter (Gusman EtAl., 2009). The waves penetrated about 500 meters inland, killed more than 200 people, and left 3900 homeless (Pararas-Carayannis, 1977: Natawidjaja EtAl, 2006; Borrero EtAl., 2006). What was unusual about this earthquake was the fact that it had a very large magnitude for a shock with a normal faulting focal mechanism, in the southern segment of the Sunda Trench where other tsunamigenic earthquakes have occurrred in the past (Kopp, 2011) and that the tsunami waves had great height amplitude. Another destructive tsunamis occurred in 12 December 1992 at Flores Island and yet another one in 1994 in the same region (Pararas-Carayannis, 1992, 1994), but because of the tsunami's source orientation towards the southwest, no significant wave was recorded or observed on the shores of the Andaman Sea.

6. CONCLUSIONS

The Sumatra fault has been reactivated due to the lateral escape of the Sumatra forearc sliver plate, and as a result of the continuous oblique convergence and subduction with the Indo-Australian plate to the south. The seismic stress on the Sumatra-Andaman megathrust is continuing. Megathrust earthquakes with moment magnitutes of Mw=9 or more, similar to the 26 December 2004, at convergent tectonic plate boundaries closer to the oceanic trench west of Sumatra and the offshore islands, can be expected to generate very destuctive tsunamis in the future, along populated coastal areas of Indonesia, but also in other countries bordering the Indian Ocean. Given the high rate of continuous northward movement of the Sunda plate at a yearly rate of up to 68 mm/year as it collides with
Eurasia, it is estimated that major earthquakes on the Sumatra-Andaman megathrust region

– including the Sumatra Fault System and its NNW extension to Nicobar and Andaman Islands South of Myanmar - a major earthquake can be expected to occur at intervals of about 40 years more or less.

Future major earthquakes on this megathrust region can be expected to generate destructive tsunamis that may result in great losses of life and property in countries bordering the Andaman Sea Basin, Sumatra and the Indian Ocean, but hopefully to a much lesser extent than in 2004, now that better programs of warning, preparedness, and public education have been adopted for this immediate region, and tsunami warning systems have been instituted. In spite of such programs, the destructiveness of future events can be expected to be significant in the Andaman Sea basin, coastal areas of Sumatra and countries bordering the Indian Ocean, thus programs of preparedness and of public education must be continuous.

Continuous population growth rate and increased use of coastal areas, as well as rapid industrialization, excessive urbanization or lack of adequate planning, will contribute significantly to the vulnerability of coastal cities in Indonesia, Thailand, Bangladesh, India, and other countries bordering the Indian Ocean. Large metropolitan coastal cities like the Mumbai Metropolitan Region (MMR), will be particularly vulnerable to future tsunami disasters. The high population density and the uneven growth rate in similar metropolitan coastal areas will result in several environmental collateral problems. Effective strategies for mitigating future tsunami disasters will require more than warning systems or sophisticated instrumentation for detection and measurements of earthquake and tsunami parameters and the communication of warnings. Effective strategies for tsunami and other collateral disaster mitigation will require the adoptation of coastal management policies that integrate wisely economic developmental activities, land use, and engineering standards into a holistic framework of environmental goals that can provide maximum public safety and effective tools for sustainability following tsunami disasters in such urban coastal regions.

REFERENCES

Ambrasseys, N. and Bilham, R., 2003, *"Earthquakes and Associated Deformation in North Baluchistan 1892-2001"*, Bulletin of the Seismological Society of America, Vol .93, No. 4, p. 1573 - 1605.

Bapat, A. (1882). *"Tsunamis and earthquakes in the Bay of Bengal",* Tsunami Newsletter, International Tsunami Information Center, Honolulu, Volume XV, No. 3, 36-37.

Bates, R.L.; Jackson, J.A. (1987). *Glossary of geology (Third ed.).* American Geological Institute. p. 668. ISBN 9780913312896.

Berninghausen, W. H., (1966). Tsunamis and Seismic Seiches reported from regions adjacent to the Indian Ocean, Bull. Seism. Soc. Am., 56 (1), 69-74.

Bilham, R, R. Engdahl, N.Feld, and S.P. Sayabala (2005). Partial and complete rupture of the Indo-Andaman plate boundary 1847-2004, Seism. Res. Lett., 76 (3), 299-311.

Borrero, J.C.; Sieh K.; Chlieh, M. & Synolakis C.E. (December 26, 2006*). "*Tsunami inundation modelling for western Sumatra". Proceedings of the National Academy of Sciences. 103 (52): 19673

Booth, A.L.; Chamberlain, C.P.; Kidd, W.S.F.; Zeitler, P.K. (2009). "Constraints on the metamorphic evolution of the eastern Himalayan syntaxis from geochronologic and petrologic studies of Namche Barwa". *Bulletin of the Geological Society of America*. **124** (3–4): 385–407. doi:10.1130/B26041.1.

Bulletin Seismological Society of America, 2005, Tsunamis and Seismic Seiches reported from regions adjacent to the Indian Ocean, Bull. Seism. Soc. Am., 56 (1),pp. 69-74.

Byrne Daniel E., Sykes Lynn R. Davis Dan M., 1992. *"Great thrust earthquakes and aseismic slip along the plate boundary of the Makran subduction zone"*. JOURNAL OF GEOPHYSICAL RESEARCH, VOL. 97, NO. B1, PAGES 449–478, 1992

Closs, H., Bungenstock, H., Hinz, K., 1969. *"Ergebnisse seismischer Untersuchungen im nrdlichen Arabischen Meer: ein Beitrag zur internationalen Indischen Ozean Expedition."* METEOR Forschungsergebnisse, Reihe C, 2, 28 pp. Flueh, E. R., Kukowski, N., Reichert, C. (Editors). FS Sonne Cruise Report SO-123 - MAMUT, Maskat - Maskat 07.09. - 03.10.1997, GEOMAR Rep. 62, 292 pp.

Cummins P. R., 2007, Austrakian National University. *"The potential for giant tsunamigenic earthquakes in the northern Bay of Bengal"*. Nature 449(7158):75-8, October 2007 DOI:10.1038/nature06088

Dasgupta, S., Pande, P., Ganguly, D., Iqbal, Z, Sanyal, K, Venkatraman, N.V., Dasgupta, S., Sural, B., Harendranath, L., Mazumdar, K., Sanyal, S., Roy, K., Das, L.K., Misra, P.S., Gupta, H., *"Seismotectonic Atlas of India and its Environs"*, Geological Survey of India, 2000.

Dorostian A., Gheitanchi M. R., 2003, *"SEISMICITY OF MAKRAN*" European Geophysical Society 2003. *Tectonics of a Lateral Transition Between Subduction and Collision:The Zagros-Makran Transfer Deformation Zone (SE IRAN)"*, Geophysical Research Abstracts, Vol. 5, 01210, 2003.

Fahmi M. N., Realita A., and Madlazim, 2022. *"RUPTURE KINEMATIC PROCESS OF THE MW 5.9 SERAM EARTHQUAKE IMAGED BY BACK-PROJECTION TECHNIQUE FOLLOWED BY THE TSUNAMI"*. Science of Tsunami Hazards,Vol. 41, N4, pp 370-382.

Fruehn, J., White, R. S. and Minshull, T. A., 1997. *"Internal deformation and compaction of* Haider H., LodhiH.A.; LeVeque R. J. "Tsunami simulations for Karachi and Bombay: Sensitivity to source parameters of the 1945 Makran earthquake the Makran accretionary wedge", Terra Nova, 9: 101-104.

Gusman, A. R.; Tanioka, Y.; Matsumoto, H.; Iwasaki, S. (2009). *"Analysis of the Tsunami Generated by the Great 1977 Sumba Earthquake that Occurred in Indonesia"*, *Bulletin of the Seismological Society of America, **99** (4): 2169–*

Hamilton, W., 1979. "Tectonics of the Indonesian region"/ *U.S. Geological Survey Prof. Paper 1078*.

Heck, N.H. (1947). List of seismic sea waves, Bull.Seism. Soc. Am., 37, 269-286.

Heidarzadeh M., Pirooz M. D., Zaker N. H.,. Yalciner A.C., Mokhtari M., Esmaeily, 2008. *Historical tsunami in the Makran Subduction Zone off the southern coasts of Iran and Pakistan and results of numerical modeling*. Ocean Engineering 35 (2008) 774–786 www.elsevier.com/locate/oceaneng

Jacob, K. H. and Quittmeyer, R. L., 1979. *"The Makran region of Pakistan and Iran: Trench-arc system with active plate subduction".* In: Farah, A. and de Jong, K. A. (Editors), Geodynamics of Pakistan: 305-317.

Kopp, H. (2011). *"The Java convergent margin: structure, seismogenisis and subduction processes*". In Hall, Robert; Cottam, Michael A.; Wilson, Moyra E. J. (eds.*)*. The SE Asian Gateway: History and Tectonics of the Australia—Asia Collision. Bath: Geological Society of London. pp. 111–*138.* ISBN 9781862393295

Macmurdo, Captain (1821). Account of the earthquake which occurred in India in June 1819, Edinburgh Phil.J. 4, 106-109.

Middlemiss, C.S., *"The Kangra Earthquake of 4th April 1905",* Memoirs of the Geological Survey of India, vol. 38, 1910 (1981 Reprint).

Minshull, T. A., White, R. S., Barton, P. J. and Collier, J. S., 1992. Deformation at plate boundaries around the Gulf of Oman, Marine Geology, 104: 265-277.

Mokhtari, M. and Farahbod, A.M. 2005. *"Tsunami Occurrence in the Makran Region".* Tsunami Seminar, Tehran, 26 February 2005

Natawidjaja, D.H.; Sieh K.; Chlieh M.; Galetzka J.; Suwargadi B.W.; Cheng H.; Edwards R.L.; Avouac J.-P. & Ward S. N. (2006). *"Source parameters of the great Sumatran megathrust earthquakes* of 1797 and 1833 inferred from coral microatolls "(PDF). *Journal of Geophysical Research*. **111**(B06403): n/a. Bibcode:2006JGRB..111.6403N. doi:10.1029/2005JB004025. hdl:10220/8480

Newcomb, K.R. and McCann, W.R. (1987). Seismic history and tectonics of the Sunda Arc, JGR, 92 (B1), 421-439.

Ortiz, M., and Bilham, R. (2003). Source Area and Rupture Parametres of the 31 December 1881 Mw=7.9 Car Nicobar Earthquake estimated from tsunamis recorded in the Bay of Bengal, J. Geophys. Res- Solid Earth, 108(4), ESE 11, 1-16.

Pakistan Meterological Department 2005. *"History of Tsunamis in Pakistan/Arabian Sea",* Report, January 2005.

Pararas-Carayannis G, 1967; "Source Mechanism Study of the Alaska Earthquake and Tsunami of 27 March 1964, The Water Waves". Pacific Science. Vol. XXI, No. 3, July 1967. Seehttp://www.drgeorgepc.com/Earthquake1964Alaska.html, and https://www.yumpu.com/en/document/read/48535641/a-study-of-the-source mechanism-of-the-alaska-earthquake-and-

Pararas-Carayannis, G., 1978. *"The Earthquake and Tsunamis of 19 August 1977 in the Lesser Sunda Islands of Indonesia".* ITIC Progres Reports for 1976-1977 prepared for the 1978 Sixth Session of ITSU in Manila, Philippines. http://drgeorgepc.com/Tsunami1977Indonesia.html

Pararas-Carayannis, G. 1989. *"Five-Year Plan for The Development of A Regional Warning System in the Southwest Pacific".* A Report prepared to the United Nations Development Program (UNDP), New York, May 1989, 21 p**.**

Pararas-Carayannis, G., 1992. *"The Earthquake and Tsunami of 2 September 1992 in Nicaragua"* http://drgeorgepc.com/Tsunami1992Nicaragua.html

Pararas-Carayannis. G. 1998. The Earthquake and Tsunami of 17 July 1998 in Papua-New Guinea. On site field survey for the United Nations Development Program (UNDP) as part of a Five Year Plan for the Development of a Regional Tsunami Warning System in the Southwest Pacific Ocean. http://www.drgeorgepc.com/Tsunami1998PNG.html

Pararas-Carayannis, G., 2000. ASSESSMENT OF INDIA'S VULNERABILITY FROM POTENTIALLY DESTRUCTIVE EARTHQUAKES AND TSUNAMIS - Land Use and Engineering Guidelines in Alleviating Future Disaster Impacts and Losses. Main Presentation at Conference of

Pararas-Carayannis, G., 2001a. *"The Earthquake of 25 January 2001 in India"*

Pararas-Carayannis, G., 2001b. *"The Earthquake and Tsunami of 28 November 1945 in Southern Pakistan"* http://drgeorgepc.com/Tsunami1945Pakistan.html

Pararas-Carayannis, G. 2001c. *"The Great Tsunami of August 26, 1883 from the Explosion of the Krakatau Volcano ("Krakatoa") in Indonesia"* http://drgeorgepc.com/Tsunami1883Krakatoa.html

Pararas-Carayannis, G., 2003. *"Near and far-field effects of tsunamis generated by the paroxysmal eruptions, explosions, caldera collapses and massive slope failures of the Krakatau volcano in Indonesia on August 26-27, 1883"*. Presentation for the International Seminar/Workshop on Tsunami "In Memoriam 120 Years of Krakatau Eruption - Tsunami And Lesson Learned From Large Tsunami", August 26th - 29th 2003, Jakarta and Anyer, Indonesia; Journal of Tsunami Hazards, Volume 21, Number 4, pp. 191-222, 2003. http://drgeorgepc.com/Tsunami1883Krakatau.html

Pararas-Carayannis, G., 2005a. *"The Great Earthquake and Tsunami of 26 December 2004 in Southeast Asia and the Indian Ocean",* http://drgeorgepc.com/Tsunami2004Indonesia.html

Pararas-Carayannis, G., 2005b. *"The Earthquake and Tsunami of 26 June 1941 in the Andaman Sea"*. http://drgeorgepc.com/Tsunami1941AndamanSea.html

Pararas-Carayannis, G., 2005c. *"The Great Earthquake and Tsunami of 1833 off the coast of Central Sumatra in Indonesia"* http://drgeorgepc.com/Tsunami1833Indonesia.html

Pararas-Carayannis, G., 2005d. *"The Great Earthquake and Tsunami of 28 March 2005 in Sumatra, Indonesia"*, http://drgeorgepc.com/Tsunami2005ndonesia.html

Pararas-Carayannis, G., 2006a, "*Potential of tsunami generation along the Makran Subduction Zone in the Northern Arabian Sea – Case Study: The Earthquake and Tsunami of 28 November 1945"*, 3rd Tsunami Symposium of the Tsunami Society May 23-25, 2006, East-West Center, Un. of Hawaii, Honolulu, Hawaii, Science of Tsunami Hazards Vol 24(5), 2006 http://drgeorgepc.com/TsunamiPotentialMakranSZ.html

Pararas-Carayannis, G., 2006b. *" The Earthquake and Tsunami of 17 July 2006 in Southern Java, Indonesia"* http://drgeorgepc.com/Tsunami2006IndoJava.html

Pararas-Carayannis, G. 2006b. The Earthquake and Tsunami of 28 November 1945 in Southern Pakistan http://drgeorgepc.com/Tsunami1945Pakistan.html

Pararas-Carayannis, G. 2006c. *Alexander the Great – Impact of the 325 B.C, Tsunami in the North Arabian Sea Upon his Fleet.* http://drgeorgepc.com/Tsunami325BCIndiaAlexander.html

Pararas-Carayannis, G., 2007a. *"The Earthquake of 31 May 1935, near Quetta (Balochistan), Pakistan"* http://drgeorgepc.com/Earthquake1935PakistanQuetta.html

Pararas-Carayannis, G. 2007b, *"The Earthquakes and Tsunami of September 12, 2007 in Indonesia"*, http://drgeorgepc.com/Tsunami2007Indonesia.html

Pendse, C. G. (1945). The Mekran earthquake of the 28th November 1945, India Met. Deptt. Scientific Notes, 10, 141-145.

Permana, H.; Singh S.C. & Research Team (2010). *"Submarine mass movement and localized tsunami potentiality of Mentawai Basin, Sumatera, Indonesia"*. Retrieved 2011-06-01.

Platt, J. P., Leggett, J. K., Young, J., Raza, H. and Alam, S., 1985. *"Large-scale sediment underplating in the Makran accretionary prism, Southwest Pakistan",* Geology, 13: 507-511.

Quittmeyer, R.C., and Jacob, K.H., 1979, *"Historical and Modern Seismicity of Pakistan, Afghanistan, N.W. India and S.E. Iran",* Bulletin of the Seismological Society of America, 69/3, pp. 773-823, 1979

Ramanathan, K., and Mukherji, S., 1938, *"A seismological study of the Baluchistan, Quetta, earthquake of May 31, 1935"*, Records of the Geological Survey of India, Vol. 73, p. 483 – 513.

Rastogi B.K. & Jaiswal R.K., 2006, *"A Catalog of Tsunamis in the Indian Ocean"*. National Geophysical Research Institute, Hyderabad, India; Science of Tsunami Hazards, Vol. 25, No. 3, pages 128-143 (2006).

Singh S.C & Moeremans R., 2017. *"Anatomy of the Andaman–Nicobar subduction system from seismic reflection data"*. Geological Society, London Memoirs, Vol. 47, pp 193-204 https://doi.org/10.1144/M47.13

Sinvhal, H., Khattri, K.N., Rai, K. and V.K. Gaur. (1978), *"Neotectonics and time-space seismicity of the Andaman Nicobar region"*, Bulletin of the Seismological Society of America, Volume 68, No. 2, 399-409.

Verma, R.K., Mukhopadhyay, M. and N.C. Bhuin. (1978), *"Seismicity, gravity and tectonics in the Andaman Sea"*, in *"Geodynamics of the Western Pacific"*, Proceedings of the International Conference on Geodynamics of the Western Pacific - Indonesian Region, March 1978, Tokyo, Advances 'in Earth and Planetary Science 6, Supplement Issue of Journal of Physics of the Earth, edited by S. Uyeda, R.W. Murphy and K. Kobayashi, Center for Academic Publications, Japan Scientific Societies Press, Tokyo, 233-248.

Wang Yu, Sieh Kerry, Thura Soe Tun, Lai Kuang-Yin, Myint Than, 2014. "Active tectonics and earthquake potential of the Myanmar region". Journal of Geophysical Research, Vol 119, Issue 4, pp.3767-3822 https://doi.org/10.1002/2013JB010762

White, R. S., Louden, K. E., 1983, *"The Makran Continental Margin: Structure of a Thickly Sedimented Convergent Plate Boundary"*, In: J. S. Watkinsand C. L. Drake (Editors), Studies in Continental Margin Geology. Mem. Am. Ass. Petrol. Geol. 34: 499-518.

ISSN 8755-6839

SCIENCE OF **TSUNAMI HAZARDS**

Journal of Tsunami Society International

Volume 42 Number 3 2023

EFFECTIVE TSUNAMI PROTECTION IN JAPAN - REVIEW AND DISCUSSION OF NEEDED MEASURES

Yuuji Tauchi

Uchiya 7-7-25, Minami-ku, Saitama-shi, 336-0034 Saitama, Japan
E-mail: tauchi@jcom.zaq.ne.jp

ABSTRACT

The 11 March 2011 Tohoku earthquake and tsunami, also known as the Great Sendai severe disaster and as the "Heisei" tsunami, occurred off the northeastern coast of Japan's main Island of Honshu, resulting in extensive destruction and the death of 22,000 people.
Also, tsunami waves struck the Fukushima nuclear power plant on the coast, thus setting in motion a major accident and spreading long-lasting radioactive material in the ocean, with far-reaching impact on marine life in the North-West Pacific Ocean. Besides the large magnitude of the destructive earthquake, the main factors responsible for the great loss of life was due to the fact that existing tsunami protective countermeasures, such as seawalls, were inadequate in providing protection given the extreme height of the 2011 tsunami waves. The seawall was overtopped by these waves and large sections were destroyed by the accompanying debris flow, thus reaching further into the harbor. Subsequently, waves traveling up the river, transformed into a river-type of tsunami, overtopping river embankments, flooding the surrounding areas, and causing great loss of life and destruction, as in the past 115 years caused by great magnitude earthquakes and destructive tsunami events. These were: 1) The magnitude Mw=8.5 tsunami generating Meiji Sanriku earthquake of 15 June 1896 in Japan; 2) The magnitude Mw=8.4 tsunami generating Showa Sanriku earthquake of 3 March 1933 in Japan; 3) The magnitude Mw= Mw=7.7 Hokkaido Nansei-Oki tsunami generating earthquake of 12 July 1993; and 4) The magnitude Mw=9.4-9 Valdivia-Chile earthquake and tsunami of 22 May1960.

The present study examines Japan's government countermeasures in providing effective tsunami predictive and protection measures from such extreme and catastrophic tsunami recurrences in the future, and particularly against the threat of river tsunamis.

1. INTRODUCTION

The most significant aspect in taking effective tsunami protection measures is the accuracy of predicting the heights of expected waves and their potential extend of inundation. Recently, the Japanese government and the media announced that the accuracy of the tsunami height prediction ranges considerably from one half to as much as two times or more (Kinki District Transport Bureau, 2011; Pararas-Carayannis, 2014). For example, if the predicted height of a tsunami is 10 m, its actual height on the shore may vary from 5–20 meters, which indicates a rather broad range of four times in the inaccuracy of its evaluation. When the 2011 tsunami struck Japan, experts repeatedly stated "unexpected" occurrences about the damage that could be expected.

Given to the insufficient height of the existing seawalls, the tsunami could easily flow over them and afflict the residents near the coastline, who expected protection from the existing seawall and did not flee. The officially established narrow danger zone of the tsunami hazard map further aggravated the disaster, because the waves reached beyond the predicted range and affected residents seeking refuge in areas that were previously considered to be safe. Consequently, the inadequate height of the existing tsunami shelters acted as a fatal trap for many of the residents. Given such high vulnerability from extreme events, it is highly significant to have accurate data and information in order to ensure more effective protection for the people residing in coastal areas, and to safeguard against future recurrences.

The obvious question is on how the height of a needed protective seawall can be effectively determined, if the actual tsunami height ranges from 0.5–2 times of the predicted height? If the forecasts predict a tsunami of 10 meters in height, a 10-m-high seawall would be insufficient against a tsunami of 20 meters in height. In the past, seawalls were built in Japan based on estimates of tsunami heights that struck the coast (Yasunori et al. 2012**)**. However, such estimates of offshore tsunami heights often differ substantially from what actually can occur within an enclosed body of water of a bay or a harbor, due to many other reasons. For example, when tsunami waves reach closer to shore, they become compressed, their wavelengths are shortened, and their energies and heights may increase considerably due to the stage of the tide, effects of refraction or resonance, or due to combining with waves approaching from different directions. Thus, a tsunami wave which may have been only one meter or less in deep ocean, may increase in height to thirty to thirty-five meters when sweeping over the shore, and its run-up and inundation may be significantly greater traveling up a river, transforming into a river-type of tsunami (known as fluvial tsunami), reversing the river flow and overtopping existing embankments, flooding and abrading surrounding areas by carrying quantities of sediments. This occurred with the 11 March 2011 Tohoku tsunami, as discussed in greater detail by the present report.

2. FACTORS WICH ALTERED THE 11 MARCH TSUNAMI ON-SHORE AND INLAND RIVER TRANSFORMATION

Besides the overtopping and partially destroying sections of the existing coastal seawall, the 11 March 2011 Tohoku tsunami also inundated rivers and streams forming a bore (also known as a fluvial tsunami) that reversed their flows, causing extensive flooding and great damage to communities far inland. The series of waves that flooded, drained away and then re-flooded the land, a process which lasted long as subsequent waves arrived. Such flooding of the coast

and of up-river regions usually varies based on the direction of approach of the tsunami waves. If the tsunami approaches diagonally a bay-front, as often is the case, an existing cape usually blocks the full impact, thus resulting in smaller waves reaching the bay. Accordingly, small seawalls have been constructed to withstand the relatively smaller tsunami waves. However, we must evaluate a scenario in which a tsunami approaches directly the front of the seawall. Fortunately since 2011 and currently, the Japanese government has expanded efforts to implement tsunami countermeasures presuming that a tsunami of the same magnitude will recur again at a given location. This assumption is somewhat incomprehensive and can be ineffective in the bay-front tsunami impact scenario. The historic record documents such an outcome.

For example the Kitakami General Branch of the seawall, facing the mouth of the Kitakami River in Ishinomaki City of the Miyagi Prefecture, was constructed five years ago as a preventive measure for tsunami protection (Shimbun, 2011). This structure is situated on land and is designated as an evacuation site as extends up to a height of 6.5 m, which is 1 m higher than the highest tsunami water level, assumed at 5.5 m (Shimbun, 2011). However, this structure was completely destroyed by an enormous wave of height greater than 8 m in 2011. Among the 49 individuals who took refuge at this section of the branch, only three individuals—two adults and one child—survived (Shimbun, 2011). Teruyoshi Makino, 42, a city employee, stated, "The Evacuation was perfect, but the force of the tsunami exceeded the limit." Based on past tsunami data, the Okawa Elementary School had been marked as a safe zone on the tsunami hazard map (Shimpo, 2011). Ishinomaki City had designated the Okawa Elementary School as a tsunami evacuation center, which was only 1m above sea level. On the day of the disaster, 74 students and teachers seeking shelter in the school grounds succumbed under the force of the tsunami waves. If this site had not been designated as a tsunami evacuation site, the individuals would have climbed the mountain behind and could have potentially survived.

Numerous other fatalities were recorded at sites that had been designated as "shelter zones" in the hazard map created with the tsunami height prediction model that was being used. However, at that time, the Japanese government had created a tsunami hazard map using the same method based on the assumption that most severe conditions of flooding had been considered in issuing such a "Tsunami Flooding Forecast Map". This incorrect assumption and the hazard map that was issued were apparently inadequate in identifying "safe shelter zones", that can safeguard individuals from such disastrous future events. Thus, studies were subsequently initiated for the purpose of developing an accurate method of predicting tsunami heights which can be used to create more effective and safer tsunami hazard maps and thus maximize the likelihood of survival. The tsunami prediction system currently employed by the Meteorological Agency is discussed as well in the subsequent section (JMA- Japan Meteorological Agency, 1999). The JMA methodology involves supposition of crustal deformation caused by earthquakes along known fault zones, and estimates of tsunami generative areas, as discussed in the following section.

3. NUMERICAL SIMULATION OF TSUNAMI WAVES – EXISTING FOCAL MECHANISMS OF THEIR GENERATION

The simulation for determining the focal mechanisms of tsunami generation by local or distant major earthquakes, as well as the heights and arrival times of tsunami waves on the coasts of Japan or anywhere else in the Pacific Ocean or elsewhere, can be broadly classified into two

stages, one being a calculation of seafloor crustal deformation and another being the tsunami propagation and its height alterations due to refraction, diffraction, and maximum energy focusing.

The seafloor crustal deformation caused by earthquakes can be theoretically evaluated, based on assumption of the movement along major faults. The fault parameters can be estimated based on 1) the horizontal position and depth of the fault, 2) its size, 3) its orientation, 4) on its inclination, and 5) the direction and magnitude of the resulting slip.

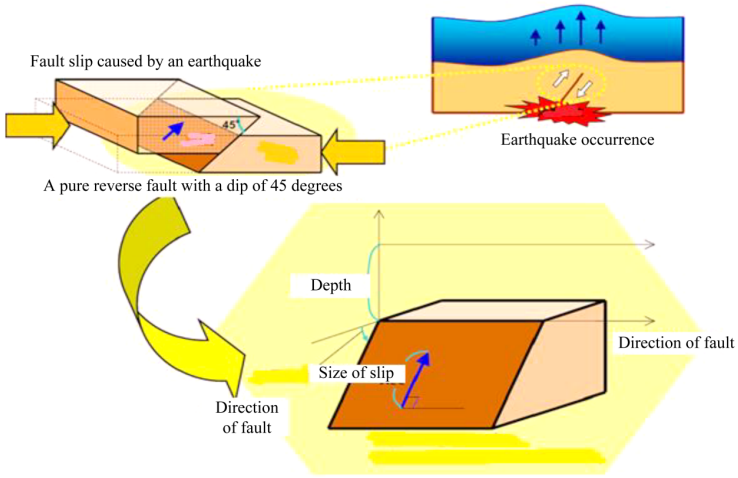

Fig. 1 Schematic of earthquake source faults causing tsunami

The direction of the fault can be determined from the data of known past earthquakes. The horizontal position, depth, and size of the fault along with the magnitude of slip, can be estimated from the magnitude. In addition, the inclination and slip direction of the fault can be set as being a pure reverse fault with a maximum inclination of 45° (Fig. 1 above), which corresponds to the generation of the largest possible tsunami. Accordingly, this study conducted extensive simulations to ensure adequate prevention and mitigation response to earthquakes of any size at any location, which could generate tsunami waves, and which particularly impact on Japan. Figure 1 is a schematic of such undersea earthquake source fault movement, which could generate a destructive tsunami based on maximum source displacements and focusing of propagation

In particular, this study considered approximately 1,500 faults in the horizontal direction at six distinct depths varying from 0 and 100 km and four magnitudes. Thereafter, a tsunami propagation calculation was applied.

However, the tsunami height calculation may be scientifically incorrect, as there may be other earthquake parameters, factors and deviations which may not have been considered. One such deviation can be clearly seen from the logarithmic graph of Figure 2 where the average slip in meters of a seismic fault is plotted in terms of an earthquake's seismic moment (Miyakoshi Lab EtAl, 2015)

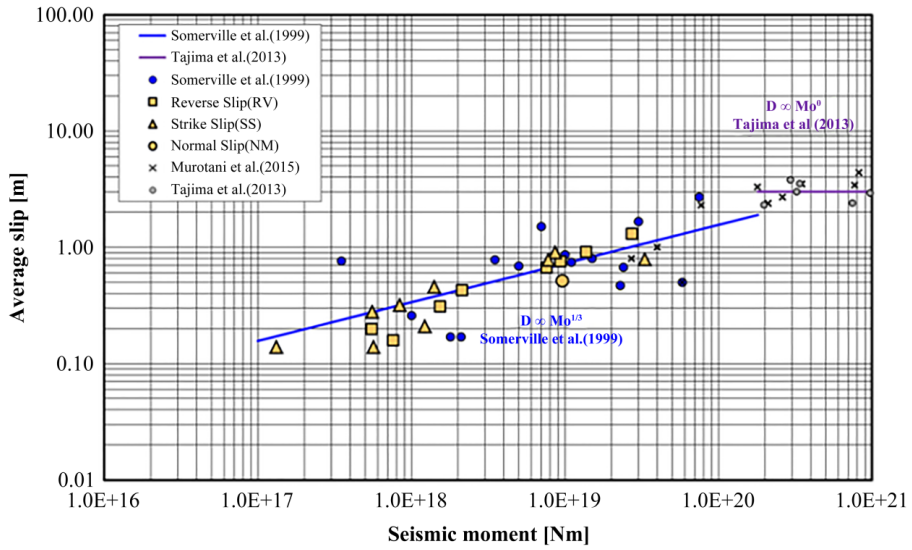

Fig. 2 Average slip in meters of a seismic fault in terms of an earthquake's seismic moment *(Miyakoshi Lab Et Al, 2015).*

The straight line passing through the center of the previous seismic data in Figure 2 represents the formula reported by Somerville (1999). The average slip (m) at any seismic moment (Nm) can be calculated using this formula.

Notably, the tsunami height calculated from the average slip (m) represents an average tsunami height; therefore, a fundamental mistake would be made when using this formula, which yields an average value, for cases where the maximum value matters (e.g., tsunami). As depicted in Figure 2, the seismic moment is 8.0E+19 Nm and the average slip is 2.8 m, which is 2.2 times the calculated value of 1.3 m. Using the formula, the corresponding tsunami height is calculated to be 1/2.2 of the previous actual tsunami height.

This is an example in which the actual observed value considerably deviated from the calculated value because of the small amount of data. With more data, we can derive more accurate results. The concept of using a regression equation to obtain an estimated mean with the maximum value, such as an earthquake or tsunami, is fundamentally incorrect. In this calculation, the average slip corresponds to an average value, and the tsunami height calculated using the average slip denotes the average tsunami height.

Moreover, the tsunami height cannot be determined only by using the average slip. Even for the same slip amount, it varies considerably depending on its slow or rapid movement. Thus their source tsunami height calculations are wrong. Based on these numbers, they simulated the tsunami propagation process.

3.1 Terrain Tsunami Amplification

The tsunami height varies considerably depending on the topography near the coast. In addition, the tsunami waves may continue to inundate on land. Waves are converge in places with special topography, such as the tip of a cape or the rear side of a V-shaped bay, which necessitates special caution. A tsunami can surge further owing to the repeated reflections and can result in remarkably high waves by overlapping with multiple waves. Consequently, the first wave is not necessarily the biggest and the subsequent waves may be higher. In shallow water, the wave speed diminishes and the wave height increases. Moreover, complex variations can occur, such as waves over shallow water that overlap on those advancing in deep water.

However, as the tsunami propagation process is a physical phenomenon, it can be predicted according to scientific laws. Specifically, the sea surface is classified into meshes for calculation, with 15 m mesh near the coast. The precise calculations were enabled by the increased computer capacity and calculation speed.

Overall, the "prediction accuracy of tsunami height of 0.5–2 times" does not vary, because the predicted height of the first tsunami wave is incorrect. Thus, we intend to enhance this "prediction accuracy of tsunami height of 0.5–2 times" to mitigate the tsunami damage. Certain studies have suggested, "escape training" as a tsunami countermeasure (Sugiyama and Yamori, 2019). In case of an under sea earthquake, escape training predicts the height of the tsunami that will impact the coast based on the magnitude and location of the earthquake. Accordingly, a safe evacuation route can be communicated to the public via mobile phones. Recently, this has been implemented in evacuation drills in various places. However, the inaccurate predictions of tsunami height at 0.5–2 times is grossly uncertain. The safe evacuation routes for an expected tsunami height of 3 meters ceases to be safe if the tsunami wave height exceeds 3.5 meters. An individual can drown even under an excess height of 50 cm. As 3.5/3.0 = 1.17 times, individuals can succumb under a tsunami that is ≈20% higher than the predicted/expected height.

Current tsunami warnings are issued over a wide area based on tsunami heights with poor accuracy. Hence, the number of people who rely on tsunami warnings to evacuate is decreasing, and the damage caused by tsunamis is actually increasing.

A tsunami warning for a specific area should be issued based on a more accurate tsunami height prediction. However, it is impossible presently to improve the accuracy of tsunami height prediction with current methods. After an initial tsunami wave strikes a shore, and an accurate measurements of its height and travel direction are made, issuing a prompt warning for the areas where the tsunami will be reaching next is necessary.

Thus in order to establish a more effective warning system, local government agencies should have quick access to data from seafloor seismometer and tsunami measurement network devices as soon as possible in order to measure the tsunami height, and thus issue a reliable tsunami warning only to the affected areas (NEC, 2013). Therefore, it is important to regain people's trust in tsunami warnings otherwise the resulting tsunami impact and destruction will increase significantly. Thus government authorities should create new tsunami countermeasures, recognizing that the current countermeasures are inadequate and may actually increase the damage.

Nonetheless, the actual scenario is more concerning. The initial height of a tsunami impacting on land is nearly impossible to accurately predict as it can be affected by a slight changes of water depth, land topography, an earthen wall of ~1 m height, or an artificial hill. Upon visiting the

disaster area of Natori City devastated by the 2011 tsunami, the author noted two two-story wooden buildings constructed adjacent to each other on a field. Surprisingly, one building suffered no damage, whereas the ground floor of the other building—located 5m away—was devastated by the tsunami. Notably, a 1-m-high earthen wall separated the fates of these two building by blocking and diverting the tsunami direction. Unfortunately, such minor obstacles cannot be incorporated into a simulation program.

Additionally, concrete buildings in densely populated cities are structures that act as barriers and can considerably affect tsunami impact with enhancement of wave heights and gains in momentum. An example of such occurrence was broadcasted seven years after the 2011 disaster, by an NHK special television program under the title: "Kawatsunami: Unknown Truth in Seven Years of the Earthquake" (NHK Special, 2018). According to the report, the tsunami reached the Kitakami River by traveling up to a speed of 40 km/h, causing 74 fatalities at the Okawa Elementary School – which had been designated as an evacuation center – and causing 68 fatalities in the Magaki district, which was situated 5 km inland from the sea. The tsunami followed the meandering course of the river; slamming and breaching the riverbanks by a height of 2 meters, and inundating an area up to 1 km inland.

The facts presented in this broadcast demonstrated that the embankments couldn't prevent tsunami damage. Thus, the strengthening of coastal dykes does not help at all. If a river flows through the town, the tsunami can flow through the river and impact the river embankment. On the day of the 2011 disaster, 600 times the average amount of seawater flowed into the Kitakami River, thereby increasing the river discharge to a speed of 40 km/h. This signifies that even a weak tsunami is dangerous if a river is flowing with extensive amounts of added water from the sea. The water in the river is pushed back by the tsunami and rises in height, thereby creating a massive river tsunami.

On that same day, the tsunami disintegrated 190 km out of the 300-km-long seawall on the Sanriku coast (Yasunori et al. 2012), because its waves created a debris flow that lifted up the sludge and sand from the seabed. As such, river tsunamis can readily destroy river levees.

In Tagajo City, Miyagi Prefecture, a river tsunami traveled up the river in the city and impacted a building district, resulting in 188 fatalities. If buildings block the tsunami flow, the height of the water level increases. Thereafter, the flow concentrated in the gaps between the buildings, increasing its speed even more by a Bernoulli effect. The tsunami flowed specifically fast in areas with sturdy buildings and exceeded 30 km/h at maximum. Furthermore, the tsunami traveled along the road, such as a waterway, and entered the city area while turning the alley. It collided with a concrete building and altered its direction, thereby creating a complicated damaging flow.

Fumihiko Imamura, a professor at the International Research Institute of Disaster Science at Tohoku University, analyzed this Tagajo tsunami and determined that the structure of the city exacerbated the damage. Professor Imamura stated that "The density of buildings is very high, and the tsunami becomes very strong, so I think this can be called an urban torrent. There is no way to escape, and no time to escape."

Almost 30,000 rivers flow through the islands of the Japanese archipelago. The investigations and research on the threat of river tsunamis are progressing where the kind of dangers exist. A massive earthquake along the Nankai Trough is forecasted in the near future. According to the

national government's assumptions, tsunamis will hit cities across the Japan immediately after the violent tremors. Amid this threat, Osaka Prefecture is becoming increasingly concerned regarding river tsunamis, because 174 rivers flow through Osaka, and it has a population of 8.8 million residents.

In 2012, the government announced that the expected flooding areas in Osaka Prefecture were limited to regions near the coast. However, the prefectural government presumed a situation in which the river embankments and water gates fail to function, thereby creating its own estimates. The results revealed that the area of the flooded area extended to more than three times the official national assumption.

According to simulations conducted by experts, the tsunami waves can penetrate up to 2 km from the mouth of two rivers, with increasing water level near the tsunami confluence. In particular, the tsunami overflowed into areas housing commercial facilities. In case of a river with a gentle slope, the tsunami reached as far as 12 km from the river's mouth. Upon crossing the embankment, experts suggest that the tsunami will flow into the low-lying residential areas.

According to the Osaka Prefectural government, in the worst-case scenario, the number of victims would increase to 130,000, which is more than ten times the national government's estimate. Overall, Tokyo faces the greatest danger in Japan. In the 1600s, when Ieyasu Tokugawa built the Edo Castle, he reclaimed the sea to create the town of Edo by digging vertically and horizontally to carry supplies by boats. The Edogawa, Arakawa, and Sumida rivers flow through the city of Tokyo.

The flood control for the five wards of Koto has been combining Sumida, Koto, Adachi, Katsushika, and Edogawa (Koto 5 Wards Large-Scale Flood Countermeasures Council, 2022). Owing to the simultaneous occurrence of floods and storm surges, the river collapses at multiple locations, including on both banks of the Arakawa River, eventually inundated almost the entire Koto Ward. The population within the inundated area reached approximately 2.5 million. Approximately 440,000 residents will have to be evacuated from their homes, as the buildings will be completely submerged. In contrast, the number of evacuation centers in the five wards of Koto is approximately for 490,000 residents, who cannot be accommodated. In the worst-case scenario, floodwaters can remain inundated for more than two weeks, and residents will be forced to stay in a harsh environment for a long time without gas and water supply. Thus, early rescue is required to prevent damage from the vertical evacuees, but if one million residents have to be evacuated (half of the population of the inundated area), the boats owned by the Kanto police, fire departments, and the Self-Defense Forces will be employed. Regardless of full mobilization, the rescue operation would involve more than two weeks.

Nonetheless, this is only an evacuation plan, and the repair of embankments as well as the discharge of the enormous quantity of water flooding the land have not been specifically considered, which forms the scope of a future research. The destructive power of tsunamis is incomparable to storm surges and floods. Even if a weak tsunami hits Tokyo Bay, the sludge from the bottom will be swept up, and the tsunami will intensify with as it merges with the Arakawa, Edogawa, and Sumida rivers. In particular, river levees in Tokyo are thin and can be easily destroyed by tsunami laden with sludge due to the high land prices. The number of victims will surpass the number of 130,000 fatalities predicted for Osaka Prefecture. Notably, the Koto 5 Ward Crisis Management and Disaster Prevention Division is unaware of river tsunamis flowing up rivers.

CONCLUSIONS

Knowledge and understanding about the complicated nature of the tsunami hazard is imminent for effective protection countermeasures. The recently introduced method of escape training may prove to be ineffective. In case a weak tsunami impacts Tokyo or Osaka, a wide area will be flooded by a river tsunami, and economic activity will cease for several years. Although the economic center of Osaka is located higher than the mean sea level, the center of Tokyo's economy is situated below the sea level. Moreover, the current communication network, power grid, gas, water, and other facilities are based on underground tunnels. Thus, draining of floodwater will require months of time. Four years ago, Osaka started to prepare against the threat of river tsunamis. However, no such effort has been yet adopted by the Tokyo government. Thus, adequate efforts must be undertaken to ensure protection against the potential tsunami hazard.

REFERENCES

Japan Meteorological Agency. (1999). Mechanism for predicting tsunamis. (Translated). URL: https://www.data.jma.go.jp/svd/eqev/data/tsunami/ryoteki.html (accessed on 3.1.2023)

Kinki district transport bureau. (2011). A collection of case studies of ships encountering tsunamis: learn from the behavior of ships encountering tsunamis in the Great East Japan Earthquake. p68. URL: http://www.mlit.go.jp/common/000212285.pdf

Koto 5-wards large-scale flood countermeasures council. (2022). Toward realization of zero victims: 5 wards along the coast of Tokyo. (Translated). URL: https://www.city.edogawa.tokyo.jp/e007/bosaianzen/bosai/kojo/koto5_daikibo_suigai.html (accessed on 3.1.2023)

Miyakoshi Lab, Irikura, K., & Kamae, K. (2015). Reexamination of scaling law of source parameters for domestic inland crustal earthquakes based on source inversion using strong motion records. *Journal of Earthquake Engineering*, *15*(7), 141–156. https://www.jstage.jst.go.jp/article/jaee/15/7/15_7_141/_pdf/-char/ja

NEC. (2013). Commencement of laying of the Japan Trench submarine earthquake and tsunami observation network. (Translated). URL: https://jpn.nec.com/press/201307/20130709_02.html (accessed on 3.1.2023)

NHK special. (2018). "River Tsunami" - seven years after the earthquake, unknown threat~. (Translated). URL: https://www.nhk.jp/p/special/ts/2NY2QQLPM3/blog/bl/pneAjJR3gn/bp/ppO3E5yLkp/ (accessed on 3.1.2023)

Pararas-Carayannis, G., (2014). The Great Tohoku-Oki Earthquake and Tsunami of March 11, 2011 in Japan: A Critical Review and Evaluation of the Tsunami Source Mechanism. *Pure Appl. Geophys.* **171,** 3257–3278 (2014). https://doi.org/10.1007/s00024 0130677 https://ui.adsabs.harvard.edu/abs/2014PApGe.171.3257P/abstract

- https://ieeexplore.ieee.org/document/6106909

Shimbun, A. (2011). “No way, even here” Tsunami fangs in designated evacuation shelter Miyagi. (Translated). URL: https://www.asahi.com/special/10005/TKY201103210377.html (accessed on 3.1.2023)

Shimpo, K. (2011). The tragedy of the tsunami that hit Okawa Elementary School, Ishinomaki. (Translated) URL: http://memory.ever.jp/tsunami/higeki_okawa.html (accessed on 3.1.2023)

Somerville, P., Irikura, K., Graves, R., Sawada, S., Wald, D., Abrahamson, N., et al. (1999). Characterizing crustal earthquake slip models for the prediction of strong ground motion. *Seismological Research Letters*, *70*(1), 59–80. https://doi.org/10.1785/gssrl.70.1.59

ISSN 8755-6839

SCIENCE OF **TSUNAMI HAZARDS**

Journal of Tsunami Society International

Volume 42 Number 3 2023

COASTAL EFFECTS, TSUNAMI AND SEICHING ASSOCIATED WITH THE KAHRAMANMARAŞ TURKEY-SYRIA TWIN EARTHQUAKES AND AFTERSHOCK SEQUENCE OF FEBRUARY 2023

Aggeliki Barberopoulou[1], George Malaperdas[2], Sarah Firth[1]

[1] Corresponding author: Department of Urban & Environmental Policy & Planning, Tufts University, Medford, MA 02155 Aggeliki.Barberopoulou@tufts.edu

[2] Department of History, Archaeology and Cultural Resources Management, University of the Peloponnese, old camp Kalamata GR

ABSTRACT- A strong M7.8 earthquake (02/06/2023; 01:17:36.1 UTC) followed by a second event (M7.5) on the same day (10:24:49 UTC) in Central Turkey caused extensive damage and fatalities (>> 50,000 in Turkey and Syria). Ground shaking exceeding 1.0 g in some locations (USGS, EMSC), structural damage, and multiple secondary effects were documented by Turkish and Greek reconnaissance teams in preliminary reports (e.g., (Lekkas, et al., 2023), reports to the EMSC). The M7+ earthquakes were widely felt in Turkey and in neighboring countries, such as Greece, the Balkan region, and Italy, as far as 1200 km and beyond. Flooding was also reported in few locations, including the bay of Alexandretta and in Salqin, Idlib, Syria. Sea level stations recorded a small tsunami, and tsunami runup was observed in Cyprus and Turkey. Through security cameras and personal cellphone footage, seismic seiches were recorded across Turkey and Cyprus. Some localities even reported multiple incidences of seiches over the course of the earthquake sequence in the same body of water. Observations of seiches are rare in the Eastern Mediterranean and are therefore especially valuable to document. Most importantly, the set of observations collected here is one-of-a-kind dataset (the most extensive dataset in Turkey and a unique dataset of seiche observations for Cyprus). Spatial analysis of seiche observations may also be valuable in documenting areas prone to liquefaction and vice versa, with particular use in the study of older or historical earthquakes. In this paper, we document the coastal effects of the Kahramanmaras Turkey earthquakes, followed by a first-order analysis. Satellite images were also processed to showcase the extent of flooding that followed the large twin earthquakes and lasted at least 3 days around the bay of Alexandretta. The source of flooding likely is a combination of subsidence, liquefaction and the tsunami that ensued. Tsunami amplitudes were small but clearly recorded in few stations; the tsunami's genesis mechanism is in debate.

Keywords: *tsunami; seiche, Turkey, coastal effects, historical tsunami records*

Vol. 42 No 3, page 257 (2023)

1. INTRODUCTION

On February 6, 2023 (01:17:36.1 UTC), a strong shallow M7.8 earthquake occurred approximately 30 km WNW of Gaziantep city, in Southeastern Turkey (CSEM/EMSC), and about twice that distance from the border with Syria (USGS, EMSC; Figure 1). Hundreds of aftershocks ensued within hours of the mainshock (USGS; the largest M6.7).

The two earthquakes are associated with the Eastern Anatolian Fault zone (EAF; Duman & Emre, 2013), a ~600km sinistral strike-slip fault zone which forms the boundary between the Arabian and the Anatolian plates. It is characterized by a narrow deformation zone to the NNE and a wider deformation zone to the SSW. Although the predominant motion of the EAF is strike-slip, normal or reverse motions are also sometimes observed along the fault zone. The two M7+ earthquakes happened in a region that is seismically active but had been relatively quiescent in the last century ((Sesetyan, Stucchi, Castellli, & Gomez Capera; Taymaz, Ganas, Melgar, Crowell, & Ocalan, 2023) and references therein). According to (Sesetyan, Stucchi, Castellli, & Gomez Capera) preliminary report, about a dozen earthquakes of M6.5 or greater occurred in the last millennium (1000-1900) in the general region of the twin Turkey earthquakes, with the largest one in Antakya in 1822 (Mw7.74). In the 20th century, several M6+ occurred in the EAF, the most recent and largest a Ms6.8 in 1971 (e.g., Sandvol et al., 2003).

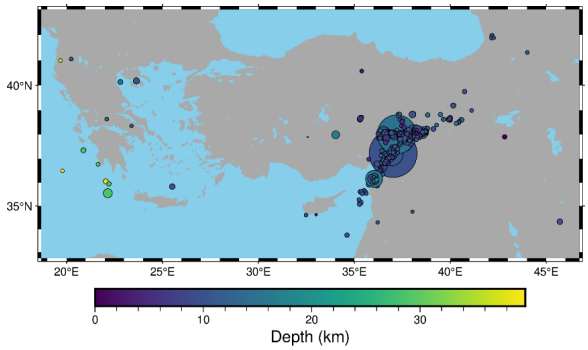

Fig. 1. Seismicity in the month following the M7.8 Pacarzik earthquake (02/06 – 03/15, 2023). Graduated symbols and colors represent magnitude and depth respectively.

The February 6, 2023, earthquakes caused widespread devastation through ground shaking and secondary effects, which included landslides, liquefaction and subsidence (e.g.,(Lekkas, et al., 2023), special reports to EMSC). A tsunami was observed and recorded (see Table 1, Figure 2) by few tide gauge stations on the coasts of Turkey and Cyprus (unfortunately, however, not all tide gauge stations nearby were operating). Additionally, seismic seiching was observed from the main M7.8 earthquake, the M7.5 event, as well as from a large aftershock. In this article, we discuss the coastal effects associated with the twin earthquakes and provide a first order analysis of the water level records and other relevant data collected after the two earthquakes.

Strike-slip faults such as the EAF are generally not associated with tsunamis because a tsunami generating mechanism requires vertical uplift of the water column. However, it is now

more widely accepted that strike slip fault earthquakes can sometimes generate tsunamis because multi-segmented strike-slip fault systems with step overs can locally produce vertical uplift or subsidence with the potential of a tsunami (e.g., Estrada et al., 2021). Given the locations of the M7+ earthquakes, the likely cause of this tsunami is rather interesting and a source of a discussion.

Seismic seiches may also be observed during the onset of ground shaking locally, or with the arrival of seismic waves from distant earthquakes (McGarr and Vorhis, 1968; Barberopoulou et al., 2004; Barberopoulou et al., 2006). Seismic seiching is a term used to describe the surface oscillations generated in enclosed or semi-enclosed water basins due to earthquake ground motions (Kvale, 1955; Rabinovich 2009; Barberopoulou et al., 2004; Barberopoulou, 2008;(Bondevik, Gjevik, & Sorensen, 2013). Such oscillations have previously been associated with distant, regional, and local earthquakes. However, through seismic and spatial analyses, it has been suggested that they are associated with the presence of thick (>1 km thick), unconsolidated sediments (Barberopoulou et al. 2004, 2006 & 2008; McGarr, 1968). Only a handful of earthquakes have relatively sufficient data to understand the occurrence of standing waves due to seismic motions (e.g., 1964 Alaska earthquake; 2002 Denali earthquake).

2. WATER LEVEL DATA AND METHODS

2.1 TSUNAMI OBSERVATIONS

The data used here are tide gauge records from national or global networks and information obtained from global tsunami databases (NOAA-NEIC; IOC-UNESCO; (Danezis, Nikolaidis, Mettas, Hadjimitsis, Kokosis, & Kleanthous, 2020)). Data from tide gauges were obtained from the IOC UNESCO portal for four stations in Turkey (Table 1; Figure 2). The other stations from Cyprus are old piezometric stations not in operation except for one (Lemessos; Danezis, personal communication; (Danezis, Nikolaidis, Mettas, Hadjimitsis, Kokosis, & Kleanthous, 2020)). There are about 10 tide gauge stations within a radius of 350 km from the bay of Alexandretta that are part of national or regional networks; but, unfortunately, not all of them were functional on February 6, 2023. Table 1 and Figure 2 includes a list of operating stations and those that did not record anything because they were down, malfunctioned or are not providing data to the IOC-UNESCO portal due to permanent damage. The tsunami database at NEIC was also searched for complimentary information (Table 2, Figure 3)
personal request and is not available through the IOC-UNESCO portal therefore this estimate may be lower than actual number of stations.

Table 1. List of operating and non-operating stations in the vicinity of the bay of Alexandretta (see Figure 2)

Tide Gauge (name)	Country	Longitude	Latitude	Operating on 02/06/2023
Iskenderun	Turkey	36.17676926	36.59423065	Yes
Arsuz (Hatay)	Turkey	35.88519	36.41559	Yes
Erdemli	Turkey	34.25538719	36.56372892	Yes
Tasucu	Turkey	33.83622742	36.28146362	Yes
Bozyazi	Turkey	32.94131088	36.09741974	Yes

Paphos	Cyprus	32.408819	34.755128	No
Zygi	Cyprus	33.338375	34.727083	No
Larnaca	Cyprus	33.640823	34.916181	No
Paralimni	Cyprus	34.036877	35.038288	No
Lemessos	Cyprus	N/A?	N/A?	Yes

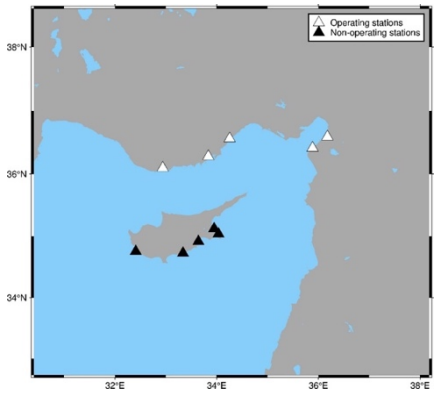

Figure 2. Stations from the IOC-UNESCO portal for which data is available for download for 02/06/2023. White triangles represent stations which have recorded water levels on February 6th, 2023, while black stations were either down or do not have data recorded on the specified date.

Table 2. Tsunami Runup observations as reported by the National Environment Institute (NCEI)

	Country	Location	Latitude	Longitude	Distance from source (km)	First wave arrival (day)	Initial wave arrival (hr)	First Wave Arrival (mins)	Travel (hrs)	Travel (mins)	Max Water Height (m)	Period (first wave in mins)
0	Cyprus	Paralimni	35.03829	34.03688	359	NaN	NaN	NaN	NaN	NaN	0.25	NaN
1	Cyprus	Gazimagusa	35.12320	33.94950	359	6.0	2.0	27.0	NaN	36.0	0.17	NaN
2	Cyprus	Kerinya	35.34100	33.33400	390	NaN	NaN	NaN	0.0	48.0	NaN	NaN
3	Turkey	Erdemli	36.56370	34.25540	257	6.0	2.0	10.0	0.0	48.0	0.13	7.0
4	Turkey	Iskenderun	36.59423	36.17677	100	6.0	2.0	49.0	0.0	25.0	0.12	7.0

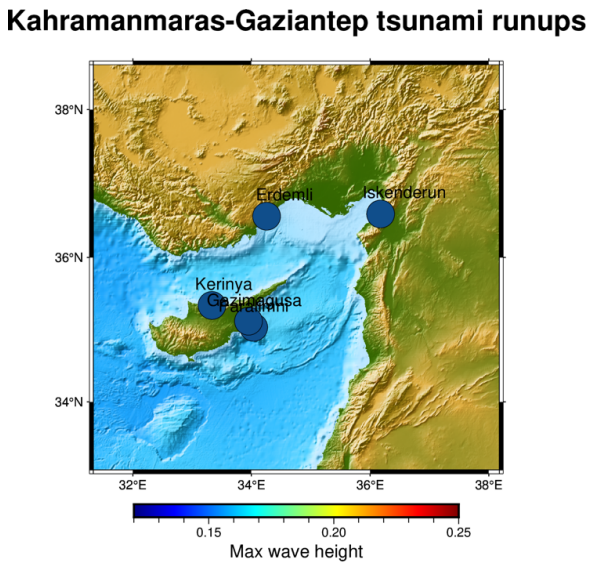

Figure 3. Spatial distribution of tsunami runup data (Table 2) as provided by NCEI.

2.2 WATER LEVEL DATA PROCESSING

Tide gauge records were first decided and then low pass filtered with a 3-pole Butterworth filter to remove high frequencies and recover the longer periods in the recorded signal that are associated with the tsunami (Figure 4, Figure 5). If the predicted
tide did not fit well any of the waveforms (Figure 5), the tide gauge record was further filtered to remove any tidal long period remnants in the signal. The clearest signal above noise in the raw data is evident in the Erdemli and Iskenderun stations, the closest to the epicenter (Figure 4). The maximum wave height (peak to trough) from the stations processed here does not exceed 25cm (Iskenderun station). Fourier spectra of the signals were calculated to show the dominant frequencies in the recorded signals (Figure 5, Figure 6).

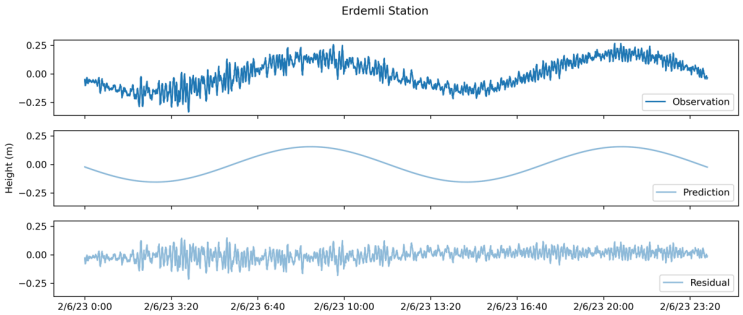

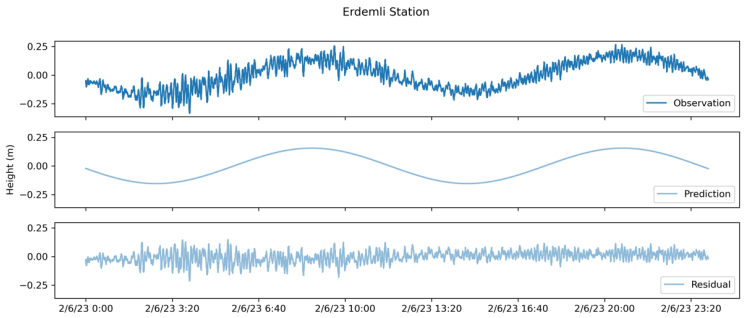

Unknown

Formatted: Font color: Black

Figure 4. Raw tide gauge data (24 hours recording starting at February 6th, 2023, 00:00 UTC time)

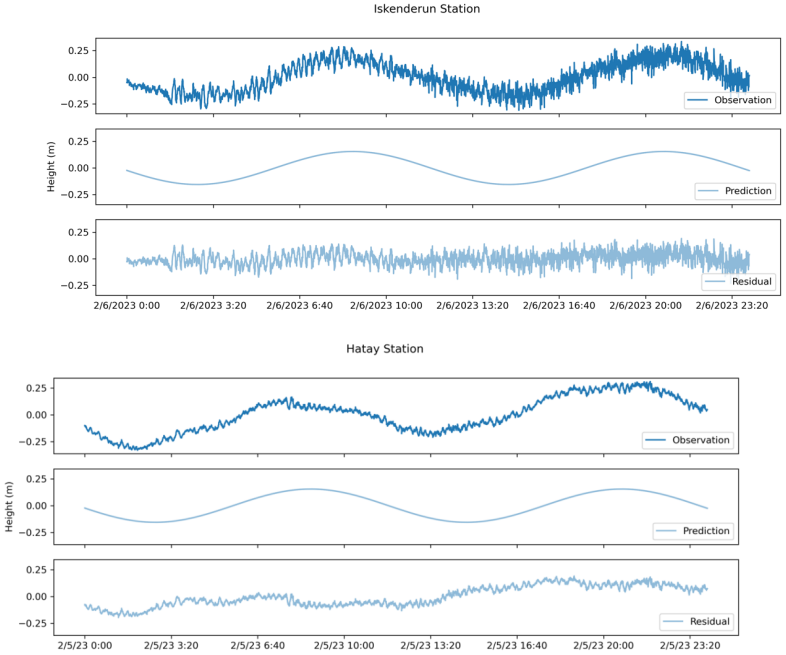

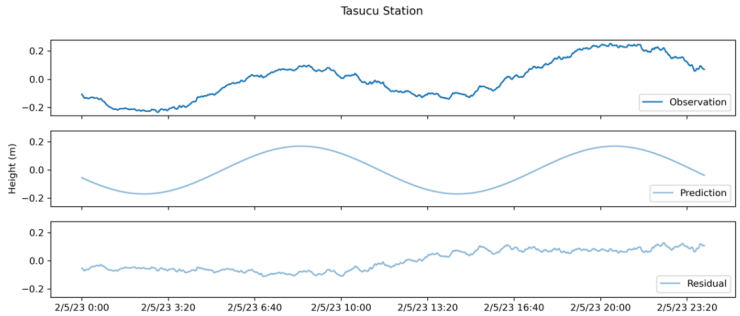

Figure 5. Detided and low pass filtered recordings (from top to bottom) for the Erdemli, Iskenderun, Lemessos, Hatay and Tasucu stations. Only 3 out of the 5 stations listed here recorded a sufficiently strong signal from the tsunami (M7.8 earthquake occurred at UTC 01:17).

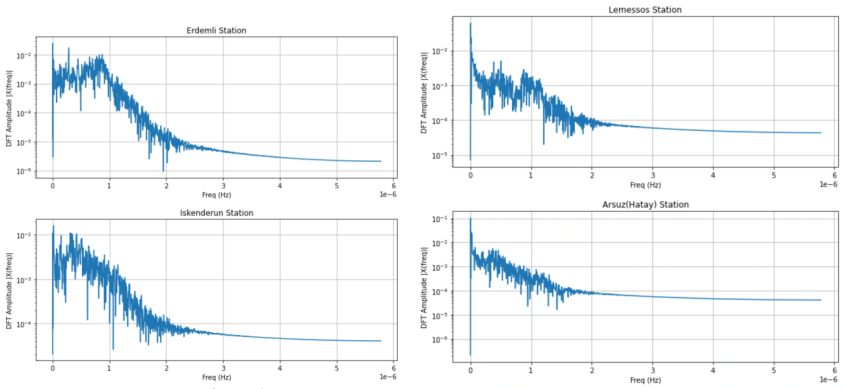

Figure 6. Fourier Spectra of 4 tide gauge stations for which water level records were obtained for the February 6, 2023 earthquake.

3 SEICHING

3.1 OBSERVATIONS

.

The data obtained and used here are video recordings of sloshing from eyewitness accounts reported through social media and news agencies, security camera footage, and related information from global database repositories. More than fifteen seiching observations associated with the Turkey earthquakes of February 6, 2023, were collected (Table 3, Figure 7, and Figure 8). The majority of these observations were from swimming pools, while few others appear to be from outdoor water tanks (for irrigation, etc.). Two observations do not fall in the last 2 categories: one was from a fountain and another from a large home aquarium. All the

observations, therefore, are from regularly shaped man-made basins (mostly rectangular). Many observations were recorded on pool security cameras because they were at hotels or other commercial buildings where cameras are used widely for security reasons. For this reason, it is more common to find observations from swimming pools as opposed to other water basins. Besides security footage, other videos were recorded on smart phones by witnesses. Observations collected are not associated with the same earthquake. Some observations are associated with the M7.8 earthquake, some are associated with the M7.5 earthquake, and one is associated with one of the large aftershocks (M6.3; 2023-02-20).

Unknown

Formatted: Font color: Black

Figure 7. Spatial distribution of seiche observations from the Kahramanmaras earthquake sequence of February 6, 2023, in Turkey. The light and dark yellow stars show the relative location of the M7.8 and M7.5 earthquakes respectively to the observations, which span a 500km-by-500km area. Purple pinpoints represent observations whose locations are well constrained (i.e., with "exact" coordinates), while blue points show those observations where only the town or city could be identified. The observations are from Turkey except for two that are from Cyprus (see Table 3).

Each observation has been assigned a location and associated seismic event to the best of the authors' abilities, and the certainty of each assignment has also been noted (see Table 3). Two

observations are from Cyprus and the rest are from Turkey. Videos obtained from the web, show sloshing in non-residential and residential swimming pools (see still images taken from the videos on Figure 8), a fountain, and various other water tanks.

Based on time stamps included in some of the footage from security cameras, we have constrained the time of occurrence for about half of the observations of sloshing. For other observations, times of occurrence have been approximated through correspondence with the video creators. Basedon the times the videos were collected, observations appear to be associated with the M7.8 event (01:17 UTC; 04:17 local time), the M7.5 event at (10:24 UTC; 13:24 local time) in Gaziantep, and with a large aftershock (M6.3) on February 20th, 2023. The spatial distribution of observations collected can be seen in Figure 7, which spans an area of at least 500km x 500km.

Table 3. Seiche observations collected after February 6, 2023.

#	Country	Location	Lat	Lon	Location Certainty	Associated Event	Body of Water	Video Type
1	Turkey	Gaziantep	**37.091**	**37.375**	**Exact**	M7.8 (02/06/2023; 01:17:36.1 UTC)	Public Swimming Pool	Security camera with timer
2	Turkey	Gaziantep	**37.091**	**37.375**	**Exact**	M7.5 (02/06/2023; 10:24:49 UTC)	Public Swimming Pool	Security camera with timer
3A	Turkey	Antalya	36.893	30.61	Approx.	M7.8 (02/06/2023; 01:17:36.1 UTC)	Residential Swimming Pool	Personal cellphone
3B	Turkey	Antalya	36.893	30.61	Approx.	M7.8 (02/06/2023; 01:17:36.1 UTC)	Residential Swimming Pool	Personal cellphone
4	Turkey	Antalya	36.893	30.61	Approx.	M6.3 (2023-02-20 17:04:29)	Residential Swimming Pool	Personal cellphone
5	Turkey	Antakya	36.204	36.162	Approx.	M7.8 (02/06/2023; 01:17:36.1 UTC)	Public Swimming Pool	Security Camera
6	Turkey	Nevşehir	**38.623**	**34.717**	**Exact**	M7.5 (02/06/2023; 10:24:49 UTC)	Public Swimming Pool	Personal cellphone
7	Turkey	Kayseri	**38.733**	**35.422**	**Exact**	M7.5 (02/06/2023; 10:24:49 UTC)	Public Swimming Pool	Security camera with timer
8	Turkey	Şanlıurfa	**37.149**	**38.81**	**Exact**	M7.5 (02/06/2023; 10:24:49 UTC)	Public Swimming Pool	Security camera with timer
9A	Turkey	Erzurum	**39.918**	**41.248**	**Exact**	M7.5 (02/06/2023; 10:24:49 UTC)	Public Swimming Pool	Personal cellphone
9B	Turkey	Erzurum	**39.918**	**41.248**	**Exact**	M7.5 (02/06/2023; 10:24:49 UTC)	Public Swimming Pool	Personal cellphone
10	Turkey	Elazig	38.671	39.204	Approx.	M7.5 (02/06/2023; 10:24:49 UTC)	Fountain	Personal cellphone
11	Turkey	Alaca (Çorum)	40.17	34.842	Approx.	M7.5 (02/06/2023; 10:24:49 UTC)	Outdoor Tank	Personal cellphone
12	Turkey	Malatya	38.346	38.266	Approx.	M7.8 (02/06/2023; 01:17:36.1 UTC)	Irrigation Tank	Security camera with timer

13	Turkey	Malatya	unknown	unknown	unknown	unclear	Commercial Swimming Pool	Personal cellphone
14	Cyprus	Paralimni	35.065	33.975	Approx.	M7.8 (02/06/2023; 01:17:36.1 UTC)	Residential Swimming Pool	Personal cellphone
15	Cyprus	Paralimni	35.063	34	Approx.	M7.8 (02/06/2023; 01:17:36.1 UTC)	Non-rectangular Swimming Pool	Personal cellphone
16	Turkey	Diyabakir	37.925	40.211	Approx.	M7.8 (02/06/2023; 01:17:36.1 UTC)	Aquarium	Personal cellphone

Table 3 continued.

#	Access video	Notes
1	https://www.youtube.com/watch?v=m8pFB731vy0	First of two observations in same pool in Gaziantep
2	https://www.youtube.com/watch?v=m8pFB731vy0	Second of two observations in same pool in Gaziantep
3A	https://twitter.com/Faworimm/status/1622414362605502464	Appears to be taken at dawn. Time of recording unclear.
3B	https://twitter.com/Faworimm/status/1622420625242349570	Appears to be taken at dawn. Time of recording unclear.
4	https://twitter.com/Faworimm/status/1627723042087370775	Video posted on 2023-02-20, seems to be from aftershock.
5	https://www.youtube.com/watch?v=c9qI-KZmt9g	Large waves in backyard pools
6	https://www.youtube.com/watch?v=iWq9rJYnWbg&list=PLi5AeW_TpchzYZjWVuDJGJIJF2WCVtFQE&index=1	Water level is much lower than other pools, so easy to observe amplitude of the waves
7	https://www.youtube.com/watch?v=oEbmcHEmc2s&list=PLi5AeW_TpchzYZjWVuDJGJIJF2WCVtFQE&index=4	Video features multiple angles of same observation, as location is large sports facilty. Footage is sped up.
8	https://www.youtube.com/watch?v=IoCZvKdg6E8&list=PLi5AeW_TpchzYZjWVuDJGJIJF2WCVtFQE&index=2	Likewise, multiple angles of same observation because sports facilty has multiple cameras
9A	https://www.youtube.com/watch?v=PJ0pg9aN648&list=PLi5AeW_TpchzYZjWVuDJGJIJF2WCVtFQE&index=6	Waves run along the length of the pool; lane dividers help to clearly see wave movement
9B	https://www.youtube.com/watch?v=oxqfhtQ6_fc&list=PLi5AeW_TpchzYZjWVuDJGJIJF2WCVtFQE&index=7	Waves run along the length of the pool; lane dividers help to clearly see wave movement
10	https://youtube.com/shorts/5VHxXjBxlTk?feature=share	Fountain has ice, outside. Assigned location is not certain, may be erroneous
11	https://youtube.com/shorts/23buzravb9c?feature=share	Snowing, outside. Comment: "Çorum alaca da sarsinti aninda havuz" (The pool at the time of the shaking in Çorum, Alaca)
12	https://www.youtube.com/watch?v=9mjE1zPdUn0	Snowing, outside. Large elevated irrigation tank at farm.
13	https://www.youtube.com/shorts/5rYU_OIlgXc	Because of video angle, diffcult to see wave motion directly; however, can see water spilling out of pool.
13	https://www.youtube.com/shorts/5rYU_OIlgXc	Because of video angle, diffcult to see wave motion directly; however, can see water spilling out of pool.
14	https://www.tiktok.com/@suheiltel/video/7196862604252400897	Pool lit with underwater lights. Personal villa near coast of Cyprus.
15	https://www.facebook.com/watch/?v=877925723319970&extid=NS-UNK-UNK-UNK-AN_GK0T-GK1C&mibextid=2Rb1fB&ref=sharing	Includes following comments in English on intensity associated with this seiche: "On February 6, 2023, at 3:17 a.m. the disaster began in Turkey and the shockwaves quickly reached the island as well. It rocked us all and woke many of us up. It felt like a 4.8 and lasted a long time. Then the aftershock of 6.3 degrees was felt and was recorded at 3.28. So it was a continuous swing. All my stuff hanging on the walls waltzed "nicely" for more than 10 minutes, but everything stayed in place in the cupboards and on the shelves. No property damage was recorded on the island, at least not reported, but images have already emerged of swaying chandeliers and pools that have been hit by small waves. "
16	https://www.youtube.com/watch?v=TgUAevXStiQ	Because of glass fish tank, can clearly observe side profile of seiche instead of only from top as in other observations. Wave motion changes over course of earthquake.

The authors have made a general estimate of the periodic motion in each observation by using time stamps from the videos. The periods of oscillations vary depending on the dimensions of the body of water and the forcing exerted to it. Seiches were observed in three main categories of environment: public pools, residential pools, and outdoor water tanks. Of these three, it is easiest to determine the dimensions of public pools, as pools used for exercise and competition are typically standardized to 25m or 50m in length and allocate approximately 2.5m in width to each lane used for lap swimming (source: World Aquatics previously known as FINA). Residential pools are generally much smaller, and it is harder to estimate their size because there are no standard dimensions; however, it is still possible to estimate their size with a good degree of accuracy through comparison with other objects pictured in the video. Harder still, it is even more difficult to determine dimensions of water tanks, though it is likewise helpful to use other objects nearby to roughly estimate size. It is also important to consider whether sloshing is along the length or width of the body of water.

Quick estimations of the motion using the clock on the camera of some of the observations (Figure 8 (Left)) shows the periodic motion to be in the range of 3-5 seconds. Public swimming pools typically span either 25m or 50m in length and allocate approximately 2.5m in width to each lane. Taking observations 1 and 2 into consideration (Table 3), this public swimming pool in Gaziantep seems to be 25m long, 12.5m wide and with 5 lanes. If we use the simple formula (1) with these dimensions in mind, then the primary mode of oscillation for an Olympic sized swimming pool (L=50m) and its half equivalent (25m) are 11 and 5.5 seconds, respectively.

Figure 8. (Left) is a still image of a swimming pool sloshingalong the short side of Gaziantep. Clock on the upper left shows Monday 13 13:12 which is the local time close to the onset of the M7.5 earthquake, (Right) Still image of swimming pool sloshing along the short side in Antalaya.

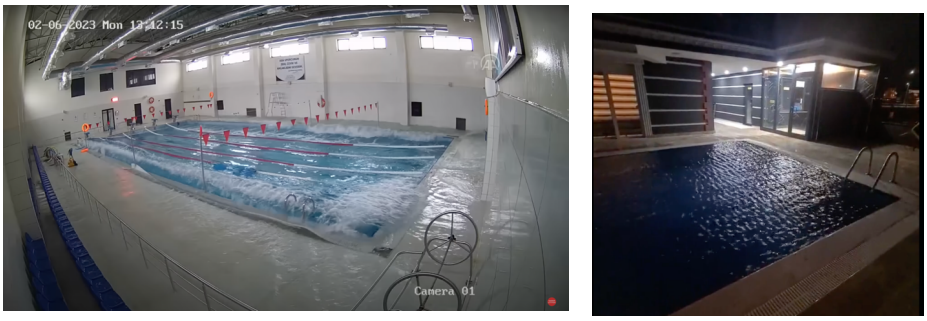

Figure 8. (Left) is a still image of a swimming pool sloshingalong the short side of Gaziantep.

Because sloshing appears to be on the short sides of various sized swimming pools (25 m, 12.5 m, 6m; sloshing appears in both cases to be along the width and not the length) the primary mode of oscillation can also occur at 2.7 seconds for the smallest sized pools. The second and third estimates (5.5, 2.7 seconds) match the approximate calculation from the video recordings in Figure 8 and therefore we can safely assume the sizes of the swimming pools are about half the

size of an Olympic swimming pool (25m x 12.5) or smaller. Videos suggest the mode of oscillation to be primary (rising on one side and fall on the other) in most cases.

$$T=2LNgD \qquad N = 1, 2, 3, \ldots..(1)$$

3.2 SEICHING HISTORY IN THE EASTERN MEDITERRANEAN (GREECE, TURKEY AND CYPRUS)

Information about seismic seiching in Greece, Turkey, or Cyprus may be found in national, regional or international databases for tsunamis – for example, the NOAA National Centers for Environmental Information (NCEI; Global Tsunami Database (previously NGDC) and regional earthquake catalogs, which discuss historical records with respect to earthquakes and tsunamis (e.g., Papazachos & Papazachou, 2003; etc.). More specifically if Turkey, Greece, and Cyprus are selected as the region of interest in NCEI, only 4 events are included as events with seiche observations (1 from Turkey and 3 from Greece) as seen below:

Table 4. Seiche observations in the eastern Mediterranean (Greece, Turkey) from the NEIC database

Year	Mo	Dy	Hr	Mn	Event Validity	Cause Code	Earthquake Magnitude	Country	Location	Latitude	Longitude
1636	9	30	18	30	0	1	7.2	Greece	Ionian Sea	38.1	20.3
1810	2	16	0	1	0	1		Greece	Crete	35.5	25
1857	9	17	22	0	0	1		Turkey	Marmara Sea	40.2	29
1949	7	23	15	3	3	1		Greece	Chios	38.718	26.482
1979	5	15	6	59	0	1	5.6	Greece	Crete	34.53	24.437

Specifically, no data exists in the Global Tsunami Database concerning seiching in Cyprus; furthermore, one event in Chios appears to be a seiche which was generated from a tsunami, and one observation is from Turkey. Two more observations are listed from Greece (Table 4). It is evident that seiching observations are a rarity in this region of the Eastern Mediterranean. To the best of our knowledge, the observations from Turkey in Table 4 are unique or of very few

documented seiches stemming from earthquake ground motions. The dataset which is presented in Table 3 is therefore of particular significance as it is unique for both Cyprus and Turkey.

The observations listed in Table 3 are the only seismic seiches that — to the best of authors knowledge — have ever been collected from Cyprus, making them especially valuable. Recorded seismic seiches from Turkey and Greece are also very few, and the dataset presented from the February 6 earthquake sequence appears to be the most extensive dataset about seismic seiches from Greece, Turkey and Cyprus to have ever been collected.

4. COASTAL FLOODING

Following the February 6, 2023, earthquakes, Iskenderun in the Hatay province was flooded. Iskenderun in the bay of Alexandretta is a coastal low-lying city in Southern Turkey (Demirkesen, 2012). Eyewitness accounts show a flow depth of knee-equivalent (~ a ft or 0.3 m,refs) for the flooding that occurred in the coastal areas of Iskenderun (Figure 9). Using eyewitness accounts, field survey results from reconnaissance reports (e.g., Figure 9, (Lekkas, et al., 2023)), we have delineated the approximate extent of flooding (230 sq km; Figure 10).

Figure 9. Photographs of the extent of the flooding from Armenia News (upper left). Trend News Agency (upper right), and Reuters (bottom)

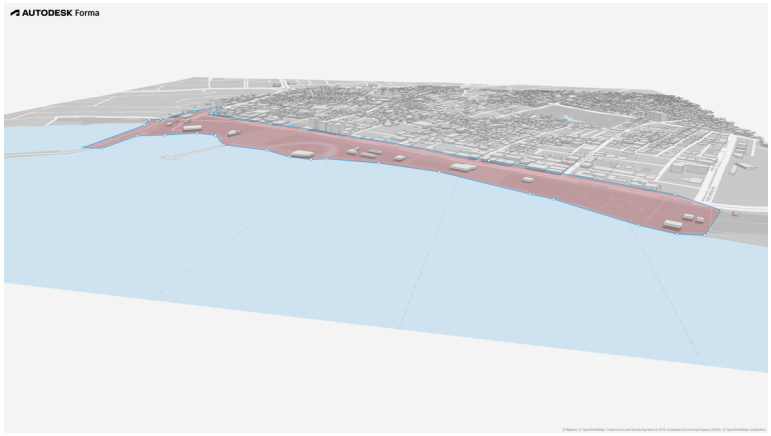

Figure 10. View of the flooded area (approximate extent) in red color in Iskenderun looking SSE, superimposed on a DTM. Extent of flooding was estimated from processed satellite imagery, eyewitness accounts, and reconnaissance reports to the EMSC (e.g. Lekkas et al. 2023)

For a more precise inundation map, we used Landsat 8 and Sentinel 2 data. The satellite images used here were taken before and after the main M7.8 event as close to the date of the earthquake as possible (Sentinel 2 images: 01/25/2023 and 02/09/2023; Landsat 8 images: 02/05/2023 and 02/06/2023). A true color composite of the Bay of Alexandretta post-earthquake (02/09/2023) is shown in Figure 11.

Figure 11. True Color Composite of the Bay of Alexandretta from the 9th of February 2023 using Sentinel 2 B-G-R bands. Red box shows Iskenderun. Flooded area was primarily on the SSW side within the box.

Because the extent of flooding is quite small (~230 sq km), we employed several different methods to capture the extent of inundation. A small extent of flooding may be difficult to capture from the processing of images of moderate resolution as is the case with Landsat 8 (30m). Specifically, true and false color composites and 2 different water indices were employed for this purpose. Landsat 8 bands 3 and 5 (30m resolution) were used in addition to Sentinel 2 Green and NIR bands (bands 3 and 8 respectively; 10m resolution).

NDWI (Normalized Difference Water Index) was used to delineate the extent of flooding observed after the earthquakes of 02/06/2023. The NDWI method is commonly used for delineating and monitoring content changes in surface water. NDWI formula is defined as follows:

$$NDWI = \frac{Green - NIR}{Green + NIR} \quad (2)$$

The following values were used as a guide to interpret results: *0,2 - 1 for water surface, 0.0 - 0.2 for flooding/humidity, -0.3-0.0 for moderate drought/non-aqueous surfaces, -1 - - 0.3, Drought/non-aqueous surfaces*.

Using Landsat 8 images of the bay of Alexandretta captured on the 5th and 6th of February 2023, we see in Figure 12 prominent water presence on the date of the Kahramanmaras earthquake (green color). More specifically, prior to the earthquake sequence of February 6, 2023, NDWI shows a general drought in the area (orange shades) and a very low water content on the ground. The next day, the index shows a large presence of water content throughout the classified image, and around the area that corresponds to Figure 10 (see red arrow pointing to green strip along the coast on Figure 12). Note that some of the water content in Figure 12 (green) is related to the snow that appears on Figure 11 and other causes.

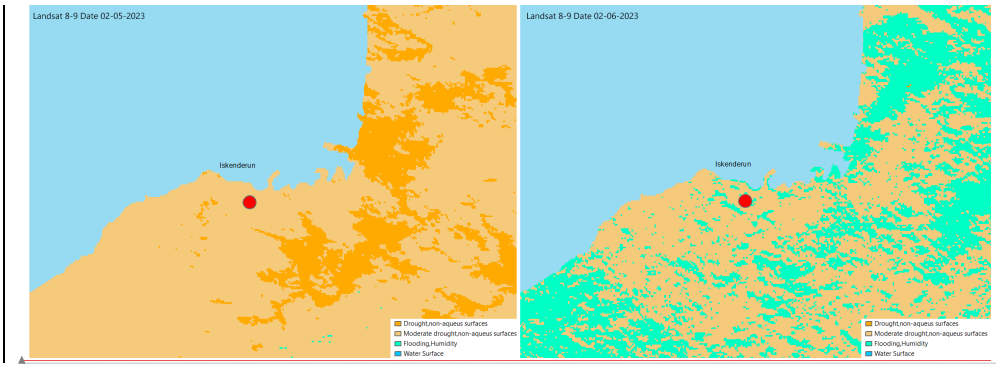

Unknown
Formatted: Font:Italic, Font color: Black

Figure 12. Before and after NDWI for Iskenderun and neighboring areas. Red dot shows central point location of flooding observed after the M7.8 February 6, 2023 earthquakes.

5. DISCUSSION/CONCLUSIONS

The coastal effects associated with the twin earthquakes of February 6, 2023Kahramanmaras Turkey earthquakes have been presented. Tsunami recordings from public portals i.e. IOC-UNESCO, were detided and fourier spectra of their frequency content were estimated. A clear tsunami signal was recorded only in a small subset of operating tide gauge stations including some in Cyprus. The best records were those closest to the Bay of Alexandretta. The tsunami records are rather interesting because of the location of the earthquake and its focal mechanism. Subsidence and liquefaction observed in Iskenderun likely have contributed to the flooding observed in the area but the degree each of these factors has played in the flooding is difficult to estimate.

A unique and one-of-a-kind dataset of seiche observations collected from Turkey and Cyprus have also been documented. The seiche observations collected after the February 6, 2023 events are especially valuable for many reasons:

- The dataset is the largest set of seiche observations that authors are aware of for the eastern Mediterranean region.
- Seismic seiche observations from Cyprus are the only ones that authors are aware of to have been documented.
- Seismic seiches are associated with multiple events from the February 6, 2023 earthquake sequence.
- A relatively large set of seismic seiches collected may allow for spatial analysis.
- Seiches may be associated with locations of liquefaction and vice versa which could further help hazard studies of past of future earthquakes of significance.

Satellite imagery from before and after the main event of February 6, 2023, from Landsat 8 and Sentinel were processed to help in delineating flood extent from the Kahramanmaras earthquakes. Specifically, Landsat 8 in combination with eyewitness accounts from media (e.g., newspapers, online), reports to the EMSC (Lekkas et al., 2023) were used to delineate the extent of flooding caused by the main M7.8 02/06/2023 event. The extent of flooding was estimated to about 230 sq km which is small and presented challenges in its exact estimation from open-source satellite imagery of moderate resolution (10-30m). Eyewitness accounts, videos and images collected from online media which were geolocated helped to delineate the extent of flooding. The causes of flooding have not been investigated in this study but likely are attributed to more than one factor such as subsidence, tsunami and liquefaction.

ACKNOWLEDGMENTS

I would like to thank Dr. Danezis of Cyprus University of Technology for providing data from the national network of Cyprus.

REFERENCES

Barberopoulou, A., Qamar, A., Pratt, T. L., Creager, K. C. & Steele, W. P. Local amplification of seismic waves from the Denali earthquake and damaging seiches in Lake Union, Seattle. Wash. Geophys. Res. Lett. 31, L03607. https://doi.org/10.1029/2003GL018569 (2004).

Barberopoulou, A. A seiche hazard study for Lake Union, Seattle. Washington. Bull. Seismol. Soc. Am. 98, 1837–1848. https://doi.org/10.1785/0120070153 (2008).

Danezis, C., M. Nikolaidis, C. Mettas, D. G Hadjimitsis, G. Kokosis, and C. Kleanthous. 2020. "Establishing an Integrated Permanent Sea-Level Monitoring Infrastructure towards the Implementation of Maritime Spatial Planning in Cyprus." Journal of Marine Science and Engineering.

Demirkesen, A.C. 2012. Multi-risk interpretation of natural hazards for settlements of the Hatay province in the east Mediterranean region, Turkey using SRTM DEM. Environ Earth Sci 65, 1895–1907. https://doi.org/10.1007/s12665-011-1171-0

Duman T. Y., O., Emre. 2013. The East Anatolian Fault: geometry, segmentation and jog characteristics, Geological Society, London, Special Publications. https://doi.org/10.1144/sp372.14

Estrada, F., González-Vida, J.M., Peláez, J.A. et al. 2021. Tsunami generation potential of a strike-slip fault tip in the westernmost Mediterranean. Sci Rep 11, 16253. https://doi.org/10.1038/s41598-021-95729-6

Hancilar, U., K. Sesetyan, E. Cakti, E. Safak, N. Yenihayat, F. S. Malcioglu, K. Donmez, T. Tetik, and H. Suleyman. 2023. "Kahramanmaraş - Gaziantep Türkiye M7.7 Earthquake - Strong Ground Motion and Building Damage Estimations." Accessed 05 24, 2023. https://www.emsc-csem.org/Doc/Additional_Earthquake_Report/1218444/Kahramanmaras-Gaziantep_Earthquake_06-02-2023_(04.17)-Bogazici_University_Earthquake_Engineering_Department.pdf.

Information, NOAA National Centers for Environmental. 2023. NCEI/WDS Global Historical Tsunami Database, 2100 BC to Present. 05 18.

Jenkins, J., B. Turner, R. Turner, G. P. Hayes, A. Sinclair, S. Davies, A. L. Parker, et al. n.d. "Seismicity of the Earth 1900–2010 Middle East and Vicinity." Open-File Report 2010–1083-K. Prod. U.S. Geological Survey. Denver, Colorado.

Kvale, A. Seismic seiches in Norway and England during the Assam earthquake of August 15, 1950. Bull. Seismol. Soc. Am. 45, 93–113.
https://doi.org/10.1785/BSSA0450020093 (1955)

Lekkas, Efthymis, PanayotisCarydis, Emmanuel Vassilakis, Spyridon Mavroulis, IoannisArgyropoulos, AndromachiSarantopoulou, Maria Mavrouli, et al. 2023. "Newsletter_29_2023_Turkey-Syria_EQ." EMSC-CSEM. February. Accessed May 17, 2023. .

Rabinovich, A. B., 2009. Seiches and Harbor Oscillations, Handbook of Coastal and Ocean Engineering, pp. 193-236

Sandvol, E., N. Turkelli, and M. Barazangi, The Eastern Turkey Seismic Experiment: Thestudy of a young continent-continent collision,Geophys. Res.Lett.,30(24), 8038, doi:10.1029/2003GL018912, 2003

Sesetyan, K., M. Stucchi, V. Castellli, and A. A. Gomez Capera. n.d. "Kahramanmaraş - Gaziantep Türkiye M7.7 Earthquake - Large historical earthquakes of the earthquake-affected region ." Accessed 05 24, 2023. https://www.emsc-csem.org/Doc/Additional_Earthquake_Report/1218444/kahramanmaras-gaziantep_earthquake_06-02-2023_large_hist_eqs.pdf.

Taymaz, T., A. Ganas, D. Melgar, B. W. Crowell, and T. Ocalan. 2023. EMSC Special Report - Earthquake sequence in Turkey, February 6th 2023. 02.

Internet

https://www.msn.com/en-xl/money/other/massive-pools-shake-during-the-64-magnitude-earthquake-in-antalya-turkey/vi-AA17NvU5 Vol. 42 No 3, page (2023) (accessed 7/14/2023).

https://news.am/eng/news/750553.html (accessed 7/14/2023).

https://en.trend.az/world/turkey/3707012.html (accessed 7/14/2023).

World aquatics, https://www.worldaquatics.com/ (accessed 08/21/2023)

Armenia News https://news.am/eng/news/750553.html (accessed 08/21/2023)

https://en.trend.az/world/turkey/3707012.html (accessed 08/21/2023)

The STAR https://www.youtube.com/watch?v=yh_pggq0rPA (accessed 08/21/2023)

ISSN 8755-6839

SCIENCE OF TSUNAMI HAZARDS

Journal of Tsunami Society International

Volume 42 Number 3 2023

TSUNAMI HAZARD: IMPACT OF DATA QUALITY ON A MODELLING AND MAPPING FRAMEWORK

Rudy VanDrie[*1], Gede Pringgana[1], Ni Nyoman Pujianiki,

[1] *Universitas Udayana Bali 60231, INDONESIA*
Email: rudyvandrie@gmail.com

ABSTRACT

The need to review the impact of tsunamis on the island of Bali and Indonesia as a whole is real and warranted. There are in excess 17,500 island, 275million people and multiple Tsunami sources. The last comprehensive assessment of tsunami risk and hazard for parts of Bali and Padang was completed in 2010 with data since identified as unsuitable in accuracy. Several problems are identified to improve tsunami hazard mapping in Indonesia, such as the role of input data accuracy consistency and density of data, a better description of hazard, and the sensitivity of hazard to input data quality. The research objectives include reviewing multiple data sets, undertaking tsunami impact modeling, and developing a data quality metric. Further there is consideration of a future framework approach to enable a nationwide roll-out of modelling on the basis the metric identifying the availability of improved quality of data. Strongly related to this is the ongoing development and review of the Indonesian BATNAS and DEMNAS data. It is recommended that version metadata be developed for the evolving data sets in time. Noting that ongoing improvement in this data is a strong candidate to trigger the need to update Tsunami Modelling and Mapping in Indonesia, either as a whole, or in specific areas as it becomes available.

Keywords: *Tsunami, hazard, models, data, quality, accuracy, DEMNAS, BATNAS, ANUGA*

1. INTRODUCTION

Indonesia is the worlds largest archipelago with over 17,500 islands (see in Figure 1 which is the 14th largest country in the world covering 1,904,569 square kilometres with 275 million people. Making it the 4th most populous country. It is one of the most tectonic seismically active countries in the world where the Indo-Australian Plate and the Pacific Plate and many sub-plates are interacting with the Eurasian plate. The 2004 Indian Ocean earthquake and 2006 Yogyakarta earthquake were two events triggering tsunami. In 2019, 15.4 million tourist visited Indonesian contributing around US$9.8 billion to GDP in 2020 making an interruption due to tsunami potentially very expensive to the entire community.

From this statement it is clear that Indonesia has significant complexity related to Tsunami impact not shared by any other nation. It has a huge number of islands (largest archipeligo in the world), a very large population, strong contribution to its economy through tourism, and sits on one of the most seismically active zones in the world. The length of coastline is estimated to be around 108,000km (second longest in the world) (Pandjaitan, 2020). The 2004 Tsunami and the 2011 Fukashima Tsunami have led to a focused, global research effort on Tsunami's and their impact, this thesis will add to this in a number of ways.

The last comprehensive assessment of Tsunami Risk and hazard undertaken at least for parts of Bali and Padang was conducted in 2009/2010 through GITEWS (GITEWS{DLR / GTZ}, 2010). "Tsunami Hazard Maps for Bali" incorporating;

- 'Multi-scenario Tsunami Hazard Maps for Bali, 1:100,000', and
- 'Multi-scenario Tsunami Hazard Maps for Southern Bali, 1:25,000',

with zoning based on wave height at coast (in line with the InaTEWS warning levels). This work was completed using Mike21 and coarse STRM (30m cell) data. This data is known to be relatively poor (Griffin etal., 2015). The earlier work (Kjell Karlsrud 2009), relied on models using a 100m grid cell using STRM and ASTER terrain data. Of some concern is the ongoing reliance and use by third parties on this mapping product (Sagala etal., 2016) to drive Disaster preparedness. Other attempts to model portions of Indonesia exist but are not comprehensive.

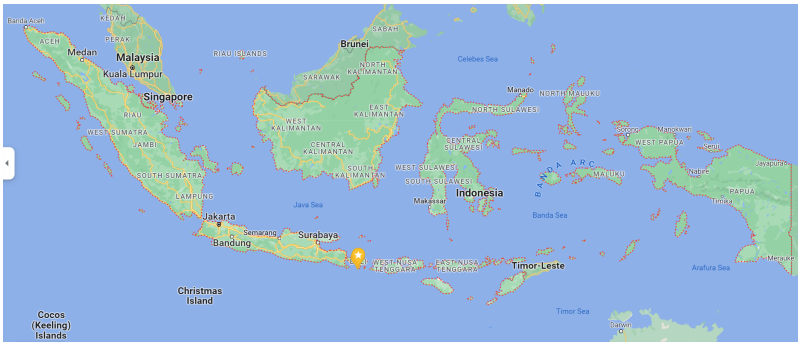

Figure 11. Indonesia Archipelago and Location of Bali

Other attempts to model portions of Indonesia exist but are not comprehensive. (Prerna etal, 2014) undertook tsunami analysis of the Andaman Islands using the STRM data set.

(Fatmawati etal., 2019) undertook run up assessments on a portion of the southern coast of Bali, but it is unknown what terrain data was used for this exercise. (Valentra Etal, 2022) undertook a tsunami impact analysis using higher resolution data in the Lombok Strait. In regard to the inclusion of Buildings research has shown a very real impact on flow behavior and resulting hazard (Murray etal., 2021).

In relation to input data accuracy, (Griffin etal., 2015) provide an assessment for the Tsunami Impact on Padang. However, the notion of a framework to control and assess the accuracy of the input is not directly discussed. It is however significant and relevant to note their findings and conclusions paraphrasing here:

"The results presented in this paper clearly demonstrate that the present generation of freely available global DEMs (i.e., ASTER and SRTM90) are not sufficiently accurate to simulate tsunami inundation with confidence.

Tsunami inundation models developed using DEMs that are currently freely available at a global scale (i.e., ASTER and SRTM) have the potential to dangerously underestimate the inundation extent. These datasets should not be used to assess tsunami inundation zones using hydrodynamic models."

Finally, globally the methods to describe a hazard from Tsunami or indeed any flowing water has not evolved from initial concepts developed in the 1970's. Whilst technology to provide analysis has improved such that there are now numerous tools that provide highly accurate simulation capacity, the core method to define the resulting hazard has remained unchanged and not open to new inputs from the new analysis methods. Hazard has and is defined primarily on momentum or the Velocity times Depth product. Although several researchers have tried to show methods of plausibly improving this (Trieste, 1988) , (VanDrie, 2008) to date no alternate methods are widely adopted beyond the original 1970's formulation of hazard. This work will touch on approaches to hazard, and the notion of using a framework to enable a systematic and consistent approach to model input assessment, model setup and production of output for mapping.

2. METHODS

The framework of thinking in this study is based on the notion that the accuracy of results from models is directly impacted by the accuracy and quality of input data. The old saying; "Rubbish-In, Rubbish-Out" is very true. However, the objective is to try to gain a metric, a notion of measurement of data accuracy and the influence on resulting output. This requires assessment of input data sets, running of multiple models over the same area utilizing each of the data sets and

finally reviewing results and the variation in results as a result of only input data differences. Refer to Figure 2 for an outline of the method and approach.

The research concept in this work is to acquire multiple data sets for two project sites. One set of multiple data sources for Ocean Floor bathymetry, one set of above Ocean terrain data. The data sets will be ranked in accuracy based on how the data has been collected. A physically measured (surveyed) data set will be deemed most accurate. For bathymetry single beam sonar is deemed most accurate on the basis that it has been manually acquired. The survey and sonar will become the point of truth data for comparisons. For the additional data sets, a comparison will be undertaken to identify how much error is in the data compared to the point of truth data. The approach here is to utilize two sites with multiple data sets that describe the terrain and bathymetry at various levels of accuracy. Based on the different data sets a tsunami model will be run for each combination of terrain+bathymetry.

The resulting inundation and hazard characteristics on the shore attacked by the tsunami will be compared for each of the models. The comparison of model results from the bathymetric data sets will provide an indication of the sensitivity of hazard based on the drowned terrain changes. The comparison of the dry terrain results for each of the bathymetric data sets, will indicate that a change in offshore data influence the on land hazard. Similarly the comparison of the multiple dry terrain data sets, keeping the bathymetry static will indicate the sensitivity of hazard definition of only the terrain change. The initial steps involve gathering the data sets. There are two distinct different types of data, point data, and surface data (grid). As such a comparison must be based on values located precisely at the points as well as over the 2 dimensional extent of the surfaces created by the points, when compared to the grid data sets.

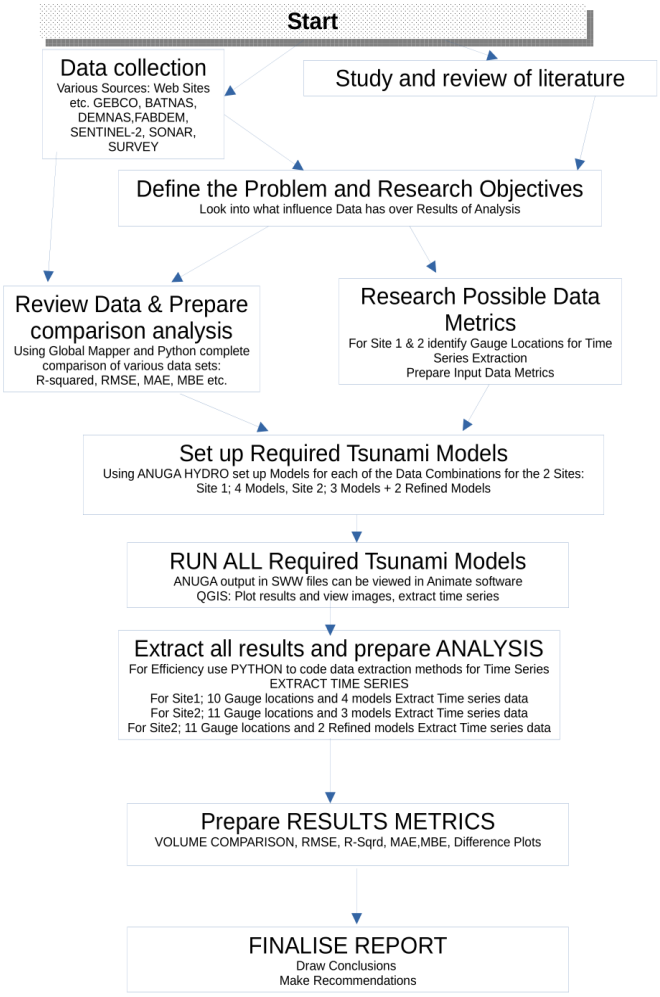

Figure 12. Process Steps

The completion of the input data analysis will attempt to identify a "Quality Metric". From each of the Terrain and Bathymetric data set combinations, a Tsunami Model will be set up apply the exact boundary conditions, such that the only variance in the model is the terrain component of either Bathymetric data or Terrain data. Once the models have all been run results will be extracted at a nominated number of GAUGE locations. The results will include the full time series of the analysis.

ANUGA HYDRO (Zoppou, Roberts, 1999), (Nielsen, Roberts, 2005) is used to model the inundation resulting from a large tsunami wave as it has been shown to replicate extreme flows very well (Mungkasi, van Drie, Roberts, 2013), (Wuppukondur, Baldock, 2020). The focus is not on the details of the type of wave, or replicating a certain event. Instead a simple 10m increase in water height is applied at the boundary which will drive the model to resolve flow characteristics. The focus again is to account for input data difference in the resulting description of hazard. ANUGA has been selected for this task for a number of reasons:

- It uses a flexibly sized triangular mesh (making it easy to produce high levels of detail only where required) (Schlurmann, Kongko, Goseberg, Natawidjaja, Sieh, 2010), which may be automated (Wright, Passalacqua, Simard, Jones, 2022)
- It is extremely stable in the most extreme flow conditions
- It is proven to be a very good model to replicate tsunami inundation
- It is not highly (or overly) sensitive to changes in surface roughness (Cárdenas, Catalán, 2022), (Van Drie, Milevski, Simon,2011).
- It has a number of very useful built-in functions to make extraction of results very easy
- Can run in Parallel (Roberts, Stals, Nielsen, 2007)

The measure of difference can be achieved in a number of ways:

- The elevation at each point directly compared
- The differences measured based on the surfaces created or available
- Using statistical functions such as RMSE, MAE, MBE etc.

The analysis to be undertaken is on the inundation data sets from the ANUGA HYDRO Models described. The data sets include water level (Stage), momentum of the moving water, bed Shear, Depth, Velocity, and Froude number. Note that, Tsunami really are or become debris flows (Synolakis, Bernard; 2006) and this may be a future trigger to re-model when models can be adequately be adapted to account for debris flows. Models may often contain errors (VanDrie, Ghetti, Milevski, 2018) which may also trigger the need for re-modelling.

The focus of this work is in understanding the influence of data quality (Schlurmann etal., 2010) or of error in input data, on the outcome of error in the results of a model to predict hazard. It is usual to take several ERROR METRICS or Key Performance Indicators (KPI's) into account in order to assess findings. Measuring forecast accuracy (or error) is not an easy task as there is no one-size-fits-all indicator. Only experimentation will show you what Key Performance Indicator (KPI) is best. The first distinction required is the difference between the precision of a forecast and its bias. Bias represents the historical average error. That is, will forecasts be, on average, too high or too low. This will give you the overall direction of the error. Precision measures how much spread is between the forecast and the actual value. The precision of a forecast gives an idea of the magnitude of the errors but not their overall direction. Ideally a model has both, is precise and is unbiased.

Forecast KPI or Error. Error simply put is the difference in a forecast and known target. Note that if the forecast overshoots the target with this definition, the error will be positive. If the forecast undershoots the demand, then the error will be negative. The bias is defined as the average error: - As a positive error on one item can offset a negative error on another item, a forecast model can achieve very low bias and not be precise at the same time. Obviously, the bias alone won't be enough to evaluate the forecast precision. But a highly biased forecast is already an indication that something is wrong in the model. The Mean Absolute Percentage Error (MAPE) is one of the most commonly used KPIs to measure forecast accuracy. MAPE is the sum of the individual absolute errors divided by the target value(s). It is the average of the percentage errors. MAPE is not a good forecast KPI as it is a poor-accuracy indicator. MAPE divides each error individually by the target, so it is skewed: high errors during low-target (numbers) will significantly impact MAPE.

Due to this, optimizing MAPE will result in a strange forecast that will most likely undershoot the target. The Mean Absolute Error (**MAE**) is a very good KPI to measure forecast accuracy. As the name implies, it is the mean of the absolute error. One of the first issues of this KPI is that it is not scaled to the average target value. If MAE is 10 for a particular item, you cannot know if this is good or bad. If your average target is 1000, it is, of course, astonishing. Still, if the average demand is 1, this is a very poor accuracy. To solve this, it is common to divide MAE by the average target to get a %. The Root Mean Squared Error (**RMSE)** is a strange KPI but a very helpful one, as we will discuss later. It is defined as the square root of the average squared error.

Actually, many algorithms (especially for machine learning) are based on the Mean Squared Error (MSE), which is directly related to RMSE. Many algorithms use MSE as it is faster to compute and easier to manipulate than RMSE. But it is not scaled to the original error (as the error is squared), resulting in a KPI that cannot be related to the original target scale. Therefore, it should not be used it to evaluate statistical forecast models.

On the question of error weighting:

Compared to MAE, RMSE does not treat each error the same. It gives more importance to the most significant errors. That means that one big error is enough to get a very bad RMSE. RMSE emphasizes the most significant errors, whereas MAE gives the same importance to each error. Generally a forecast of the median will get a good MAE and a forecast of the mean a good RMSE. MAPE promotes a very low forecast as it allocates a high weight to forecast errors when the target (numbers) is low. Optimization of RMSE will seek to be correct on average. In contrast, MAE's optimization will try to be as often overshooting the demand as undershooting the target, which means focusing on the target median. Understanding that a significant difference lies in the mathematical roots of MAE & RMSE is key. One aims at the median, the second aims at the average. The Root Mean Squared Error (RMSE) is one of the two main performance indicators for a regression model. It measures the average difference between values predicted by a model and the actual values. It provides an estimation of how well the model is able to predict the target value (accuracy). Mean Absolute Error (MAE) is one of the most commonly used loss functions for regression problems, MAE helps users to formulate learning problems into optimization problems. It also serves as an easy-to-understand quantifiable measurement of errors for

regression problems. In MAE, different errors are not weighted more or less, but the scores increase linearly with the increase in errors. The MAE score is measured as the average of the absolute error values. The Absolute is a mathematical function that makes a number positive. Mean Bias Error (**MBE**) is primarily used to estimate the average bias in the model and to decide if any steps need to be taken to correct the model bias. Mean Bias Error (MBE) captures the average bias (+ve or -ve) in the prediction. $\mathbf{R^2}$ is the coefficient of determination, and is a measure that provides information about the goodness of fit of a model. In the context of regression it is a statistical measure of how well the regression line approximates the actual data. This can be used to compare data sets given we know that if the elevations were identical in two models the results would also be. In this work the focus in understanding error utilizing: **{ $\mathbf{R^2}$, RMSE, MAE and MBE }**

3. RESULTS AND DISCUSSION

3A. Site Locations and Input Data

The locations (see in Figure 3) were selected purely on the basis of multiple data sets being available for either topography (terrain) or bathymetry as follows:

Site 1, is at Keramas, where there is Sonar data available, GEBCO, BATNAS and Sentinel-2 data. Four data sets in total. Site 2, is at Nyanyi, where there is ground survey points are available and FABDEM and DEMNAS data. Three data sets in total.

Figure 13. Location of Research Sites

For site 1 the point of truth data is assumed to be the measured SONAR data. This will be compared to the other available data sets being; GEBCO, BATNAS and Sentinel-2. The SONAR data has been filtered to below zero (Figure 4) only and contained within a manageable polygon. There are 2,211 points over an area of 715,525m^2, providing roughly a data density of 1 point per 323.62m^2. Or on average, a data point every 18m in x and y. This data can be used to create a DEM as a surface.

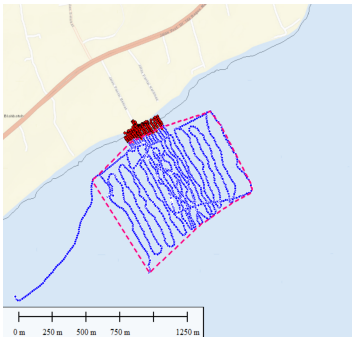

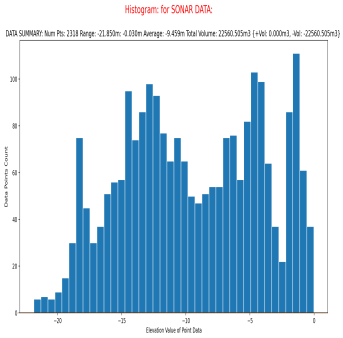

Figure 14. Site 1 SONAR data points

Figure 15. Site 1 SONAR (S) pts

Now that the SONAR data is both a DEM (Figure 6) and a histogram (Figure 5) of point values a comparison can be made of the data differences. This can be achieved both by reviewing the DEMS of the data surfaces and by reviewing the histograms of point elevation values. For the GEBCO data the elevation from the DEM surface is extracted at the same SONAR data points with now the ability to plot the histogram and then compare the differences. The same process can be completed for any other data set.

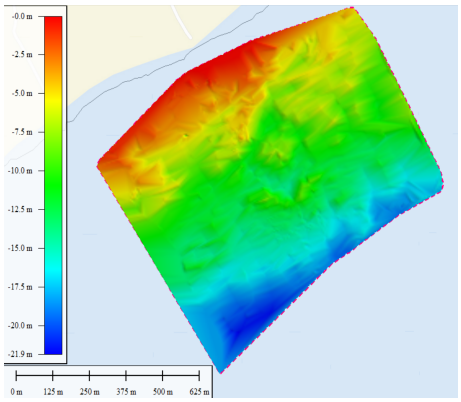

Figure 16. Site 1 SONAR (S) as DEM surface

Extracting the data from GEBCO (Figure 7 & 8) at the same data points provides a method of comparison as does the difference in the DEM as surfaces. Subtracting one surface from another surface provides the difference over the full extent of data change.

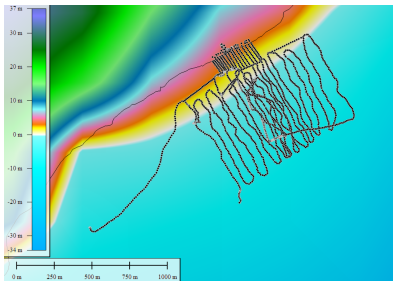

Figure 17. Site 1 GEBCO DATA (G-data)

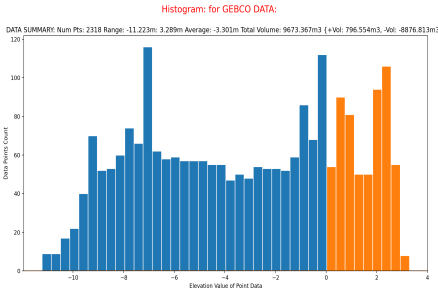

Figure 18. Site 1 GEBCO Histogram

Subtracting the point elevation values (SONAR minus GEBCO) provides a comparison histogram (Figure 9). Similar subtracting the surface DEMS (Figure 10) provides a spatial view of difference.

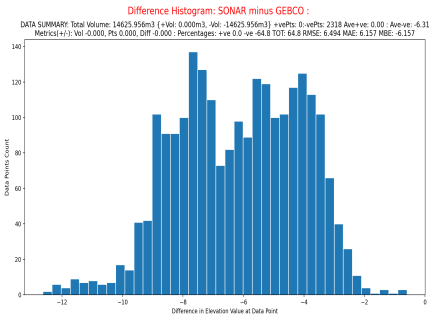

Figure 19. Site 1 Difference Histogram (S minus G)

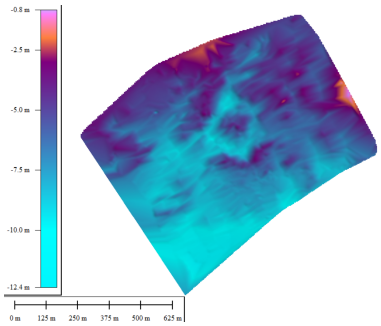

Figure 20. Site 1 DEM Difference (S minus G)

Similarly with the BATNAS data the data can be extracted at the sonar points (Figure 11 & 12) and compared to the DEM surface. The comparison of surfaces provides a very visually rich comparison. The comparison of the points as a histogram provides a more specific approach to comparison (Figure 13 & 14).

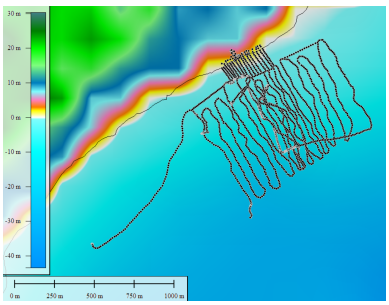

Figure 21. Site 1 BATNAS DATA (B-data)

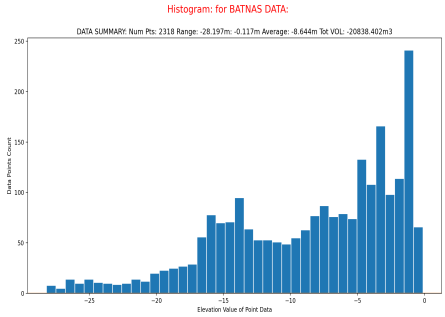

Figure 22. Site 1 BATNAS Histogram

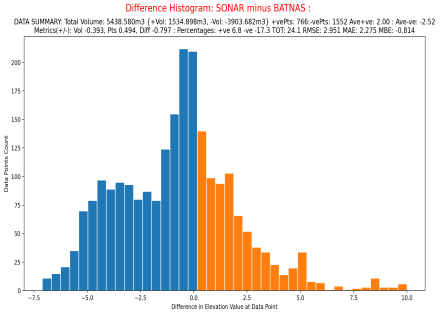

Figure 23. Site 1 Difference Histogram (S minus B)

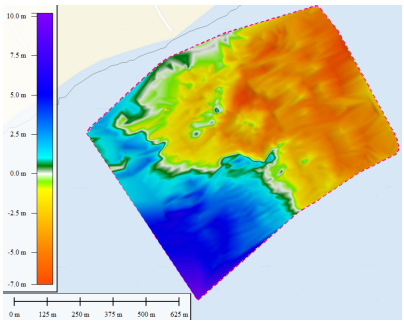

Figure 24. Site 1 DEM Difference (S minus B)

The final data set available is from Sentinel-2 as follows (Figure 15 & 16);

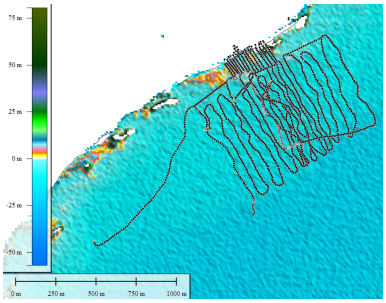

Figure 25. Site 1Sentinel-2 DATA (S2-data)

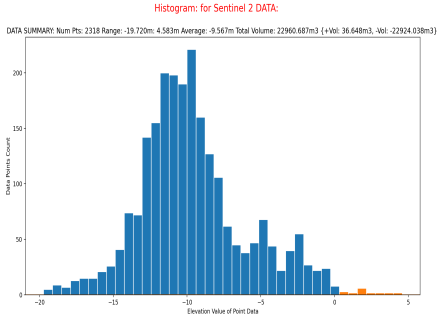

Figure 26. Site 1 S2 Histogram

Once again comparing to SONAR as points and as a DEM surface (Figure 17 & 18).

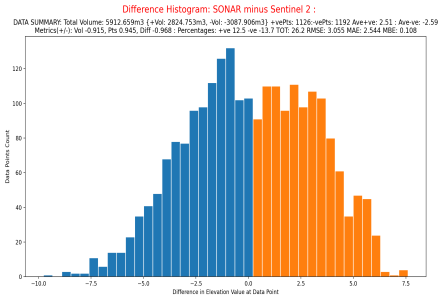

Figure 27. Site 1 Difference Histogram (S minus S2)

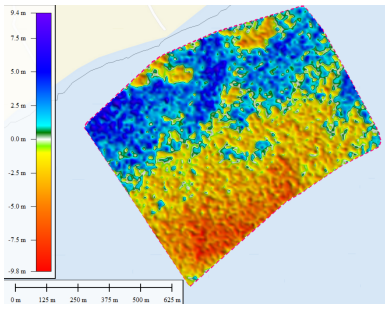

Figure 28. Site 1 DEM Difference (S minus S2)

Another approach to determining an overall difference is to compare how the surface volumes compare. For example, what is the volume contained above each of the surfaces to a specified elevation? This is relatively easy to determine and provides yet another visually rich approach to comparing differences (Figure 19).

The same approach has been applied to site 2 and its available data sets.

3B. Input Data Metrics

Looking at the input data comparing to the point of truth data for Site 1, overall the BATNAS DATA best replicates it based on 2318 points analysis. The **Points Volume Metric** of 24.1% and RMSE of 2.951. However, based on **MBE** of -0.108 the SENTINEL-2 DATA is preferred. On the basis of the **3D surface volume analysis** its suggests BATNAS the best overall candidate with SENTINEL-2 preferred for very shallow water (< 5m depth).

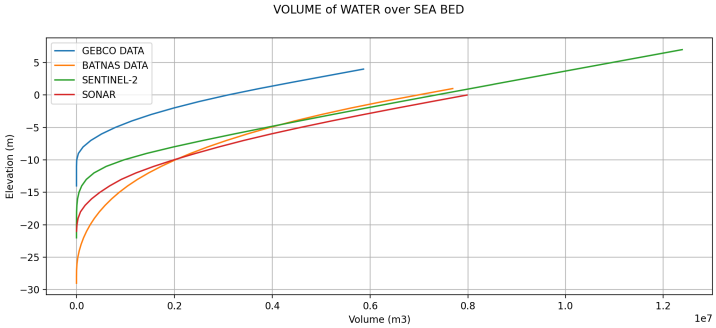

Figure 29. Comparison of water volume over sea bed surface Site 1

For Site 2, the **Points Volume Metric** suggest DEMNAS at 15.9%, which also coincides with the **MBE** of -1.104. The RMSE of 3.026 and MAE of 2.173 prefers the FABDEM data set. Reviewing the terrain based on **3D surface volume** identifies the DEMNAS DATA as the best candidate to replicate the SURVEY.

3C. Tsunami Models

The ANUGA HYDRO MODEL has been set up and run for all of the scenarios described (Figure 20 & 21). The ANUGA HYDRO model produces a single output file (*.SWW) which contains the full time history of conserved quantities (Elevation, Stage, Momentum X and Momentum Y). As it is a finite volume model velocity is not a conserved quantity in the model.

Velocity is derived from Momentum as {V = M/Depth}, where;
M = Sqrt (MomX x MomX + MomY x MomY)
Depth is Stage(Water Elevation) minus Bed Elevation.
This is important as in some model applications such as erosion the elevation can change. For all models since the focus is on the influence of terrain data change, the adopted values of surface roughness are not considered particularly important. For all model runs Manning's N is set at 0.035.

Site 1 has four (4) models with only Bathymetric data being changed between models. The mesh for all models was set at (10x10m) {100m2} cells.

Site 2 has three (3) models with only the terrain data being changed between models.
In addition a further model was set up to test the sensitivity of results to the mesh refinement. The mesh for all models was set at (10x10m) {100m2} cells, except for the refined models which used (5x5m) {25m2}. The Models have been run for 1 hour (3600 seconds in the models).

In addition any surface can be extracted and viewed in QGIS, or exported to any other GIS platform. Further for any location within the models it is possible to extract the conserved quantities and from those derive many other quantities such as:

- Depth
- Velocity
- bed Shear (VxVxD)
- Froude
- Specific Energy (VxV/2g)

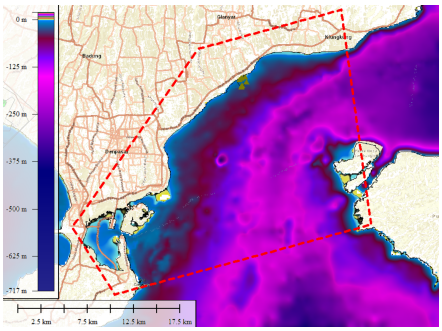

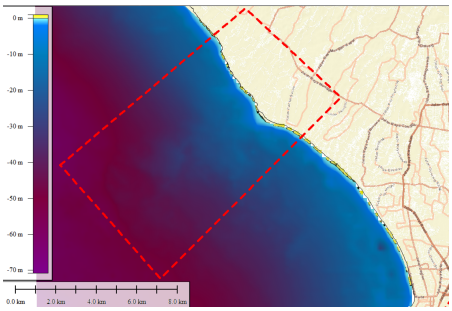

Figure 30. Site 1 Tsunami Model Extent

Figure 31. Site 2 Tsunami Model Extent

Data is to be extracted at Gauge locations for each site as indicated in (Figure 22 & 23).

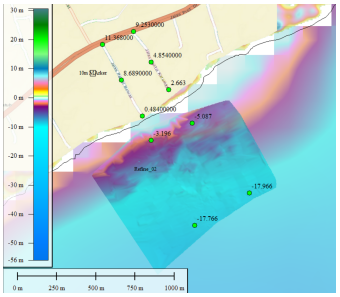

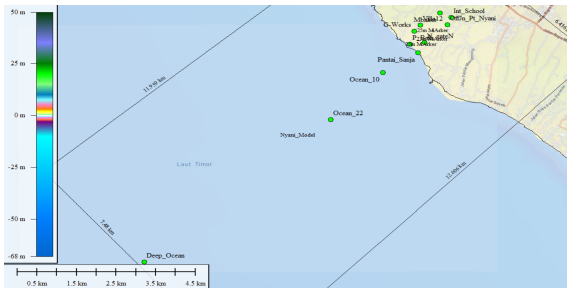

Figure 32. Site 1 Gauge Locations

Figure 33. Site 2 Gauge Locations

The models were run as described and data extracted as both time series and as a surface of maximum momentum (Hazard). For Site 1 the four models (Figure 24-27) produce the maximum momentum plots as shown and these can be used to look into the difference of hazard resulting from the difference in input data for each of the models.

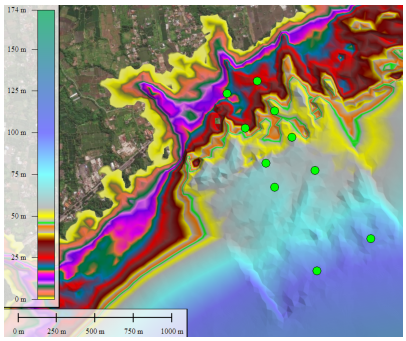

Figure 34. Max Hazard Sonar

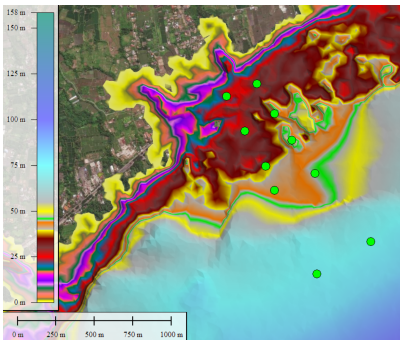

Figure 35. Max Hazard GEBCO

Visually the Gebco model is immediately different. The BATNAS and Sentinel based models are far more similar to the SONAR model, but clearly not identical.

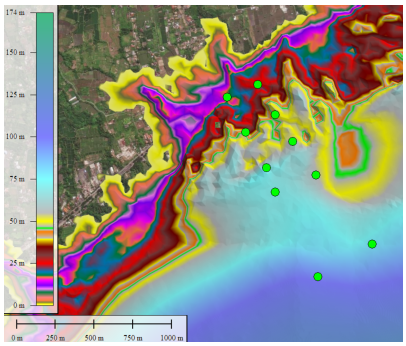

Figure 36. Max Hazard BATNAS

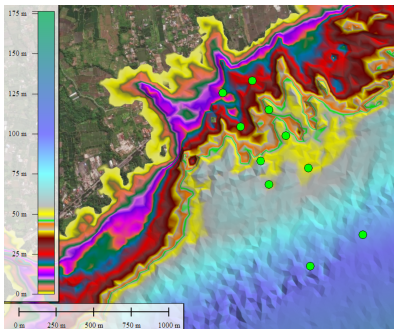

Figure 37. Max Hazard Sentinel

The differences (Figure 28) in the model results can be visually indicated by creating a difference plot of results of each of the models compared to the SONAR model results.

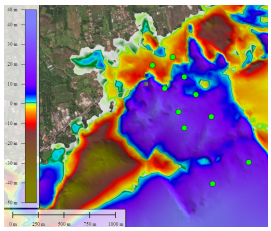

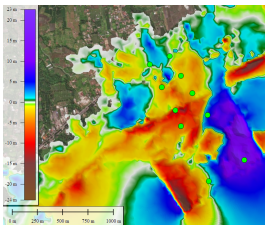

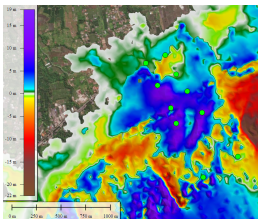

Difference Sonar-Gebco Difference Sonar-Batnas Difference Sonar-Sent

Figure 38. Comparison of Max Hazard Differences for Site 1 models

To drill into more detail time series at the gauge points will be explored further.
The Hazard is defined from Velocity times Depth (Momentum).
The maximum hazard can therefore be plotted spatially for each of the models as for site 1.

For Site 2 the following plots show the maximum momentum (Hazard) for the 3 models (Figure 29-31) run and the difference plots again indicate the resulting variations only as a result of changing the input terrain data.

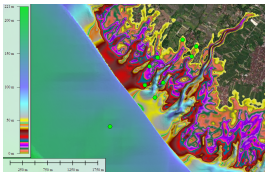

Figure 39. Max Hazard Survey

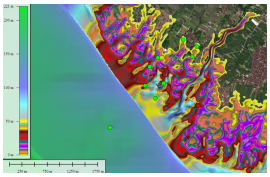

Figure 40. Max Hazard Demnas

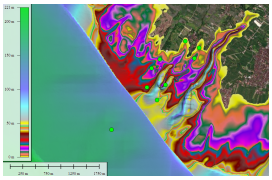

Figure 41. Max Hazard Fabdem

Once again the very obvious difference (Figure 32) here is the Fabdem data set results. Looking at the difference between model results also identifies the extent of differences.

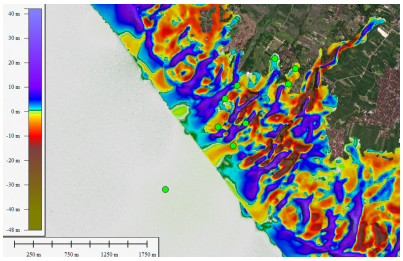

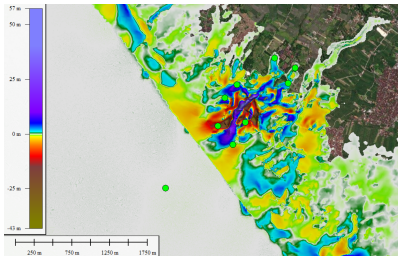

Difference Survey-Demnas Difference Survey-Fabdem

Figure 42. Comparison of Max Hazard Differences for Site 2 models

Once again further details can be extracted from time series behaviour over the entire simulation.

3D. Extracting and comparing Time Series Data

For site 1 there are 10 locations where gauge data has been extracted the following time series plots are an example of those extracted (Figure 33). Site 2 has similar plots for all its gauge points.

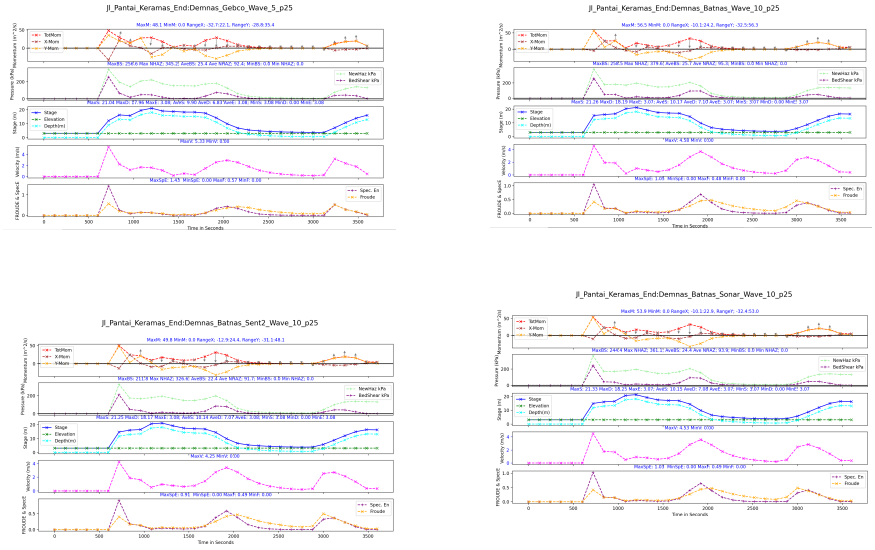

Figure 43. Time Series 4 models at Site 1: Location Jl Pantai Keramas End

The difference plots show the variation between the point of truth model (SONAR) compared to the other data models (GEBCO, BATNAS, SENTINEL). Hence, for Site 1 at each location there are three (3) difference plots (Figure 33-36) . The difference plots statistics have also been accumulated and will be presented here as a form of summary and to draw conclusions. A critically important aspect to be aware of in the nature of tsunami analysis is that of the reflective wave, or the retreating wave on land. The difference at times can be more pronounced in the retreating phase than in the initial wave attack. This is clear in the example shown in the following figures.

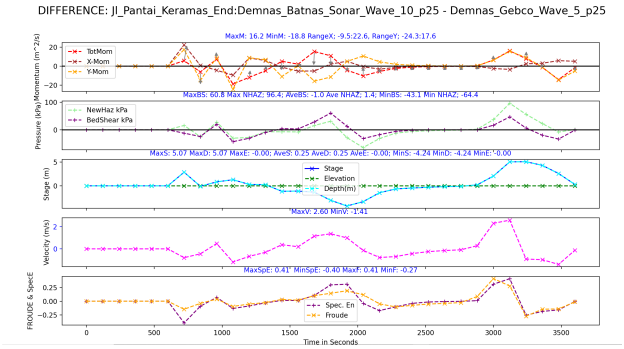

Figure 44. Site 1 Location Jl. Pantai Keramas End Difference SONAR minus GEBCO

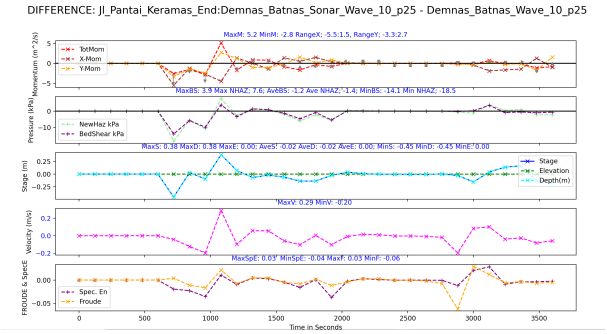

Figure 45. Site 1 Location Jl. Pantai Keramas End Difference SONAR minus BATNAS

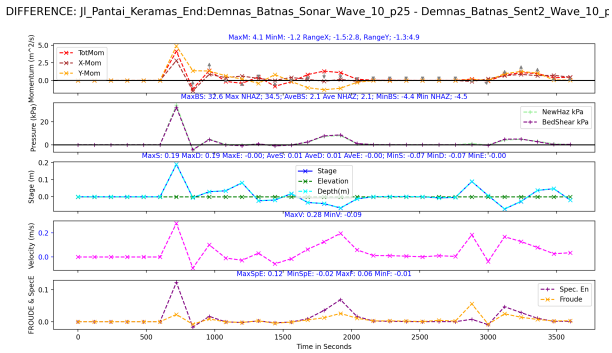

Figure 46. Site 1 Location Jl. Pantai Keramas End Difference SONAR minus SENTINEL

For the 10 Gauge Locations in 3 comparison models at Site 1 the R-squared terms show that for the Bathymetric data changes (only) the impact the surface water elevation (Stage) the least in the SENTINEL model compared to the point of truth SONAR model. Similarly Momentum is best replicated in the SENTINEL model when compared to the point of truth SONAR model. For Bed Shear and a newly considered hazard measure based on pressure, the BATNAS model best replicates the point of truth SONAR model.

For the 11 Gauge Locations in 2 comparison models at Site 2 the R-squared terms show that for the terrain changes (only) the impact on all terms, (Stage, Total Momentum, Bed Shear and the Pressure Hazard term considered), the best model to replicate the point of truth SURVEY model is the DEMNAS based model.

SITE 1:	**SITE 2: Mesh 100**
SONAR - GEBCO	**SURVEY - FABDEM**
Stage 0.9084336	Stage 0.9999042
TotM 0.7677961	TotM 0.9988720
BedShear 0.7769386	BedShear 0.9992434
NewHaz 0.8781592	NewHaz 0.9992782
SONAR - BATNAS	**SURVEY - DEMNAS**
Stage 0.9987725	**Stage 0.9999943**
TotM 0.9922413	**TotM 0.9999616**
BedShear 0.9727753	**BedShear 0.9999540**
NewHaz 0.9908819	**NewHaz 0.9999559**
SONAR - SENTINEL-2	**SITE 2: Mesh 25 (Refined)**
Stage 0.9996891	**SURVEY – DEMNAS Run1**
TotM 0.9926519	**SURVEY – DEMNAS Run2**
BedShear 0.9726684	Stage 0.9999854
NewHaz 0.9818269	TotM 0.9999705
	BedShear 0.9999627
	NewHaz 0.9999642

Table 1 R-Squared Terms for Site 1 and Site 2

The other METRICS considered for the OUTPUT results included **RMSE, MAE and MBE** as follows:

SITE 1:

Demnas_Batnas_Sonar_Wave_10_p25 - **Demnas_Gebco_Wave_5_p25**
Stage RMSE: 2.197 MAE: 1.629 MBE: 0.368
TotM RMSE: 12.728 MAE: 8.935 MBE: 4.213
BedShear RMSE: 35.566 MAE: 20.897 **MBE: -0.060**
NewHaz RMSE: 91.825 MAE: 83.827 MBE: 83.343

Demnas_Batnas_Sonar_Wave_10_p25 - **Demnas_Batnas_Wave_10_p25**
Stage RMSE: 0.252 MAE: 0.132 MBE: 0.053
TotM RMSE: 3.257 MAE: 2.171 MBE: 1.920
BedShear RMSE: 12.381 MAE: 4.442 MBE: -1.237
NewHaz RMSE: 44.880 MAE: 43.628 MBE: 43.628

Demnas_Batnas_Sonar_Wave_10_p25 -
Demnas_Batnas_Sent2_Wave_10_p25
Stage RMSE: 0.127 MAE: 0.059 MBE: 0.017
TotM RMSE: 2.616 MAE: 1.385 MBE: 1.218
BedShear RMSE: 18.781 MAE: 7.006 MBE: -4.363
NewHaz RMSE: 41.685 MAE: 40.994 MBE: 38.013

Table 2 OUTPUT METRICS for Site 1

COMMENTS:
Site 1. Bathymetric Data Change
In running multiple models and only adjusting the Bathymetric data it was found that the Closest estimate to the SONAR data was as a result of the Sentinel-2 DATA with RMSE result for Stage, Total Momentum (VxD) and a New Hazard Term. However, the best RMSE result for BedShear was the BATNAS data.

The same result was clear in the R-squared term also.

SITE 2:

BatNas_DemNas_SURV_Wave_10_p25 -
BatNas_FabDem_Wave_10_p25
Stage RMSE: 0.018 MAE: 0.006 MBE: 0.002
TotM RMSE: 2.571 MAE: 1.941 MBE: -1.160
BedShear RMSE: 8.941 MAE: 6.103 MBE: -5.356
NewHaz RMSE: 8.888 MAE: 6.082 MBE: -5.332

BatNas_DemNas_SURV_Wave_10_p25 -
Batnas_Demnas_Wave_10_p25
Stage RMSE: 0.004 MAE: 0.002 MBE: 0.001
TotM RMSE: 0.426 MAE: 0.313 MBE: -0.097
BedShear RMSE: 1.816 MAE: 1.177 MBE: -0.491
NewHaz RMSE: 1.805 MAE: 1.164 MBE: -0.481

SITE 2: REFINED:

BatNas_DemNas_SURV_Wave_10_M25 -
Batnas_Demnas_Wave_10_M25
Stage RMSE: 0.007 MAE: 0.003 MBE: -0.000
TotM RMSE: 0.364 MAE: 0.187 MBE: 0.001
BedShear RMSE: 1.743 MAE: 0.843 MBE: -0.077
NewHaz RMSE: 1.741 MAE: 0.841 MBE: -0.077

Table 3 OUTPUT METRICS for Site 2

COMMENTS:

Site 2: Terrain Data Change

In running multiple models and only adjusting the terrain it was found that the DEMNAS data provided the closest estimate to GROUND SURVEY for all terms likely to be related to hazard. The same result was shown in the R-squared term

These results have been plotted in simple graphs showing the input metric change against the output metric change, providing a measure of sensitivity (dy/dx). For site 1 input MBE the Output MBE has a sensitivity is 0.5. For site 2 the sensitivity is 1.85 as shown (Figure 37-38).

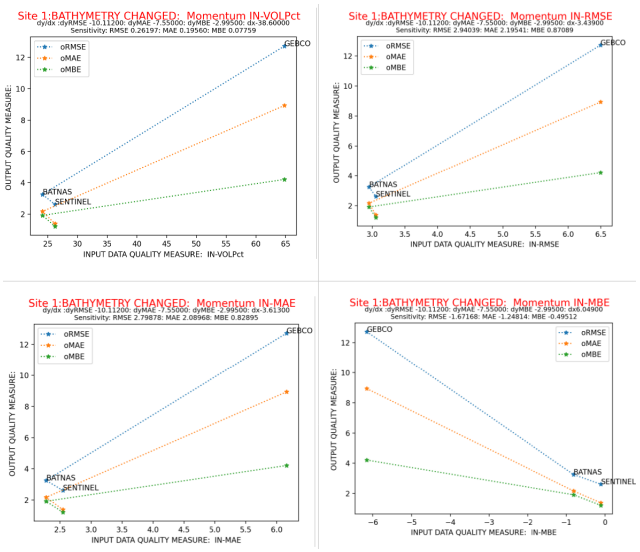

Figure 47. Site 1 RESULTS

Plotting input data and output data variability, indicates sensitivity to change.

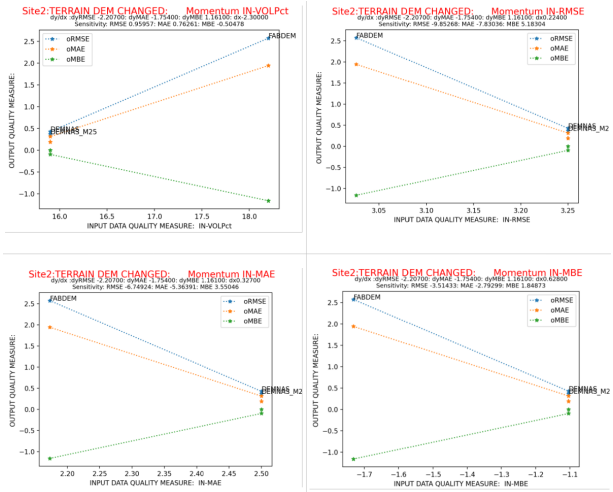

Figure 48. Site 2 RESULTS

4. CONCLUSIONS

For this body of work the objective was to identify the influence of data quality on the resulting determination of hazard for tsunami analysis. The conclusion clearly identifies better candidate metrics for inputs and results that link input data quality to output data quality. The broader objectives were to at least discuss the use of a framework, and to discuss how hazard is defined.

The following can be concluded:

1. The model topographic input data has a great influence on model results.
2. Input data quality has been shown to influence resulting outputs that define tsunami hazard.
3. Input data can be systematically reviewed by the inclusion of data metrics to compare data sets. The input metrics 3D surface volume , Points Volume Metric and Mean Bias Error (MBE) appear to perform better than Root Mean Square Error in identifying candidates for best input model DEMS.
    a. For Site 1 Identifying BATNAS as the best general candidate and SENTINEL-2 in the shallower water (<5m depth) to replicate the SONAR model. For Bathymtric DATA, the model results compared from each of the models for the sites suggests R-Squared performs well to identify a split between BATNAS and SENTINEL-2 whilst RMSE, MAE and MBE select SENTINEL-2 for Stage, Total Momentum, and the suggested new Pressure hazard term whilst identify BATNAS to perform best for Bed Shear in replicating the point of truth SONAR model.
    b. For Site 2 Identifying DEMNAS is the best general candidate to replicate the SURVEY model as land based terrain. For Terrain DATA, the model results compared from each of the models for the sites suggests R-Squared, RMSE, MAE and MBE, each identified the DEMNAS model to perform best for Stage, Total Momentum, Bed Shear and the suggested new Pressure hazard term in replicating the point of truth SURVEY model.
4. It was shown that momentum (current approach to hazard) is sensitive to changes in input data. Even though the extent of measure (range) was limited, the best consistent metric was MBE as compare to RMSE and MAE.
5. The better spread of values from a Pressure based term may be a better candidate for describing hazard compared to the current globally adopted Momentum based term. This made measuring sensitivity more pronounced.
6. Through the extent of work undertaken in relation to the findings presented, it is likely that a framework based approach would stream line many aspects of similar future ventures in tsunami analysis.

In terms of real life adoption and application, the following can be suggested. The need to update time consuming, expensive tsunami modelling requires a specific trigger. One trigger being the availability of updated and improved data. The identification of the level of improvement of new data sets can be estimated through the processes utilised in this thesis, whereby an improvement metric in output can be estimated from the improvement metric in input.

ACKNOWLEDGEMENTS

This body of work could not have been completed without the assistance and guidance of a number of people. Their assistance is greatly appreciated and acknowledged.
Thesis Primary Supervisor: Pak Gede Pringgana; Thesis Secondary Supervisor: Ibu Ni Nyoman Pujianiki; Provision of Data, and support , Pak Komang Gede Putra Airlangga
Staff in the Udayana International Office Administration

REFERENCES

Airlangga KGP (2023) “SONAR Single Beam Sounding Data Thesis: Analysis Of Sentinel-2 Image Utilization For Bathymetric Depth Extraction, (Case Study: Bali Province)".

Bonham, A.J., Hattersley, R.T.(1967),; "Low Level Causeway Water Research Laboratory Report 100".

Cárdenas, Catalán, (2022);"Accelerating Tsunami Modeling for Evacuation Studies through Modification of the Manning Roughness Values", GeoHazards 2022, 3, 492–507. https://doi.org/10.3390/ geohazards3040025

Fatmawati, Yuliara, Riandhita, Kelo, Vellicia, Reswari: (2019) "Tsunami Level Disaster Based on Simulation Scenario of Earthquake Modeling and Seismicity in South Bali 2010-2018"

Filippucci, Brocca, Bonafoni, Saltalippi, Wagner, Tarpanelli, (2022); "Sentinel-2 high-resolution data for river discharge monitoring ", Remote Sensing of Environment 281 (2022) 113255

Flouri, Kaligeris, Alexandrakis, Kampanis, and Synolakis, (2010) ;"Numerical modelling of tsunami waves: Application to the simulation of an earthquake generated tsunami"

GITEWS, DLR / GTZ, Balinese Working Group for Tsunami Hazard Mapping; (2010); "Technical Documentation: Tsunami Hazard Maps for Bali:-Multi-scenario Tsunami Hazard Maps for Bali, 1:100,000 :- Multi-scenario Tsunami Hazard Maps for Southern Bali, 1:25,000; with zoning based on wave height at coast (in line with the InaTEWS warning levels) as well as probability of areas being affected by a tsunami."

Griffin, Latief, Kongko, Harig, Horspool, Hanung, Rojali, Maher, Fuchs, Hossen, Upi, Dewanto, Rakowsky, Cummins; (2015) "An evaluation of onshore digital elevation models for modeling tsunami inundation zones"

Kjell Karlsrud [NGI]; (2009) "Tsunami Risk Reduction Measures phase 2, Tsunami Risk evaluations for Indonesia, Ref: 20061179-00-227-R"

Kuncoro, Setiawan, Kusuma, Manessa, Susetyo; (2021) “Rapid Bathymetry Detection With Sentinel Application Platform (Snap) Using Sentinel Imagery 2a”

Laksono, Widagdo, Aditama, Fauzan, Kovács; (2022) "Tsunami Hazard Zone and Multiple Scenarios of Tsunami Evacuation Route at Jetis Beach, Cilacap Regency, Indonesia"

Marras, Mandli; (2021):"Modeling and Simulation of Tsunami Impact: A Short Review of Recent Advances and Future Challenges"

Mungkasi , VanDrie, Roberts (2013),“Predictions on arrival times of water of the St. Francis dam break flood using ANUGA”, 20th International Congress on Modelling and Simulation MODSIM 2013

Murray, Shand, Higuera; (2021) "Hydrodynamic Modelling of Tsunami Inundation Behaviour in Urban Environments":Australasian Coasts & Ports 2021 Conference – Christchurch, 30 November – 3 December 2021

Nielsen, O., Roberts, S., Gray, d., McPherson, A.,Hitchman, A.(2005); "Hydrodynamic modelling of coastal inundation" :: MODSIM2005

Roberts, Nielsen, Jakeman, (2006):"Simulation of Tsunami and Flash Floods"

Roberts, Stals, Nielsen; (2007) "Parallelisation of a finite volume method for hydrodynamic inundation modelling", ISSN 1446-8735 http://anziamj.austms.org.au/ojs/index.php/ANZIAMJ/article/view/153

Saberi, Kabolizadeh, Rangzan, Abrehdary (2022); Accuracy assessment and improvement of SRTM, ASTER, FABDEM, and MERIT DEMs by polynomial and optimization algorithm: A case study (Khuzestan Province, Iran) https://doi.org/10.1515/geo-2022-0455

Schlurmann, Kongko, Goseberg, Natawidjaja, Sieh; (2010) "Near-Field Tsunami Hazard Map Padang, West Sumatra: Utilizing High Resolution Geospatial Data And Reasonable Source Scenarios"

Sukmono, Aji 1, Amarrohman, Bashit, Saputra; (2022) "The Extraction of Near- Shore Bathymetry using Sentinel-2A Satellite Imagery: Algorithms and Their Modifications" :: TEM Journal. Volume 11, Issue 1, pages 150-158, ISSN 2217-8309, DOI: 10.18421/TEM111-17, February 2022.

Sulistian, Aditya, Mugiarto, Istighfarini, Harrys, Sofian, (2021);"Pemutakhiran Digital Elevation Model Nasional Wilayah Laut" (Updating of National Ocean Digital Elevation Model, Case Study: Aceh Waters Area)

Synolakis, Bernard (2006);"Tsunami science before and beyond Boxing Day 2004", DOI: 10.1098/rsta.2006.1824

Tennakoon,(2004); "Parameterisation of 2D Hydrodynamic Models and Flood Hazard Mapping for Naga City, Philippines" ::Thesis, International Institute for Geo-Information Science and Earth Observation Enschede, The Netherlands.

Titov, V.V. (1997): Numerical modeling of long wave runup. Ph.D. thesis, University of Southern California, Los Angeles, State California,

Valentra, Rachmayani, Diastomo, Sapiie; (2022) "Potential Tsunami Due To Submarine Landslide In The South Of Bali Island: A Preliminary Study"

VanDrie, Ghetti, Milevski(2018), “Who is Responsible for Checking Flood Models?“, ASFPM Annual Conference, Phoenix Arizona, USA, 17-21 June

VanDrie R. (2008), “Is There A Better Definition Of Hazard?”,48th Annual NSW Floodplain Management Authorities Conference

Van Drie, Simon, Schymitzek (2009);"ANUGA:- the FREE Ocean Impact model", 12th NSW Local Government IT Conference, Coffs Harbour NSW

Van Drie, Milevski, Simon;(2011) "Validation of a 2-D Hydraulic Model - ANUGA, to undertake Hydrologic Analysis"; 34th IAHR (International Association for Hydro-Environment Engineering and Research),BIENNIAL CONGRESS, 33rd Hydrology and Water Resources Symposium, 10th Conference on Hydraulics in Water Engineering

Varnuska M. (2005); "Surface reconstruction of Geometrical Objects from Scattered Points", Doctoral Thesis, University Of West Bohemia Faculty of Applied Sciences

Wuppukondur, A., & Baldock, T.E.; (2020) "Modelling of tsunami wave overtopping in a converging channel" ::22nd Australasian Fluid Mechanics Conference AFMC2020, Brisbane, Australia,7-10 December 2020. Brisbane, Australia, The University of Queensland. https://doi.org/10.14264/042c06b.

Zoppou, C., and S. Roberts;(1999), "Catastrophic collapse of water supply reservoirs in urban areas" ::Journal of Hydraulic Engineering, American Society of Civil Engineering, 125(7), 686–695.

ISSN 8755-6839

SCIENCE OF **TSUNAMI HAZARDS**

Journal of Tsunami Society International

Volume 42 **Number 3** **2023**

WWW.TSUNAMISOCIETY.ORG

TSUNAMI SOCIETY INTERNATIONAL, 1325 South 33rd Avenue, Hollywood, Florida 33021, USA.